An Image Processing Based Patient-Specific Optimal Catheter Selection

dem Fachbereich Informatik
der Technischen Universität Darmstadt
genehmigte

DISSERTATION

zur Erlangung des akademischen Grades eines
Doktor-Ingenieurs (Dr.-Ing.)
von

M.Sc. Sami ur Rahman

Swat, Pakistan

Referenten der Arbeit: Prof. Dr. techn. Dieter W. Fellner
Technische Universität Darmstadt
Prof. Dr. med. Wolfram Völker
Universitätsklinikum Würzburg

Tag der Einreichung: 06.11.2012
Tag der mündlichen Prüfung: 18.12.2012

Darmstädter Dissertation
D 17
January, 2013

Acknowledgments

Many organizations and individuals helped in successful completion of this thesis. I am thankful to Prof. Dr. Dieter W. Fellner who supervised this thesis and provided all the required resources for the successful completion. Special thanks go to Dr. Stefan Wesarg for his time, valuable suggestions and technical discussions during the whole project. He took a great interest in my work and always came to my rescue during the hard times. I am also thankful to Priv. Doz. Dr. Arjan Kuijper for reading this thesis and his valuable suggestions. I am thankful for the efforts of Prof. Dr.-Ing. Georgios Sakas for arranging the PhD defense in a very short time. I want to extend my gratitude to all colleagues at the Interactive Graphics Systems Group (GRIS), especially Matthias Kirchner and Wissam El Hakimi for their active role in discussions on daily work topics. A bundle of thanks goes to Prof. Dr. Wolfram Voelker and Matthias Dobhan from Uniklinikum Wuerzburg for their help in clinical evaluation of the project. Prof. Voelker remained a great source of motivation and took time for producing clinical data for the required validation and experiments. I would like to cordially acknowledge the efforts of Muhammad Munir Khan (Hazara University), Dr Sehat ullah (University of Malakand) and Muhammad Awais (University of Bayreuth) for their help and suggestions in shaping the thesis draft. I want to extend my cordial gratitude to the Higher Education Commission (HEC) of Pakistan for giving me scholarship. Special thanks go to Shaikh Muhammad Ali, Project director at HEC, and the team at the German Academic Exchange Service (DAAD) for smooth transfer of funds. Last but not the least, I am thankful to my family for their patience, encouragement and support during my absence from home.

Erklärung zur Dissertation

Hiermit versichere ich die vorliegende Dissertation selbständig nur mit den angegebenen Quellen und Hilfsmitteln angefertigt zu haben. Alle Stellen, die aus Quellen entnommen wurden, sind als solche kenntlich gemacht. Diese Arbeit hat in gleicher oder ähnlicher Form noch keiner Prüfungsbehörde vorgelegen.

Darmstadt, den 06.11.2012 Sami ur Rahman

Abstract

Coronary angiography is performed to investigate coronary diseases of the human heart. For better visualization of the arteries, a catheter is used to inject a contrast dye into the coronary arteries. Due to the anatomical variation of the aorta and the coronary arteries in different humans, one common catheter cannot be used for all patients. The cardiologists test different catheters for a patient and select the best one according to the patient's anatomy. To overcome these problems, we propose a computer-aided catheter selection procedure. The basic idea of this approach is to obtain MR/CT images before starting angiography. From these images, the patients' arteries are segmented and some geometric parameters are computed from the segmented images. At the same time, geometric parameters are computed from the available catheters. A model is developed, which is based on these parameters from the patients' image data and parameters from the catheters. This model reduces the number of catheter choices. In the next step, the reduced number of catheters are simulated and the most optimal catheter is obtained. A series of validation tests were conducted for segmentation, geometric parameters' estimation, parameters based catheter selection and simulation model. In our experiments, we compared catheters selected in the clinic with the catheters suggested by the image processing based model. For these experiments, the ground truth data were obtained from the clinical partner. In the clinic, angiography of twenty four cases was performed. An experienced cardiologist selected catheters based on his experience and knowledge in the field. In the next step, CT/MR image data that was acquired prior to the angiography was used for the image based catheter selection model to find optimal catheters. For every patient, three most optimal catheters were suggested by the model. These three optimal catheters were ranked as first, second and third ranked catheters. Catheters suggested by the model were compared with the catheters selected by the cardiologist. It was found that in 41% cases, model based top ranked suggestions were the same as that were used in the clinic. In 25% cases, the catheters used in the clinic were the model's second ranked catheters. In 21% cases, the catheters used in the clinic were the model's third ranked catheters. In 13% cases the catheters used in the clinic were not in the list of suggested catheters. In further experiments, the clinicians graded catheters based on catheter's performance and placement in the arteries. Most optimally placed catheters were assigned good grades, and less optimal catheters were assigned bad grades. It was seen that the model suggested similar catheters to the clinically good graded catheters but suggested different catheters to the clinically bad grade catheters. All these experiments showed that the method of an image processing based catheter selection is clinically applicable, and the only requirement is to have patient's image data before starting the angiography. It was shown that this tool will be of great help for the experienced as well as the non experienced cardiologists to have a catheter suggestion before starting the angiography.

Zusammenfassung

Motivation

Herzerkrankungen sind die häufigste Todesursache in den entwickelten Ländern. In den Entwicklungsländern ist die Häufigkeit in den letzten Jahren stark angestiegen [MPN*11]. Krankheiten der Koronararterien können mittels Katheterangiographie diagnostiziert werden. Während dieses Prozesses wird ein kleiner Schnitt in den oberen Oberschenkel gemacht. Dann wird eine kleine Röhre, genannt Katheter, in die Oberschenkelarterie eingeführt und in Richtung der Aorta geschoben. Danach wird das Kontrastmittel durch den Katheter injiziert und dem Blut der kleinen Gefäße zugegeben. Hierdurch erscheint das Blutgefäß undurchsichtiger, so dass klare Bilder von kleinen Gefäßen akquiriert werden können. Während der Angiographie ist die Auswahl geeigneter Katheter eine anspruchsvolle Aufgabe. Es gibt anatomische Variationen der Aorta und der Koronararterien bei verschiedenen Menschen. Für die Katheter-Auswahl, testen die Kardiologen verschiedene Katheter für einen Patienten und wählen den Besten abhängig von der Anatomie des Patienten. Diese Prozedur ist zeitaufwändig und es besteht ein geringes Krebsrisiko durch die übermäßige Strahlenbelastung. Es ist hilfreich für die Kardiologen im voraus den optimalen Katheter zu kennen, bevor sie tatsächlich mit der Angiographie beginnen. In dieser Arbeit werden wir uns mit diesem Problem beschäftigen und ein bildverarbeitungsbasiertes Verfahren vorschlagen, das zur Auswahl eines patienten-spezifisch optimalen Katheters dient.

Stand der Technik

Die Idee der bildverarbeitungsbasierten Katheter-Auswahl ist es, MR/CT-Daten des Patienten vor Beginn der Angiographie zu akquirieren; anatomische Informationen über den Patienten aus diesen Bildern zu erhalten; und den optimalen Katheter entsprechend der Anatomie des Patienten vorzuschlagen. Wir präsentieren einen Überblick über die vorhandene Literatur im Zusammenhang mit der Segmentierung, nicht-bildverarbeitungsbasierter und bildverarbeitungsbasierter Katheter-Auswahl.
Es existieren frühere Arbeiten mit dem Schwerpunkt auf der Segmentierung der Aorta und der Koronararterien aus 3D-Bilddatensätzen. Zum Beispiel ist ein stochastisch-relaxation-basiertes Verfahren zur Segmentierung der Aorta von Rueckert et al. [RBF*97] präsentiert worden. Eine modellbasierte Segmentierung ist von Kovacs [KCA*06b, KCA*06a] vorgeschlagen worden. Wörz and Rohr [WR07, WvH*10] haben ein 3-D zylindrisches parametrisches Intensitätsmodell vorgeschlagen, das Benutzer-Interaktion verlangt. Der Thresholding-Algorithmus von Sauer et al. [SKB*08] braucht Interaktion mit dem Benutzer, um die beiden Schwellwerte zu bestimmen. Die Arbeit von Lorenz et al. [LRSB03] für

Module	Was wird getan	Neuigkeit/Erweiterung
Segmentierung	Viele halbautomatische Ansätze sind verfügbar.	Erweiterung der bisherigen Ansätze für eine vollständige automatische Segmentierung
Schätzung von Parameter	Manualle Ansätze zur Verfügung	Ansatz zur automatischen Berechnung ist erforderlich
Nicht bildverarbeitungsbasierente Katheterauswahl	Vorhandene Ansätze können verwendet werden	–
Bildverarbeitungsbasierente Katheterauswahl	Keine Ansätz sind vorhanden	Entwicklung eines neuen Ansatzes
Simulationsbasierte Katheterauswahl	Kathetersimulation für Ausbildungszwecke sind vorhanden	De aktuellen Ansätze müssen für die Katheterauswahl angepasst werden

Table A.: Liste der Forschungsgebiete, in denen neue Ansätze erforderlich sind.

die Segmentierung der Koronararterien setzt die Bestimmung von Saatpunkten in jeder Koronararterie voraus. Hennemuth [HBF*05] hat eine Methode vorgeschlagen, bei der der Benutzer einen Saatpunkt über den Verzweigungen der Herzkranzgefäße wählen muss. Wang [WL09] hat eine vollautomatische Level-Set-basierte Methode für CT-Daten vorgeschlagen, welche Parametertuning benötigt, während Shoujan [SJYW10] eine Segmentierung in Rötgenbildern vorgeschlagen hat. Die meisten dieser Methoden verwenden CT-Daten mit Sub-Millimeter-Auflösung.
Wir haben auch die Literatur über die allgemeine Anatomie und den empfohlenen Katheter untersucht. In der Arbeit von Schneider [Sch03] über Katheterauswahl ist eine detaillierte Untersuchung der verschiedenen Arten von Kathetern vorgestellt worden. Es gibt auch Arbeiten von anderen (Kirks et al. [KFHN76], Kimbiris et al. [KISB78], Brinkman [BBN*94], [BBN*94], Voda [Vod92] und Sarkar et al. [SSK09]), die auf dem Problem der Katheterauswahl gearbeitet haben, aber all diese Ansätze sind sehr allgemein gehalten und sind nicht Bildverarbeitungsmethoden.
In der Arbeit von Rubin et al. [RPJN98] wird ein halbautomatisches Verfahren zur Quantifizierung von Durchmesser und Krümmung der Aorta und ihrer Verzweigungen in CT-Daten verwendet. Eine auf diskriminativem Lernen basierende patientenspezifische Modellierung und Quantifizierung der Aorten- und Mitralklappe in 4D Herz-CT und TEE ist von Ionasec et al. [IVG*10] vorgestellt worden. Eine Studie zum Auffinden der Koronararterien-ostia und der verbundenen Objekte zur Aortenklappen-Implantation ist von John et al. [JLZ*10] vorgestellt worden. Wir haben gesehen, dass es in der Literatur einige halbautomatische Ansätze zur Berechnung einiger Parameter aus den Bilddaten gibt.
Ein weiterer Bereich, der Hilfe bei der Auswahl von Kathetern auf Basis der Bilddaten eines Patienten geben kann, ist die Simulation von Kathetern. Es gibt Ansätze für die Kathetermodellierung und simulation. In diesen Arbeiten wird der Katheter mittels FEM oder Feder-Masse-Modellen modelliert. Zu den Systemen, die FEM-Modelle verwendet haben, gehören die Arbeiten des HT Medical

Inc. [Meg96], daVinci [AR98], iCard [WCL*98], Duriez et al. [CDL*05] und NeuroCath [NC01]. Die Feder-Masse-Modelle sind von Lenoir et al. [J. 06], Alderliesten et al. [AKN04], Lauboz et al. [LBGB09, LZL*10] und Takashima et al. [TOY*09]. Allerdings sind diese Systeme noch weit von der realen Umgebung entfernt. Hinzu kommt, dass diese Systeme nicht das Problem der patientenspezifischen optimalen Katheterauswahl behandeln. In Tabelle A haben wir zusammengefasst, was getan wurde und was getan oder erweitert werden muss.

Bildverarbeitungsbasierte patientenspezifische Modelle für die Katheterauswahl

Die Grundidee dieses Ansatzes ist, MR / CT-Bilder zu erhalten, bevor die Angiographie durchgeführt wird. In diesen Bildern werden die Arterien des Patienten segmentiert. Klinisch wichtige geometrische Parameter werden aus den segmentierten Bildern sowie aus den verfügbaren Kathetern berechnet. Ein Modell, das auf Basis dieser Parameter definiert wird, reduziert die Anzahl der in Frage kommenden Katheter. Im nächsten Schritt werden die vorselektierten Katheter simuliert, um den optimalen Katheter zu bestimmen.

Segmentierung

Der erste Schritt des bildverarbeitungsbasierten Modells ist die Segmentierung der Aorta und der Koronararterien. Das Bildgebungsprotokoll, das durch unsere klinischen Partner verwendet wird, verlangt, dass das Verfahren auf speziellen MRI-Daten durchgeführt werden muss. Wärend für die Aorta Bilder mit geringer Auflösung aufgenommen werden, ist für die Koronararterien eine höhe Auflösung nötig. Diese Daten werden vor der Koronarangiographie akquiriert.

Segmentierung der ganze Aorta

Die Segmentierung der Aorta in den Bilddaten niedriger Auflösung wird schichtweise durchgeführt. Dabei wird eine Kombination aus der Hough-Transformation [Bal81] und der Fast Marching Methode (FMM) [Set99] eingesetzt.

In einem Vorverarbeitungsschritt werden die Bilddaten mit einem anisotropen Diffusionsfilter geglättet dazu wird ein Gradientengrößenfilter sowie ein Sigmoidfilter angewendet.

Ein erster Startpunkt (siehe Abbildung 3.6, Punkt S) für die FMM wird automatisch durch die Suche nach Kreisen mit den stärksten Hough Spitzen in den mit dem Gradientengrößenfilter bearbeiteten Bildern gefunden. Dann wird die Aorta wie folgt segmentiert: Absteigende Aorta: Für das rote Segment startet die Segmentierung vom Startpunkt S. Die FMM wird bei jeder Bildschicht unterhalb von Punkt S verwendet, und der Schwerpunkt der segmentierten Region wird nach unten propagiert und als Startpunkt für die Segmentierung der nächsten Scheibe verwendet. Für das grüne Segment wird die gleiche Prozedur für die Schichten oberhalb von Punkt S wiederholt, bis die Größe der segmentierten

Region schlagartig abnimmt (siehe Abbildung 3.6 Punkt P). Für die aufsteigende Aorta (blaues Segment) wird die Segmentierung am Punkt P gestartet, und die FMM wird in Abwärtsrichtung verwendet, bis die Größe der segmentierten Region schlagartig zunimmt (gerade unterhalb der Aortenklappen).

Segmentierung der Koronararterien

Die hochaufgelösten Datensätze mit den Koronararterien werden auf die gleiche Weise vorverarbeitet wie bei den niedrigaufgelösten Bildern. Zusätzlich werden zwei Bilddatensätze erstellt, die mit dem Vesselness Operator gefiltert sind [FNH*99]. Der Vesselness-Filter muss mit geeigneter Glättung der Hesse-Matrix verwendet werden, um die gesuchte Struktur zu finden. Wir setzen sigma = 1 für die Hervorhebung der Koronararterien und sigma = 4 für die Aorta. Diese beiden Datensätze dienen als zusätzliche Eingabe für die folgende Segmentierung. Zunächst wird eine starre Registrierung beider Datensätze unter Verwendung einer Mean Squares-Metrik durchgeführt, und die niedrigaufgelösten Daten werden auf die Voxelgrößen der hochaufgelösten Daten hochgesampled. Sobald die Registrierung abgeschlossen ist, wird der Schwerpunkt der bereits segmentierten Aorta in den niedrigaufgelösten Daten als Startpunkt für die hochaufgelösten Daten verwendet. Hier werden die hochaufgelösten Daten explizit segmentiert anstatt einfach die segmentierte Region aus den niedrigaufgelösten Daten zu transferieren, da wir eine genaue Abgrenzung der Aorta im Bereich der koronaren-Ostia benötigen. Die Aorta und die Koronararterien werden in zwei Schritten extrahiert, wobei jeweils eines der mit dem Vesselness-Operator gefilterten Bilder verwendet wird. Zunächst wird das mit sigma = 4 gefilterte Bild voxelweise mit dem Bild multipliziert, das mit dem Sigma-Filter vorverarbeitet wurde. Dann wird mit der FMM schichtweise nach unten und oben eine Segmentierung durchgeführt. Danach werden die dem Parameter sigma = 1 gefilterten Bilder voxelweise mit der Ausgabe der FMM addiert, und die FMM wird eneut ausgeführt, aber dieses Mal in 3D. Im letzten Schritt werden die segmentierte Aorta und die Koronararterien fusioniert, um ein einziges 3D-Modell zu erhalten.

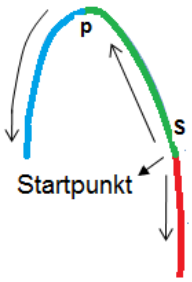

Figure A.: Segmentierung der Aorta

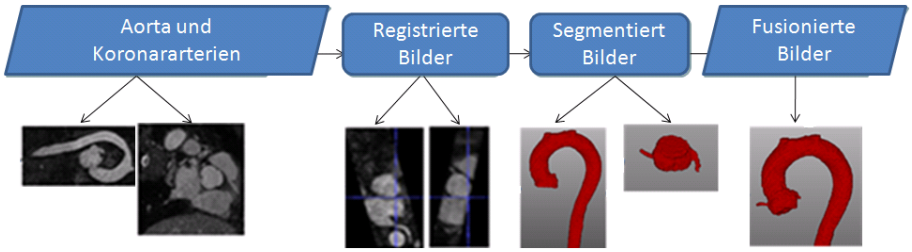

Figure B.: Segmentierungspipeline

Geometrische Parameterschätzung

Die klinisch wichtigen Parameter, die gewonnen werden, sind:
Mittellinienextraktion: Ein binäres Ausdünnungsverfahren für 3D-Bilddaten [Hom07] wird für die Mittellinienextraktion verwendet.
Durchmesser der Aorta und der Koronararterien: Zu jedem Punkt auf der Mittelline wird eine Ebene berechnet, die senkrecht zur Mittellinie steht. Entlang dieser Ebene werden die gemittelten Distanzen der Punkte auf der Oberfläche der segmentierten Region bestimmt, welche Durchmesser der Aorta und der Koronararterien bereitstellen.
Koronares Ostium: Die berechneten Werte für den Durchmesser werden an den oberen linken und rechten Endpunkten des Skeletts betrachtet (Abb. 3.20, Punkt B). Durch Berechnung des Verhältnisses zwischen dem aktuellen Wert und dem vorherigen wird der Skelettpunkt bestimmt, bei dem das Verhältnis 2,0 übersteigt. Dies zeigt an, dass dieser Punkt bereits innerhalb der Aorta liegt. Das Skelett zwischen dem vorherigen Punkt und dem entsprechenden Endpunkt des Skeletts wird als koronares Ostium markiert.

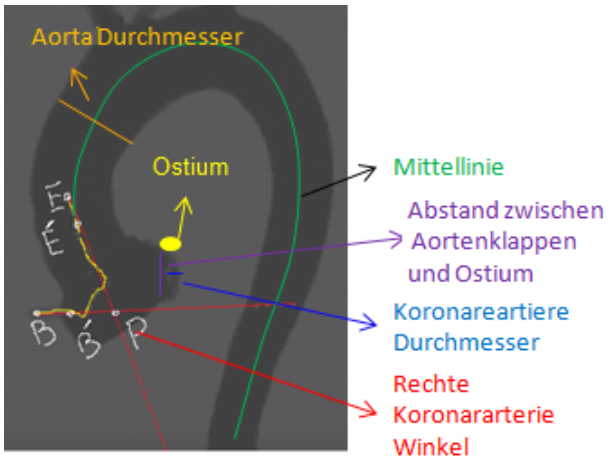

Figure C.: Mittellinie Extraktion und klinisch bedeutende Parameter

koronare Winkel: Für die Berechnung des Winkels zwischen der Aorta und den beiden Koronararterien werden die Teile des Skeletts, die zu den Koronararterien beziehungsweise zur aufsteigenden Aorta gehören, auf eine 2D Ebene projiziert. Gerade Linien werden für diese projizierten Segmente interpoliert und die entsprechenden Winkel zwischen ihnen berechnet.
Position der Aortenklappen: Schließlich wird die Position der Aortenklappen, die bereits während der Segmentierung der gesamten Aorta geschätzt wurde, verfeinert. Dazu werden die Bildintensitäten der Voxel aus den niedrigaufgelösten Daten betrachtet, die innerhalb des segmentierten Bereiches und die in Schichten nahe der geschätzten Position der Klappen liegen. Die Klappen erscheinen im Vergleich zum Aorta-Lumen als dunkel. Daher werden die Schichten aufwärts durchgegangen, startend von der Schicht, die die anfänglich abgeschätzte Aortenklappenposition beinhaltet. Es wird nach der ersten Schicht gesucht, bei der die Durschnittsintensität innerhalb der segmentierten Region um den Faktor 1,5 ansteigt. Die darunterliegende Schicht wird als Position der Aortenklappe betrachtet.

Modelle

In diesem Abschnitt werden bildverarbeitungsbasierte, patientenspezifische Modelle zur Auswahl optimaler Katheter präsentiert. Basierend auf Vorgaben der Klinik werden verschiedene Parameter aus

den Bilddaten eines Patienten und für den Katheter definiert. Da die Optimalitätsbedingungen für die linken und rechten Koronararterien unterschiedlich sind, werden jeweils getrennte Modelle definiert.

Modell für die Rechte Koronarangiographie

Die Kurven der Katheter und die Kurven, die durch die Aorta und die rechte Koronararterie (RKA) gebildet werden (siehe Abbildung D (b) gelbe Kurve), werden berücksichtigt. Die Kathter-Kurvenlänge (KKL) und Katheter-Kurvenwinkel (KKW) der verfügbaren Katheter sowie Kurvenlänge der RKA (RKAKL) und Kurvenwinkel der RKA (RKACW) werden berechnet, und ein quantitatives Mass für die optimale Auswahl eines Katheters wird definiert. Die folgende Kostenfunktion ist definiert, um jedem Katheter Kosten für einen bestimmten Patienten zuzuordnen. Der optimale Katheter (OK) wird als das Minimum aller Kosten KK_i für alle betrachteten Katheter i bestimmt:

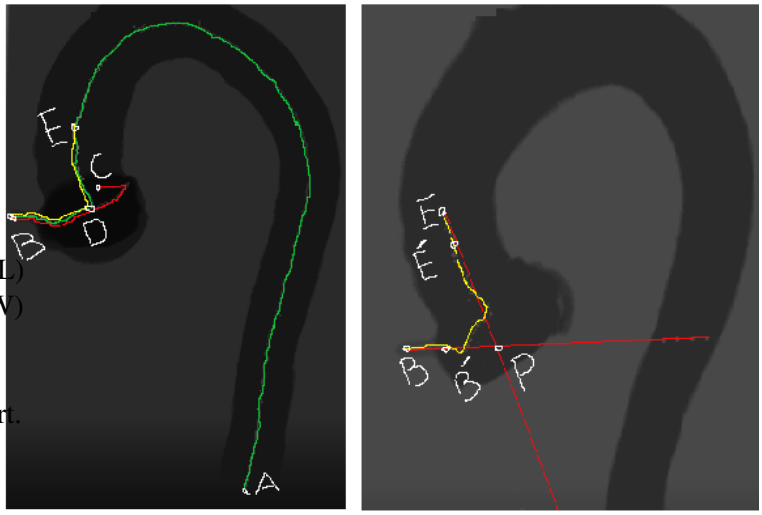

Figure D.: Rechte Koronararterie Kurve Berechnung

$$OK = \arg\min_i \{KK_i\} \tag{A}$$

wobei i der i^{te} Katheter ist und

$$KK_i = a\sqrt{\left(\frac{1}{N_{KL}}\left((KKL)_i - RKACL\right)\right)^2} + b\sqrt{\left(\frac{1}{N_{KW}}\left((KKW)_i - RKAKW\right)\right)^2} \tag{B}$$

mit N_{KL} und N_{KW} die Normierungsfaktoren für die Kurvenlänge und Kurvenwinkel sind. Die Koeffizienten a und b sind Gewichte, die jedem Term der Formel zugewiesen werden. Diese Gewichte sind jedoch heuristische Werte, die aus der Bedeutung der einzelnen Parameter abgeleitet wurden.

Modell für die linke Koronarangiographie

Für das Modell für die linke Koronarangiographie werden klinisch wichtige Parameter aus den Bilddaten des Patienten extrahiert und die Parameter der Katheter berechnet. Die Winkel und die Längen der beiden Kurven eines Katheters (grün und gelb in Abbildung E (b)) werden betrachtet.

Die gelbe Kurve wird als *Katheter-Kurve 1 (KK1)* und die grüne Kurve als *Katheter-Kurve 2 (KK2)* bezeichnet. KK1L ist die Länge von KK1. KK2W ist der Winkel von KK2. Der Abstand zwischen KK1 und KK2 (weißes Segment in Abbildung E (b)) wird mit KSSL bezeichnet. Wir betrachten die folgenden Parameter aus den Bilddaten des Patienten (siehe Abbildung E (a)):

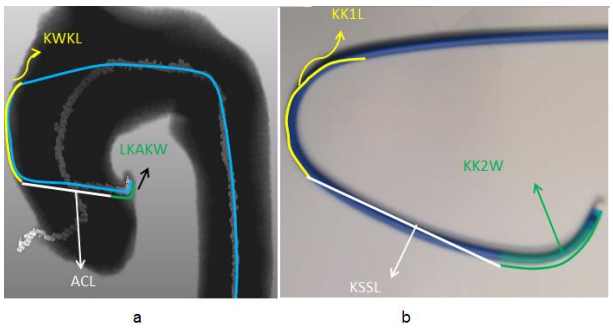

Figure E.: Parameter von den Arterien (a), Parameter der Katheter (b)

- Die gelbe Kurve ist die kontralaterale Wandkurve (KWK)
- Die grüne Kurve ist die linke Koronararterien-Kurve (LKAK)
- Die Länge des KWK (KWKL)
- Der Winkel von LKAK (LKAKW)
- Der Abstand zwischen KWK und LKAK (weiße Linie in Abbildung E) wird als Aorta Cavity Länge (ACL) bezeichnet.

Im nächsten Schritt wird ein Modell in Form einer Kostenfunktion definiert. Der optimale Katheter (OK) wird als das Minimum aller kosten KK_i für alle betrachteten Katheter i bestimmt:

$$OK = \arg\min_i \{KK_i\} \tag{C}$$

wobei i der i^{te} Katheter ist und

$$KK_i = a\sqrt{\left(\frac{1}{N_1}\left((KSSL)_i - ACL\right)\right)^2} + b\sqrt{\left(\frac{1}{N_2}\left((KK1L)_i - KWKL\right)\right)^2} + c\sqrt{\left(\frac{1}{N_3}\left((KK2W)_i - LKAKW\right)\right)^2} \tag{D}$$

mit N_1, N_2 und N_3 als Normierungsfaktoren und a, b und c die Gewichte für jeden Term der Formel. Diese Gewichte sind jedoch heuristische Werte, die aus der Bedeutung der einzelnen Parameter abgeleitet wurden.

Simulation

Um die Wahl des optimalen Katheters durch den geometrischen Ansatz weiter zu verfeinern, wird eine ausgewählte Menge von Kathetern simuliert, um die finalen Platzierungen der Katheter nach der Simulation zu ermitteln. Für die Simulation werden die Arterien basierend auf den MR/CT-Daten des

Patienten simuliert, die vor dem Eingriff erfasst wurden. Ein Oberflächennetz der Arterien wird aus den segmentierten Bildern mit einer Reihe von VTK-Filtern [SML06] erstellt. Die Katheter werden als endliche beam elements modelliert. Bei der Simulation verschiedener Katheter, wird die endgültige Platzierung aller Katheter bestimmt, und gewählt wird dann der Katheter, der entlang des optimalen Weges verläuft. Die Simulation erfolgt mit Hilfe der Bibliothek *Simulation Open Framework Architecture* (SOFA) [ACF*07]

Um den optimalen Katheter zu ermitteln, wird mit Hilfe des klinisch bestätigten optimalen Wegs untersucht, wie nah die verschiedenen Katheter an dessen Mittellinie platziert werden. Dafür wird der optimale Weg (OP) in N äquidistante Punkte aufgeteilt. Ebenso wird jeder Katheter k nach der Platzierung durch die Simulation in N äquidistante Punkte geteilt. Für die Berechnung des Abstands zwischen Katheter k und der ACL wird die folgende Formel benutzt:

$$distanceCatheter_k = \sum_{i=1}^{N} \left(\sqrt{(Catheter_{ki} - OP_i)^2} \right) \tag{E}$$

wobei $Catheter_{ki}$ der i^{te} Punkt des Katheters k ist und OP_i der i^{te} Punkt des OP.

Ergebnisse

Eine klinische Studie wurde durchgeführt, in der gezeigt wurde, dass das Modell in der Lage ist, den optimalen Katheter vor der eigentliche Angiographie zu bestimmen. Eine Reihe von Validierungen wurde für die Segmentierung, die geometrische Parameterschätzung, für das parameterbasierte Katheterselektionsmodell und das Simulationsmodell untersucht. Die Segmentierungsergebnisse wurden mit den Ergebnissen des ITK-SNAP Tools verglichen, sowie visuell validiert. Es wurde gezeigt, dass eine komplett automatische Initialisierung und Terminierung des Segmentierungsprozesses weniger als eine Minute benötigt. Nach erfolgreicher Segmentierung wurde die nächste Validierung für die Berechnung der unterschiedlichen geometrischen Parameter durchgeführt. Die automatisch berechneten Werte wurde mit den manuell ermittelten verglichen. Der durchschnittliche Fehler zwischen manueller und automatischer Berechnung war kleiner als 1 *mm*. Der wichtigste Schritt des Validierungsprozesses war der Wahl des Katheters basierend auf dem geometrischen Modell. Für diese Validierung wurden Referenzdaten von den klinischen Partnern bereitgestellt, die auf Basis von 24 in der Klinik durchgeführten Angiographien erstellt wurden. Ein erfahrener Kardiologe wählte die passenden Katheter basierend auf seiner Erfahrung und seines Expertenwissens. Im nächsten Schritt wurde das bildbasierte Katheterselektionsmodell auf die CT/MR-Daten angewendet, die vor der Angiographie aufgenommen wurden. Katheter wurden für jeden Patienten vorgeschlagen. Die vom Modell vorgeschlagenen Katheter wurden mit den Kathetern verglichen, die vom Kardiologen vorgeschlagen wurden. Für das rechte Modell waren in 41% der Fälle der erste vom Modell vorgeschlagene Katheter identisch mit dem, der vom Kardiologen gewählt wurde. In 25% der Fälle war die Wahl des Kardiologen der zweite Vorschlag, und in 25% der Fälle der dritte Vorschlag. In 9% der Fälle war die Wahl des Kardiologen nicht in den Vorschlägen enthalten. Für die linke Koronararterie war in 41% der Fälle der erste Vorschlag des

Modells identisch mit der Wahl des Kardiologen. In 25% der Fälle war die Wahl des Kardiologen der zweite Vorschlag des Modells, und für 17% der Fälle der dritte Vorschlag. In 17% der Fälle war die Wahl des Kardiologen nicht in den Vorschlägen enthalten. Insgesamt wurden in diesen Experimenten 25 Katheter verwendet. Es wurde gezeigt, dass die Methode klinisch anwendbar ist. Die einzige Anforderung ist, dass Bilddaten vom Patienten vor der Angiographie aufgenommen werden. Die Methode ist vollständig automatisch und benötigte zwei Minuten für Segmentierung und Katheterauswahl. Um das auf geometrischen Parametern basierende Modell weiter zu verfeinern, wurde eine Simulation durchgeführt. Die Simulation wurde benutzt, weil das geometrische Modell nicht die Deformierbarkeit der Katheter in Betracht zieht, und auch Arterien als feste Körper betrachtet.

All diese Tests zeigen, dass die Methode der bildverarbeitungsbasierten Katheterauswahl klinisch anwendbar ist und die einzige Anforderung hat, dass vor der Angiographie Bilddaten des Patienten aufgenommen werden.

Zusammenfassung und Ausblick

In dieser Arbeit haben wir Modelle präsentiert, die von unterschiedlichen MR- und CT-Bildern Information sammeln und patientenspezifische Informationen für die Behandlungsplanung und Diagnose bereitstellen. Die Beiträge sind Modelle zum Sammeln nützlicher Information von unterschiedlichen Bildern, Modelle zum Planen von Angiographien und simulationsbasierte Entscheidungsunterstützung vor der eigentlichen Prozedur. Unser erster Beitrag ist das Sammeln von Informationen aus verschiedenen 3D-Bildern. In dieser Arbeit haben wir eine Idee vorgestellt, um Bildinformation durch Segmentierung und Registrierung zu fusionieren. Dies ist das erste Mal, dass ein vollständig automatisches Segmentierungsmodell für die Aorta und die Koronararterien präsentiert wurde. Der zweite Beitrag liegt im Gebiet der quantitativen Messung von verschiedenen klinisch relevanten Parametern. Ein 3D-Modell wird aus den 3D-MR- und -CT-Bildern erstellt, und dann werden die klinisch relevanten Parameter automatisch berechnet. Der wichtigste Beitrag dieser Arbeit ist in dem Gebiet der Katheterangiographie und Katheterauswahl. Unterschiedliche Modelle wurden definiert für die sehr schwierige Aufgabe der Katheterauswahl. In dieser Arbeit wurden verschiedene bildverarbeitungsbasierte Modelle für die optimale Katheterauswahl definiert. Diese Modelle sind in der Lage, die gängige Selektionsstrategie durch Versuch und Irrtum zu ersetzen. Es wurde gezeigt, dass die Methode klinisch anwendbar ist und die einzige Anforderung ist, Patientendaten vor der Angiographie aufzunehmen. Die komplette Methode ist vollständig automatisch und benötigt zwei Minuten zur Segmentierung und zum Vorschlagen eines Katheters.

Verbesserung der Modelle

Die Algorithmen, die in dieser Arbeit entwickelt wurden, können verbessert werden, um allgemeiner und robuster zu werden. Es gibt viele Richtungen, in denen die aktuellen Ansätze verbessert werden können. In den aufgenommenen MR- und CT-Bildern ist die Orientierung der aufgenommen Bilder

gleich, mit einer leichten Abweichung in der Rotation und Translation. Der aktuelle Segmentierungsalgorithmus geht von diesen Standardausrichtungen aus. Der Algorithmus kann verändert werden, so dass er unabhängig von der initialen Orientierung wird. Genauso erwartet der Algorithmus zur automatischen Parameterschätzung die Standardausrichtung, und auch dieser kann verändert werden, so dass er unabhängig von der Orientierung wird. Die Berechnung der Aortenklappen kann ebenfalls verbessert werden, indem Anatomieinformation berücksichtigt wird. Die derzeitigen Berechnungen verwenden lediglich Intensitätsinformationen für die Identifikation der Aortenklappen. Eine weitere Verbesserungsmöglichkeit ist, die Allgemeinheit des Segmentierungsverfahrens zu erhöhen. Der aktuelle Ansatz wurde für die spezielle klinische Anforderung entwickelt, dass Bilder der Koronararterien und der Aorta separat aufgenommen werden. Allerdings kann der Algorithmus erweitert werden, um Bilder zu segmentieren, die sowohl die Aorta als auch die Koronararterien enthalten. Für die Simulation wird FEM benutzt, welche sehr langsam ist und Realzeitberechnungen unmöglich macht. Um Berechnungen in echtzeit zu ermöglichen, muss die FEM durch eine andere Technik ersetzt werden, die schneller ist, wie das Feder-Masse-Modell.

Ausblick

Die verschiedenen Richtung für eine Erweiterung sind Gehirn-Angiographie, Herz-Katheterisierung, die Entwicklung neuer Katheter sowie die Fusion von 3D- und 4D-Bilddaten. Das aktuelle Modell zum Vorschlagen optimaler Katheter kann erweitert werden, um die Katetherauswahl bei der zerebralen Angiographie zu ermöglichen. Die Behandlung und Diagnose von Schlaganfällen und arterivenous malformation benötigt die Gehirn Katheterisierung, und aufgrund der komplexen Arterienstrukturen ist die Auswahl eines passenden Katheters schwierig. Die in dieser Arbeit entwickelten Modelle können auf das Problem der Katetherauswahl in der zerebralen Angiographie angepasst werden. Ein andere Forschungsrichtung ist die Herzkatheterisierung. Das Passieren der Aortenklappen während der Katheterisierung des linken Teils des Herzens ist ebenfalls ein zeitraubender Prozess. Die Kardiologen finden einen geeigneten Katheter, um die Aortenklappen zu passieren, mit einer Versuch und Irrtum-Strategie. Die existierenden Modelle für die Katheterauswahl können hier verwendet werden, indem ihre Parameter angepasst werden. Die Arbeit kann auch erweitert werden, um neue Katheter zu entwickeln. In dieser Arbeit wurde eine Studie von der Anatomie von verschiedenen Patienten gemacht und unterschiedliche Katheter wurden untersucht. Es wurde festgestellt, dass die Parameter der verfügbaren Katheter nicht gut zur gegebenen Patientenanatomie passen. Die Idee, neue Katheter zu entwickeln, die die Bedürfnisse von vielen Patienten erfüllen, kann ein interessantes Forschungsgebiet sein. Eine andere Erweiterung der aktuellen Arbeit ist die Fusion von 3D-Bildern von unterschiedlichen Teilen des menschlichen Körpers. Zum Beispiel können die Aortenklappen hochaufgelöst aufgenommen werden (da sie relativ klein sind), und die Aorta mit niedriger Auflösung. Klinisch wäre es wünschenswert, die hochaufgelösten Aortenklappen und die niedrigaufgelöste Aorta in einem einzigen 3D Bild zu kombinieren, und dies wird die Zeit reduzieren, in der der Patient Strahlung ausgesetzt ist.

Contents

1. Catheter Selection Problem During Catheter Angiography

1.1. Motivation

Cardiac diseases have become the leading cause of death in the developed countries. In the developing countries, it has increased at a fast rate in the recent years [MPN*11]. According to the WHO survey [MPN*11], 31% deaths are caused due to the cardiovascular diseases (CVD) (see Figure 1.1). It is the leading cause of death all over the world. In 2008, 17.3 million people have died from CVDs where 7.3 million were due to coronary heart diseases. The survey shows that 80 % of CVD deaths took place in low and middle-income countries. It is forecasted that by 2030, almost 23.6 million people will die annually from CVDs.

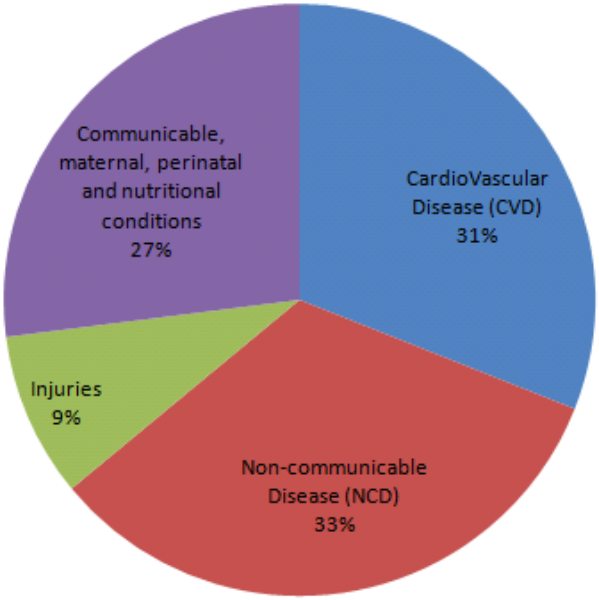

Figure 1.1.: Comparison of the major causes of deaths.

Atherosclerosis is the process in the blood vessels that results in coronary heart diseases and heart attack. In this process cholesterol and fatty materials are deposited inside the central cavity of the

arteries. Due to these fatty materials, the inner surface of the blood vessel becomes irregular and the lumen becomes narrow (see Figure 1.2). Due to this narrowness, it becomes difficult for the blood

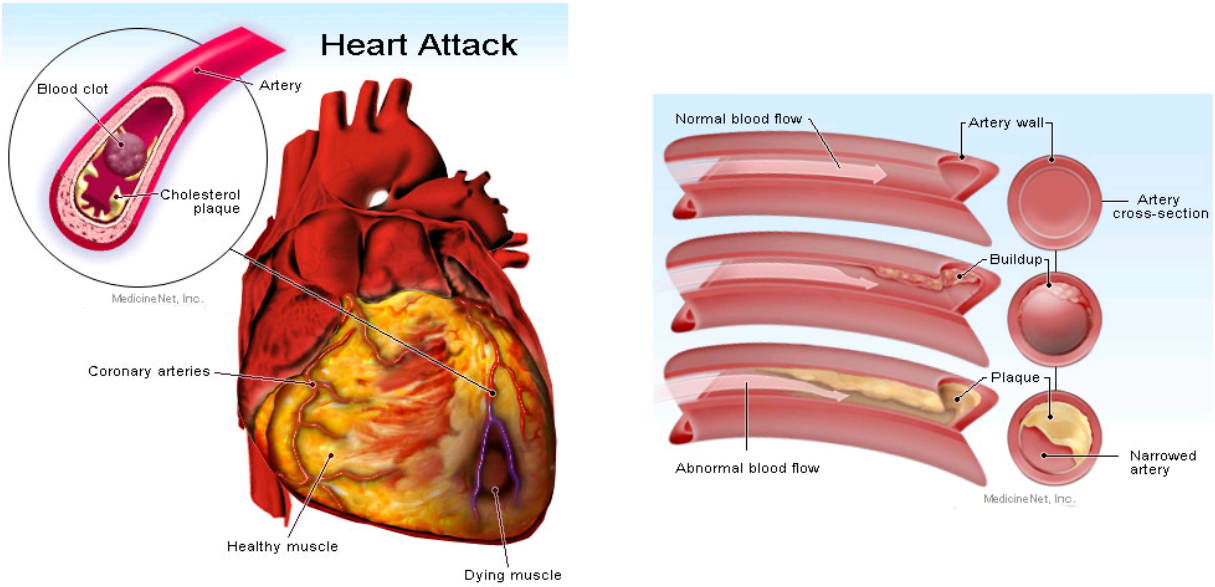

Figure 1.2.: Creation of blood clot in the arteries that causes heart attack.

to flow easily. Sometimes the plague ruptures and form a blood clot. This blood clot in coronary arteries causes heart attack. The coronary arteries diseases are diagnosed by going through catheter angiography. Catheter angiography is also called coronary angiography or coronary catheterization. It is a medical imaging technique used to visualize the arteries, veins and the heart chambers. It is performed to investigate the presence of any obstruction in the coronary arteries. During this process, a small incision is made in the upper thigh, and a small tube called catheter is inserted into the femoral artery and is threaded towards the aorta (see Figure 1.3). Then the contrast agent is injected through the catheter and is added to the blood in the small vessels. It renders the blood vessels more opaque and then clear images of the small vessels are obtained. Due to the anatomical variation of the aorta and coronary arteries in different humans, one common catheter cannot be used for all patients. The cardiologists test different catheters for a patient and select the best one according to the patient's anatomy. This procedure is time consuming and there is a slight chance of cancer from excessive exposure to radiation. It is also possible that a catheter -not matching the internal anatomy- punctures the artery and causes internal bleeding. It will be more helpful for the cardiologists to know in advance the optimal catheter before they actually start angiography. In this thesis, we will handle this problem and will suggest an image processing based patient-specific optimal catheter. In this chapter, we will introduce the basic concepts and will briefly explain coronary heart diseases, coronary angiography, variations in arteries' anatomy, catheters' variation and challenges during catheter selection. The chapter is organized as follows: In Section 1.2, cardiac diseases and its causes, and the diagnostic procedure is introduced. We

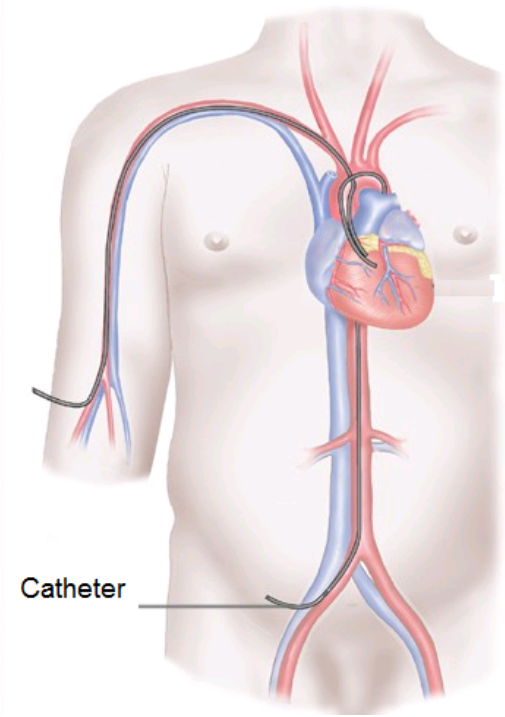

Figure 1.3.: Illustration of coronary angiography. A small incision is made in the upper thigh or arm, and a small tube called a catheter is inserted into the femoral artery and is threaded towards the aorta. Then contrast material is injected through the catheter and is added to the blood in the small vessels. It renders the blood vessels more opaque and then clear images of the small vessels are obtained using X-Rays [NHS12].

explain catheter angiography, the instruments (catheters and guidewires) used during the procedure and the catheter selection challenges that are faced during angiography. In Section 1.3, the catheter selection is explained. We discuss how human aorta and coronary arteries vary due to the aneurysm and stenosis. We also discuss the different anomalous cases of the coronary arteries. The variation in the coronary arteries and guidewire is also discussed. We explain why it is important to select an optimal catheter before starting the procedure and discuss the risks and problems that are faced during catheter selection procedure. In Section 1.4, we give an idea about how these challenges can be overcome by selecting an optimal catheter before starting the procedure. Summary of the chapter is given at the end.

1.2. Cardiac Diseases and Diagnosis

There are different types of heart diseases, but our focus is treatment of coronary arteries diseases using coronary angiography.

1.2.1. Coronary Arteries Diseases and Heart Attack

The heart is a muscular organ that pumps oxygen and nutrients to all parts of the body. Atherosclerosis is the process in the blood vessels that results in coronary heart diseases and heart attack. Atherosclerosis is a complex process that continues for many years. In this process cholesterol and fatty materials are deposited inside the lumen (central cavity) of the arteries. Due to these fatty materials, the inner surface of the blood vessels becomes irregular and the lumen becomes narrow (see Figure 1.2). Due to this narrowness, it becomes difficult for the blood to flow easily. Sometimes the plaque ruptures and forms a blood clot. This blood clot in the coronary arteries causes heart attack. The general factors causing the process of atherosclerosis includes physical inactivity, tobacco use, unhealthy diet and harmful use of alcohol. Catheter angiography is used to diagnose these cardiac diseases.

1.2.2. Catheter Angiography

Catheter angiography is also called coronary angiography or coronary catheterization. It is a medical imaging technique used to visualize the arteries, veins and the heart chambers. It is performed to investigate the presence of any obstruction in the coronary arteries. During angiography, a small incision is made in the upper thigh, and a small tube called a catheter is inserted into the femoral artery and is threaded towards the aorta (see Figure 1.3). Then contrast material is injected through the catheter and is added to the blood in the small vessels. It renders the blood vessels more opaque and then clear images of the small vessels are obtained using X-Rays. These images are called angiograms [LUM11].

Coronary angiography is useful for diagnosing different conditions and getting guidance for treatment. The results of coronary angiography are used to know whether there is a serious condition where the supply of blood is suddenly blocked due to blood clot. It is also used to investigate angina– a chest pain caused when the blood supply to the heart is restricted. It is also needed to investigate a heart disease when blood supply to the heart is blocked or interrupted by formation of fatty substances in the coronary arteries. Coronary angiography is used to investigate whether the arteries have been narrowed down and need widening using coronary angioplasty. Cardiologists perform angiography for artery bypass graft, which is a surgical procedure of diverting blood around narrow or clogged arteries to improve blood flow to the heart. It is also important for getting guidance for aortic valves replacement, which is a surgical process to treat problems affecting the aortic valve. In the next section we discuss the catheter selection problem.

1.3. Catheter Selection Problem

During catheter angiography, the cardiologists need to select an appropriate catheter for a patient. In this section, we explain the anatomical variation of the aorta and coronary arteries as well as the variation in the catheters' shape and show how this variation in the human anatomy and catheters make it challenging to select a proper catheter.

1.3.1. Human Anatomy Variation

There exist anatomical variations of the aorta and coronary arteries between different humans. This shape variation may be due to the age, height or weight. The aorta shape also changes due to some diseases like aneurysm or stenosis. There also exist variations in the structure of the coronary arteries, and some patients have an anomalous structure of the coronary arteries. In this section, we discuss these variations in the aorta and coronary arteries.

1.3.1.1. Normal Versus Abnormal Aorta

Sometimes the aorta deviates from its normal shape either due to aneurysm or stenosis. An aortic aneurysm is the concept of swelling of the aorta. This represents some weakness in the wall of the aorta. Aortic stenosis or coarctation is the concept of narrowing of the aorta (see Figure 1.4). These different conditions affect the catheter selection decision.

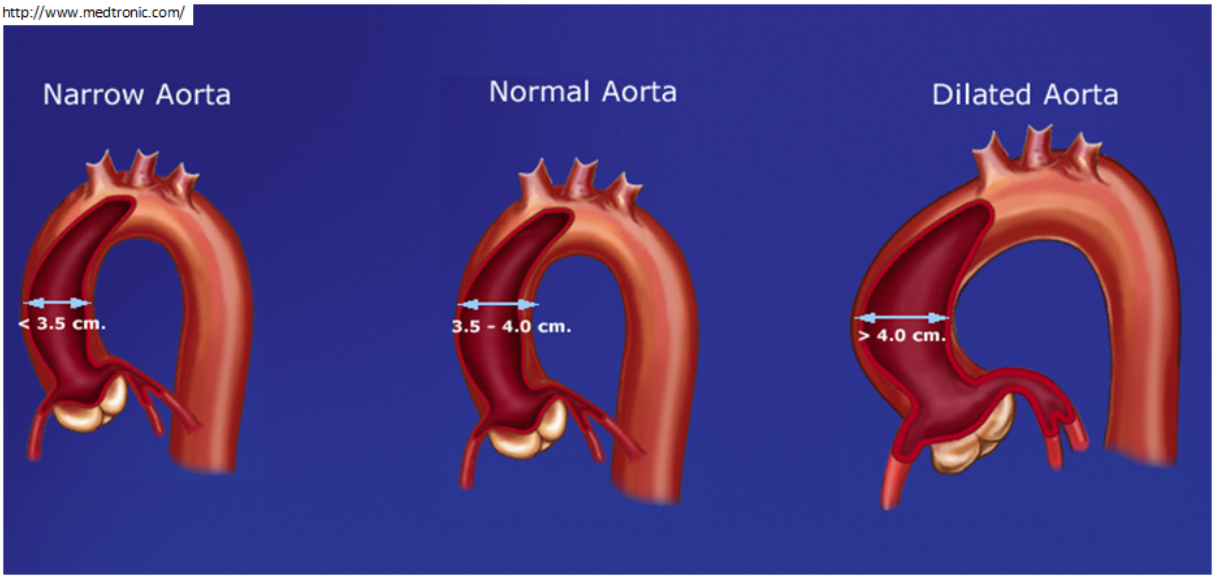

Figure 1.4.: Anatomical variation of the aorta due to aneurysm and stenosis.

1.3.1.2. Coronary Arteries Takeoff

Coronary arteries depart from the aorta and the position and the angle of the depart of the coronary arteries is called takeoff. It is very important to know about the takeoff of the coronary arteries. The nature of the takeoff plays a significant role in the catheter selection. If the coronary arteries depart the aorta at an abnormally high distance above the aortic valves, then such takeoff is called a high takeoff (see Figure 1.5 A). Another takeoff is a horizontal takeoff i.e., a takeoff which is at right angle to the ascending aorta (see Figure 1.5 B). A takeoff that makes an angle less than 90 degrees is called inferior takeoff (see Figure 1.5 C) and a takeoff with an angle greater than 90 degrees is called superior takeoff (see Figure 1.5 D).

1.3.1.3. Anomalous Origin of the Coronary Arteries

There exist cases where the origin of the coronary arteries deviates from the normal origin. Trivellato et al. [TAL80] have defined the following criteria for the normality of the coronary arteries.

- The two normal aortic origin points are the right and left ostia.
- The right coronary artery follows the atrioventricular groove.
- The left atrioventricular groove and anterior interventricular groove are followed by the course for the left coronary artery.
- The posterior descending branch originates from either the right or left coronary artery.
- The coronary arteries terminate at the myocardial capillary level.

We are restricting our discussion to the variation based on geometry and not function. We are only interested in the geometrical variations because these affect the catheter selection decision. The common anomalies are as follows:
Normally, there are two coronary cusps from which the coronary arteries arises but in some situations, there is one cusp from where the right coronary artery arises. The left coronary artery arises from pulmonary artery. In normal cases, right coronary artery originates from right atrioventricular groove, but in some cases it may originate from the left ostium. Kosar et al. [PK09] in his study found that in some cases the sinus node artery (SNA) originated from the right coronary artery (RCA) or from the circumflex artery (Cx) or from the left main coronary artery (LMCA). Sometimes SNA originates from the right sinus valsalva with a separate ostium. In some cases the left main coronary artery is absent. In Figure 1.6 the left main coronary artery is absent, and the left anterior descending and circumflex artery originate from the left coronary sinus with separate ostia. In Figure 1.7 the right coronary artery originates from the left coronary sinus. In Figure 1.8 the left main coronary artery originating from the right coronary sinus and following prepulmonic course. The sinoatrial node artery originates from an anomalous left main coronary artery. In Figure 1.9 (open arrow) the left main coronary artery originating from the right coronary sinus. Kimbiris et al. [KISB78] have presented a study of the anomalous origin of the coronary arteries. A summary of their study is given in Figure 1.10.

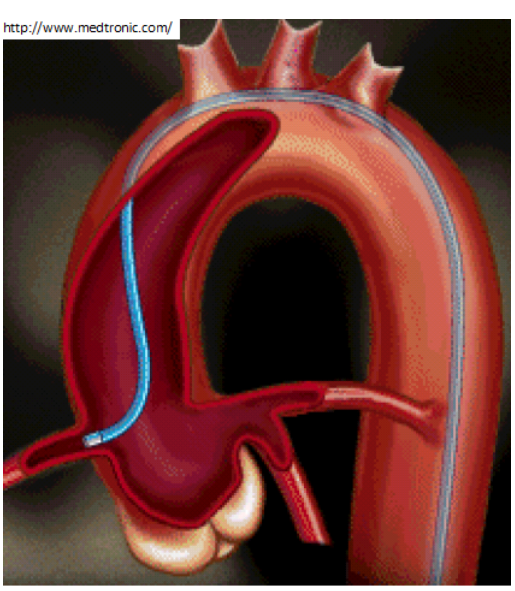

(a) High takeoff: Coronary artery departs the aorta at an abnormally high distance (> 1.5 cm) above the aortic valve.

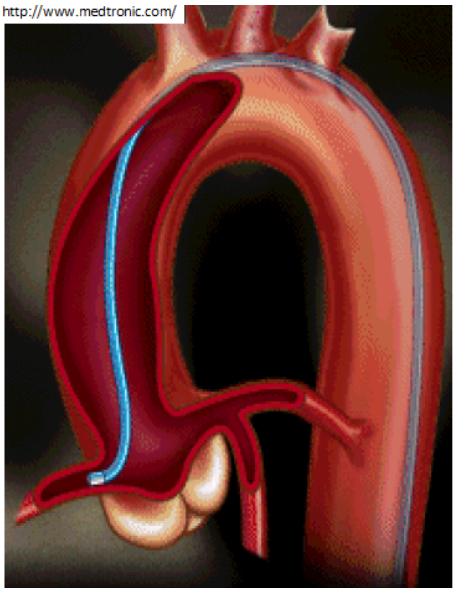

(b) Horizontal Takeoff: Coronary artery departs at right angle from the ascending aorta.

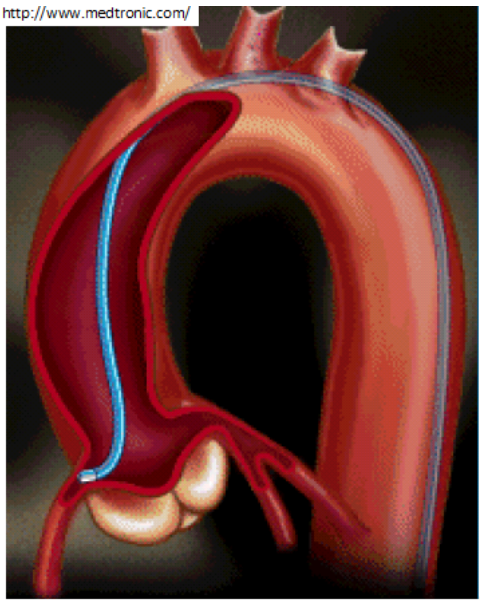

(c) Inferior takeoff: Coronary artery departs from the ascending aorta making an angle less than 90 degree.

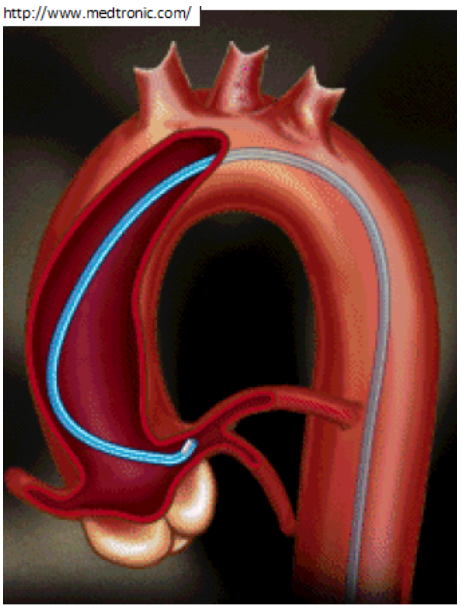

(d) Superior takeoff: Coronary artery departs from the ascending aorta making an angle greater than 90 degree.

Figure 1.5.: Different types of the coronary arteries' takeoff from the ascending aorta.

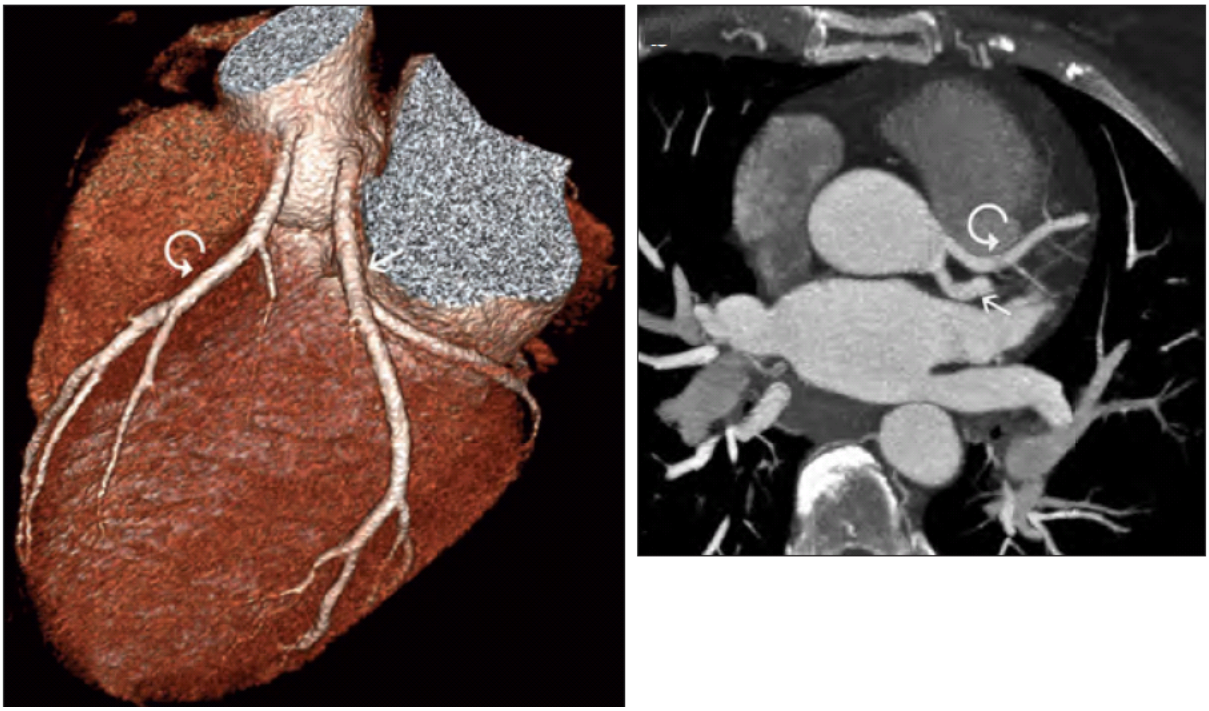

Figure 1.6.: In this anomalous case, left main coronary artery is absent and the left anterior descending (LAD) (curved arrow) and circumflex artery (arrow) originates from the left coronary sinus with separate ostia [PK09].

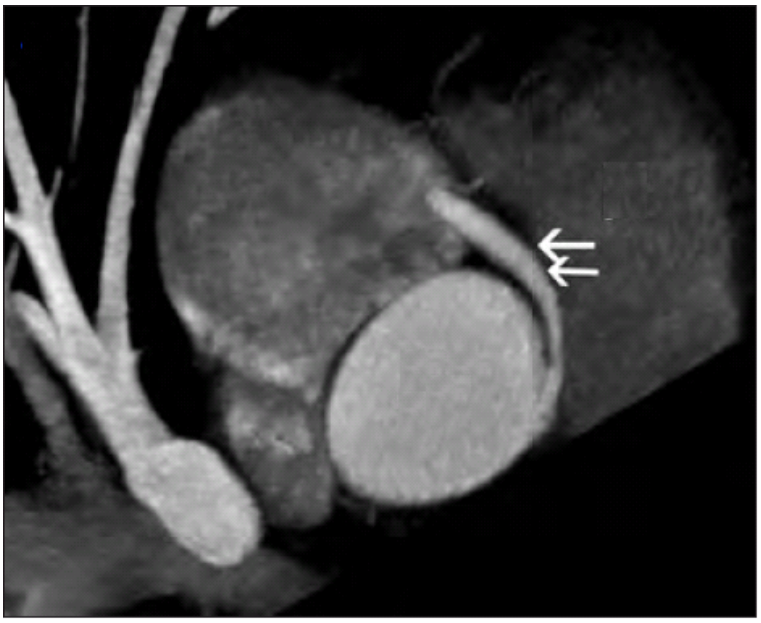

Figure 1.7.: Anomalous right coronary artery: The right coronary artery (double arrows) originates from the left coronary sinus [PK09].

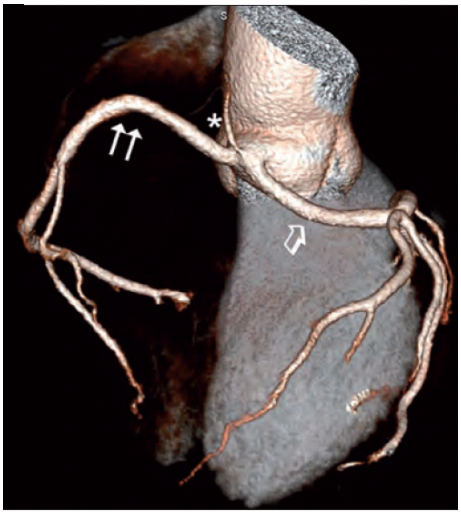

Figure 1.8.: Anomalous left coronary artery: The left main coronary artery (open arrow) originating from the right coronary sinus and following prepulmonic course. The sinoatrial node artery (asterisk) originates from the anomalous left main coronary artery [PK09].

Figure 1.9.: Anomalous left coronary artery: Left main coronary artery (open arrow) originating from the right coronary sinus [PK09].

These variations in anatomies as well as the presence of anomalous cases make the selection of an optimal catheter difficult.

1.3.2. Catheters and Guidewires Variation

Catheters and guidewires are used to transfer a contrast agent to the location of interest during coronary angiography. Catheters are small tubes inserted into the femoral artery and pushed inside the aorta towards the coronary arteries. These are made of varieties of polymers which include silicone rubber, latex, and thermoplastic elastomer. Guidewires are made of steel and are used to provide additional stiffness to the catheters for successful insertion of catheters. Guidewire helps to make the curved catheter straight so that it can be pushed towards the aorta lumen. There is a large number of catheters (more than 300), some are shown in Figure 1.13. There are also different types of guidewires. Catheters and guidewires vary in diameter, stiffness, tip shape, and length.

Diameter

Catheters and guidewires vary in diameters. The diameter is usually represented by the French units of measurements. It is commonly abbreviated as Fr. The higher the number, the larger the diameter of the catheter. The diameter of a round catheter can be determined as $D(mm) = Fr/3$. The diameter should be as small as possible to accomplish the task. In Figure 1.12 the different available diameter ranges for the catheters are shown.

Length

ANOMALOUS CORONARY ARTERIES/*Kimbiris et al.*

Anomaly	No. of patients	CAD	Aortic valve disease	Mitral valve prolapse	IHSS	Misc	No heart disease
LCF from RSV	26	6	7	2	1	4	6
Both coronary arteries from LSV	12	2	2	2		3	3
Both coronary arteries from RSV	4	2					2*
LAD from RSV	2				1	1	
First septal perforator	1	1					
Total	45	11	9	4	2	8	11

*One patient had an acute myocardial infarction.
Abbreviations: CAD = coronary artery disease; LCF = left circumflex artery; LSV = left sinus of Valsalva; RSV = right sinus of Valsalva; LAD = left anterior descending artery; IHSS = idiopathic hypertrophic subaortic stenosis; Misc = miscellaneous.

Figure 1.10.: Anomalous coronary arteries [KISB78]

The length of the catheter and guidewire should be long enough so that it reaches the target position. The catheters' length ranges from from 65 to 100 cm.

Tip shape

Catheter tip is designed for a particular task. The nature of the tip's curve angle, curve length and number of curves represent the purpose of a catheter.

Stiffness

Catheters vary not only in shape but also in stiffness. Softer catheters lead to fewer complications, but sometimes it becomes very difficult to catheterize some arteries without a certain level of stiffness for the catheters. We have measured different segments of each catheter and have found that the same catheter has different levels of stiffness at different segments (see Chapter 4, Table 4.8).

1.3.3. Catheter Selection Problem

Due to the anatomical variation of the aorta and coronary arteries in different humans, one common catheter cannot be used for all patients. The cardiologists test different catheters for a patient and select

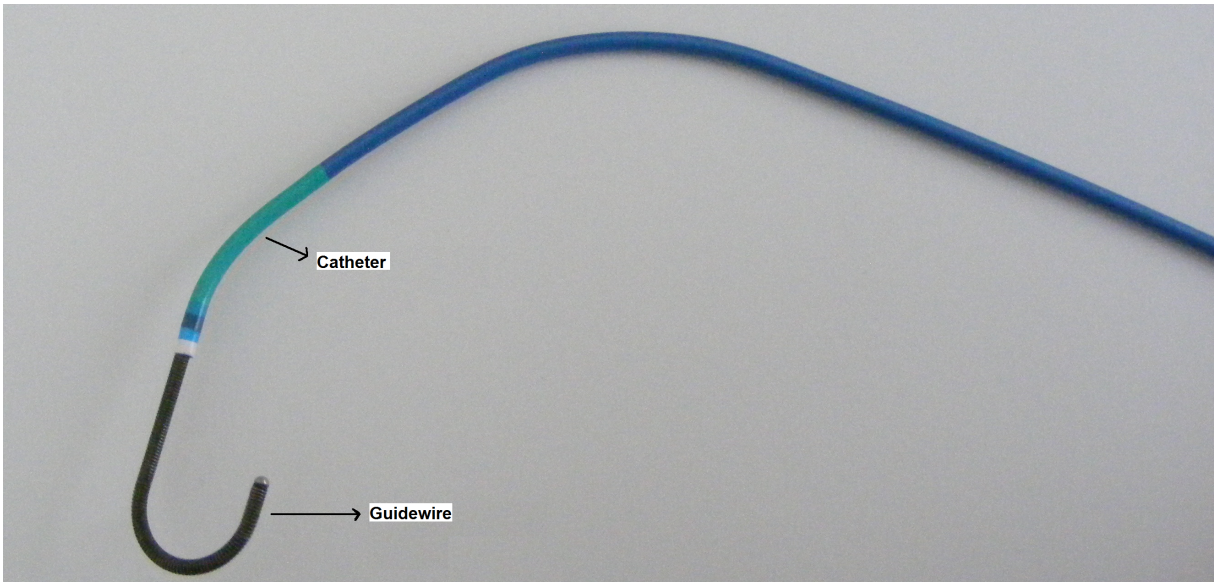

Figure 1.11.: Catheter and Guidewire.

the best one according to the patient's anatomy. This procedure is time consuming and there is a slight chance of cancer from excessive exposure to radiation. It is also possible that a catheter -not matching the internal anatomy- punctures the artery and causes internal bleeding. It will be more helpful for the cardiologists to know in advance the optimal catheter before they actually start angiography. In the next Section, we give our idea for solving this problem.

1.4. Proposed Solution: Image Processing Based Patient-Specific Model for Catheter Selection

In this thesis, a technique based on image processing, is suggested for catheter selection. This technique will enable cardiologists to have patient-specific catheter suggestions before starting angiography. The only requirement for this system is to have patient's MR/CT data before starting angiography. The required arteries i.e., the aorta and coronary arteries will be segmented from these image data. In the next step, some clinically important geometric parameters will be computed from the segmented images. At the same time, clinically important geometric parameters will be computed from all the available catheters. Based on these parameters from the patient image data and parameters from the catheters, a model will be developed that will be able to suggest few optimal catheters for a given patient. These few choices will be further refined by a simulation model. The contribution in this thesis include *an automatic segmentation model for the aorta and the coronary arteries, automatic computation of the geometric parameters from the segmented image data, a geometric parameters*

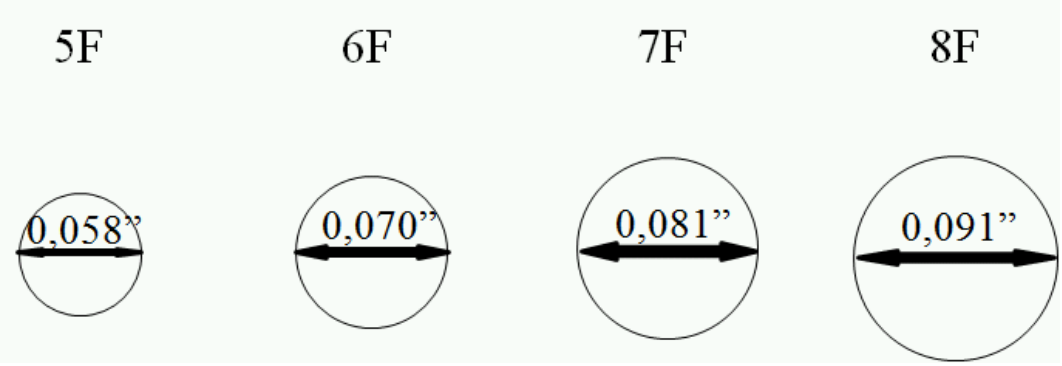

Figure 1.12.: The different available diameter ranges for the catheters.

based model for reducing the catheter choices and a simulation based model for refining the reduced choices.

1.5. Summary

In this chapter, challenges of “catheter selection during coronary angiography” were discussed. We presented the challenges faced during coronary angiography due to the variation of human anatomy and catheters’ variation. We discussed how the aorta and coronary arteries very in different humans and also discussed the variation in catheters. In the end, we talked about the risks of selecting incorrect catheter and suggest an image processing based catheter selection procedure. In the next chapter, the current approaches related to catheter selection will be presented, and the details of our procedure will be given in Chapter 3.

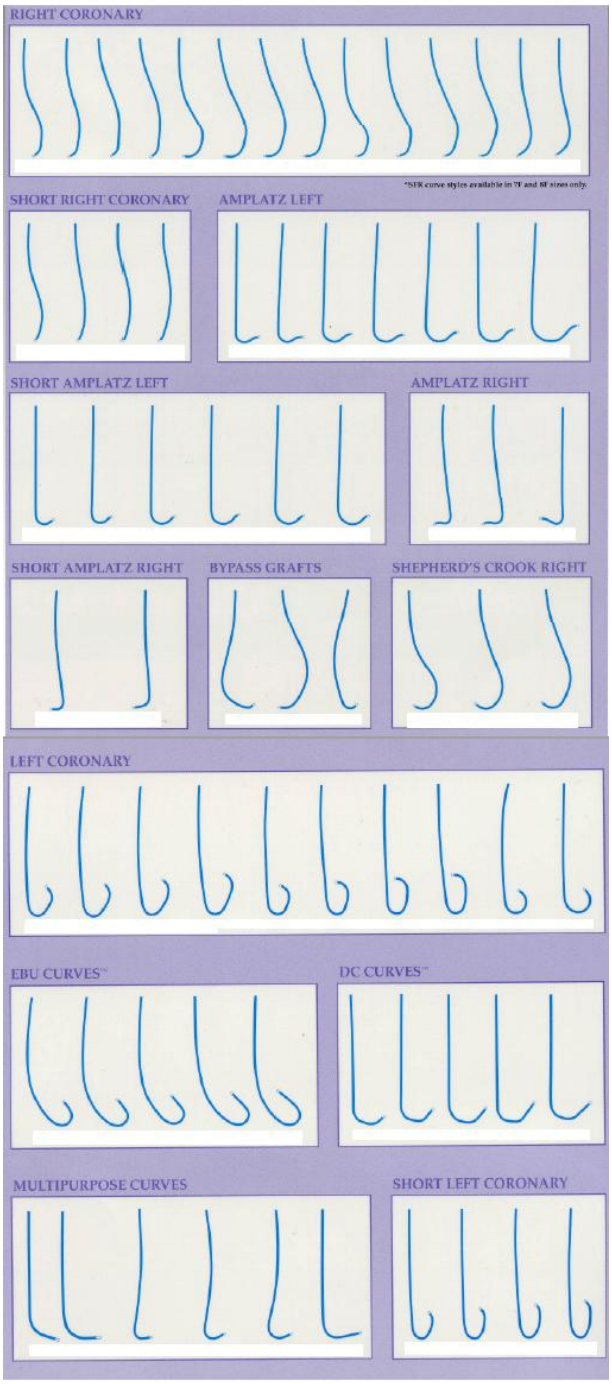

Figure 1.13.: Various types of catheters.

2. Related Work

2.1. Introduction

The goal of this thesis is to assist cardiologist selecting an optimal catheter before starting angiography. This image processing based catheter selection technique will help cardiologists to avoid the process of *trial and error* based catheter selection and will also reduce the chances of internal arteries' injuries. The idea of an image processing based catheter selection model is to acquire MR/CT data of a patient before starting angiography; obtain patient's anatomical information from these images; and suggest an optimal catheter according to the patient's anatomy. A two step approach will be followed for suggesting an optimal catheter. In the first step, rigid parameters will be defined from the patient image data and parameters from the catheters, and these parameters will be used to reduce the large number of choices to few choices. In the second step, these reduced number of catheters will be simulated to find an optimal catheter. This image processing based catheter selection algorithm is accomplished following a series of sub tasks. The first step is segmenting the aorta and coronary arteries from the images. The next step is skeletonization and centerline extraction. Then some geometric parameters will be computed from the segmented images and parameters from the available catheters will be defined. Then a parameter based model will be defined to reduce the large set of catheters' choices. The last step will be simulating the reduced number of catheters and finally finding an optimal catheter choice. In this chapter, we will present a survey of the available literature related to each of the above steps of our procedure. This chapter is organized as follows: In Section 2.2, we will introduce the current approaches related to the aorta and coronary arteries segmentation. The available skeletonization algorithms will be presented in Section 2.3. In Section 2.4, we will present a survey of the medical literature related to general catheter selection approaches. In Section 2.5, it will be discussed whether any patient-specific catheter selection strategy is available in the literature. A survey of the catheter simulation will be presented in Section 3.5. At the end, we will give a summary of the areas where we need either an extension of the current work or need new approaches.

2.2. Arteries Segmentation

The first step of an image processing based catheter selection approach is arteries' segmentation. A lot of work has been done related to the aorta and coronary arteries segmentation. The imaging protocol used by our clinical partner dictates that the planning has to be performed on specifically acquired MRI data. On one hand, a low resolution 3D data set covering the complete ascending as well as large parts of

the descending aorta is acquired. And on the other hand, a high resolution data set containing only that part of the aorta where the ostia are located, is provided. The combination of the information contained in these two MRI data sets serve as the basis for the computation of several geometrical parameters. In this section, we will explore the available literature for the aorta and the coronary arteries segmentation, and we will discuss whether the existing approaches can be used in our problem.

2.2.1. Aorta Segmentation

Aorta segmentation has been remained an active research field for long time. In the literature, there exist different approaches for the aorta segmentation. There exist semiautomatic and automatic approaches. We present common approaches that have been used for the aorta segmentation.
A region growing based algorithm is presented by Pohle et al. [Poh01]. In this approach, the algorithm learns its homogeneity criterion automatically from characteristics of the regions to be segmented. In the presented algorithm, parameters of the homogeneity criterion are estimated from sample locations in the region. Another algorithm combining local watershed transform and the region based deformable model, is presented by Tek et al. [TAA05]. In this approach, first watersheds are computed in the whole image, and then the regions are merged, and segmented structures are computed. Wink et al. [WNV00] present a technique for vessels segmentation. In this approach, after the manual determination of at least two initial points of the central vessel axis, an iterative tracking process is started. In every iteration, the vessel axis is extended by one point. At this candidate position, a plane perpendicular to the central vessel axis is constructed. From this point, a number of rays are cast until the border of the vessel is encountered (see Figure 2.1). This method is good in condition where there is high contrast but with low contrast it will be unable to mark the boundaries. A two level thresholding algorithm of Sauer et

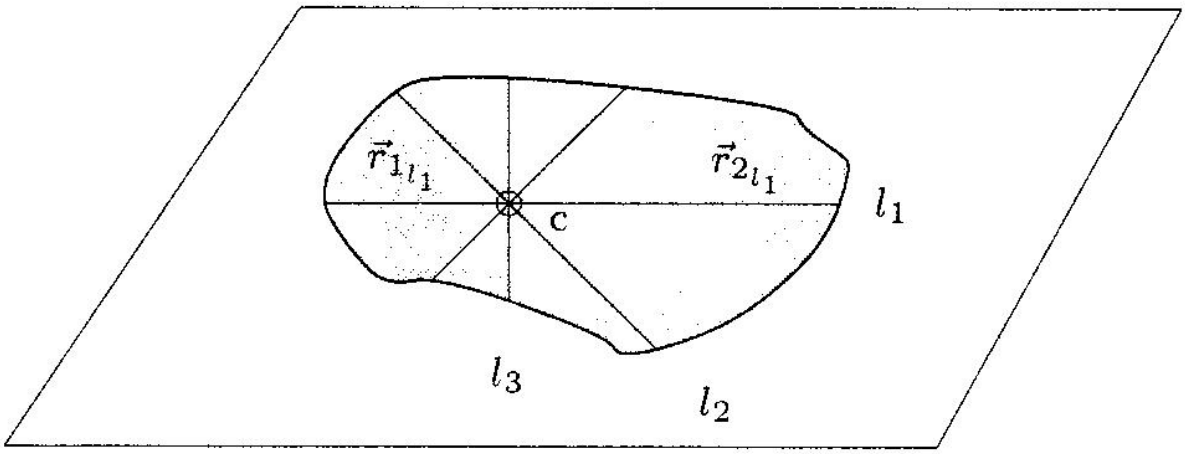

Figure 2.1.: Vessel segmentation: Based on a user defined starting point, a number of rays are cast until the border of the vessel is encountered [WNV00].

al. [SKB*08] needs user interaction for the two thresholding levels (see Figure. 2.2).

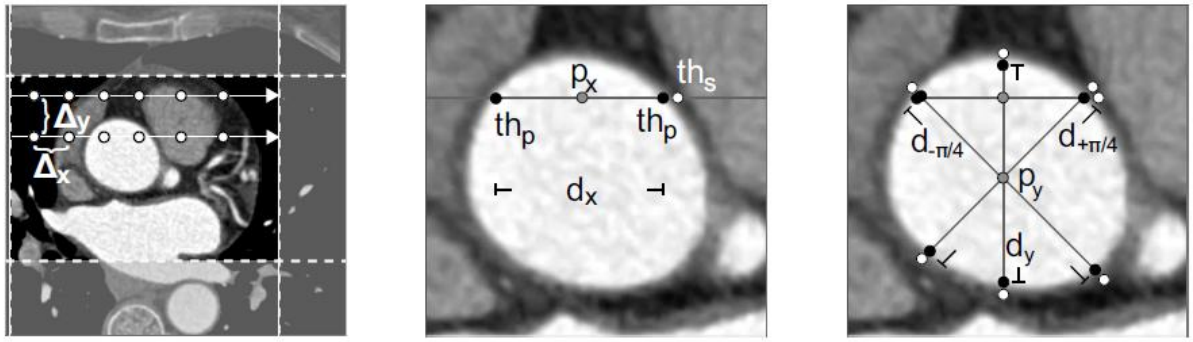

(a) VOI and ray propagation (b) Extension in x-direction (c) Candidate point p_y

Figure 2.2.: Detection of the ascending aorta. Within a predefined volume of interest (VOI), search rays are propagated (a) following a two-level threshold approach to compute the extension in x-direction (b) and afterwards in y-direction as well as in direction of the two angle bisectors (c). If geometric constraints are fulfilled, the point p_y is added to the list of ascending aorta candidates [SKB*08].

A neural network based method for the aorta detection in magnetic resonance images is presented by Katz et al. [KM90]. In this method, the network is trained with hand-drawn masks using the back propagation algorithm. Then multiple neural nets are created, and a final neural net is trained to incorporate the output of a primary target detector. Using Marginal Space Learning (MSL) for segmenting the aorta, is presented by Zheng et al. [ZJL*10, JLZ*10]. In this method, discriminative learning is applied to train a detector. Rueckert et al. [RBF*97] presents an automatic tracking of the aorta using MR images. It is a stochastic relaxation based method for the aorta segmentation. In this approach, they first consider a rough estimate of the location and diameter of the aorta which is obtained by applying a multi scale medial-response function using the available *a-priori* knowledge. In the next step, they refine this estimate using an energy-minimizing deformable model which is defined in a Markov-random-field (MRF) framework. The disadvantage of the method is finding the proper values for the optimization function, and the method is sensitive to noise. It takes three minutes for segmentation. A generalized cylinders based vessel axis extraction and border estimation model is presented by Verdon [VBM*96]. In this method, first an initial vessel axis is initialized manually and then slices are extracted from the 3D data volume perpendicular to this axis. Blood vessel contours are extracted with maximum gradient position. A Kalman filter based 3-D cylindrical parametric intensity model is developed by Wörz and Rohr [WR07, WvH*10]. This model needs user interaction for the initialization. A model-based segmentation is proposed by Kovacs [KCA*06b, KCA*06a]. Here, the centerline is generated using Hough transform (see Figure 2.3) and then an initial rough deformable model is generated using the aorta centerline and diameter. This initialization is then optimized using the mass-spring analogy as described in [Zse05]. It takes six minutes for the segmentation.

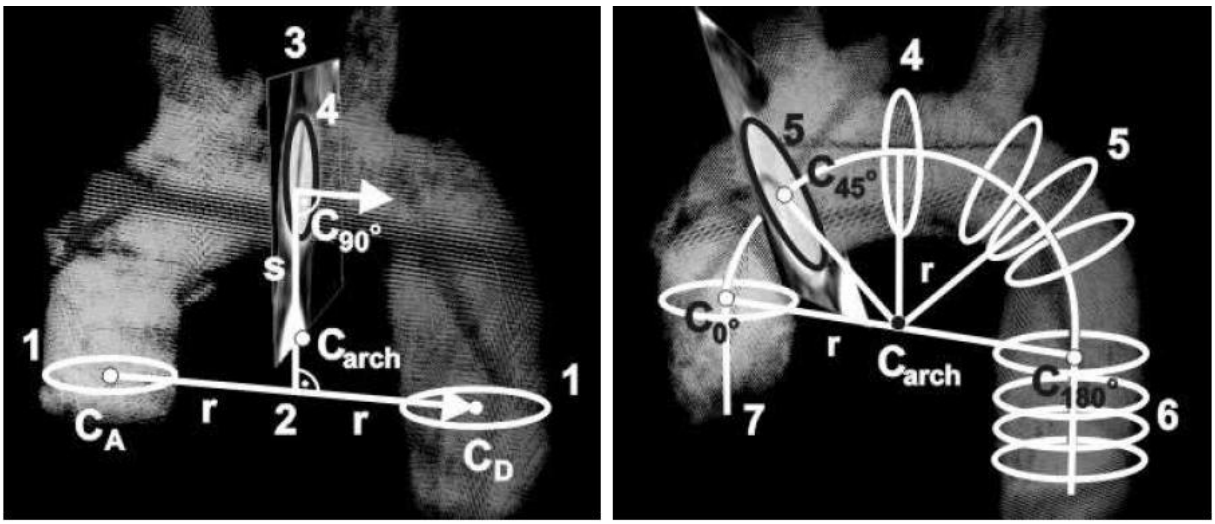

Figure 2.3.: Model based segmentation: (a) The three initial circles estimates the parameters of the aortic arch. (b) the aortic arch refinement [KCA*06b]

Deformable models are effective models for segmenting anatomic structures. These models exploit information derived from the image data together with *a-priori* knowledge about the location, size and shape of these structures. Deformable models were first proposed by Kass et al. [KWT88] for segmenting the contour of 2D images. These models are based on an initial estimate, and the model is deformed by minimizing its energy function. The energy function has two major terms. The internal energy characterizes the bending deformation, and the external energy characterizes the image forces that attract the model towards the features. A survey about the deformable models for medical image analysis is by McInerney and Terzopoulos [MT96]. An automated segmentation method for the segmentation of the aorta in 4D (3D+time) cardiovascular magnetic resonance (MR) image data is presented by Zhao et al. [ZZW*06]. This method combines the level set and optimal surface segmentation algorithms. This algorithm tries to determine the final aortic surfaces in all 16 cardiac phases in a single optimization process. Deschamps et al. [DC02] presents an approach based on Fast Marching and level sets method for vessels and vascular trees. They especially consider thin structures and modify the front propagation such that the front propagation freezes close to the boundaries and propagate only in the small area along the arteries.

2.2.2. Coronary Arteries Segmentation

Coronary arteries are the two blood vessels that originate from the aorta. These arteries carry oxygen-rich blood to the heart muscles. Coronary arteries have been extensively studied due to its significance

related to cardiac diseases. There are many algorithms developed for the coronary arteries segmentation. The work of Lorenz et al. [LRSB03] for coronary arteries segmentation uses front propagation approach. It can extract all major branches of the coronary arteries. The segmentation needs to select the seed point for each coronary artery. The Corkscrew algorithm [WF04] for the coronary arteries segmentation can be considered as a variant of the region-growing algorithm. On a locally thresholded image, linear search paths, cycling standard 3D directions, are followed until the vessel wall is found. The algorithm requires the definition of the start point and end point of the centerline path. Hennemuth [HBF*05] proposes a method where the user has to select a seed point above the branching points of the coronary arteries, and then the coronary arteries are segmented using region growing method. An automatic coronary artery segmentation in X-ray images is described by Fallavollita [FC06] where a 4-step filter is suggested in order to enhance vessel contours. In the first step, a homomorphic filter used to denoise the fluoroscopic image. In the second step, the Perona-Malik anisotropic diffusion method [PM90a] is used to reduce and remove both noise and texture from the fluoroscopic image. In the third step, shock filter is used that results in a robust and stable deblurring process. Wang [WL09] proposes a fully automated level set based method for CT data which needs parameter tunning. In their approach, the main branches of the coronary arteries are extracted from the volume data sets by using a localized region-based level set framework [Yan06]. In the next step, calcified voxels are removed by a post processing step. The centerline of the coronary arteries is extracted by a mesh contraction algorithm [ATC*08]. Shoujan et al. [SJYW10] presents an automatic segmentation of coronary angiograms based on fuzzy inferring and probabilistic tracking. The segmentation is done in two steps. In a preprocessing step, multi scale Gabor filtering is used to enhance vessel features. In second step, a seed point is selected using the vessel features map. Then two operators, a probabilistic tracking operator (PTO) and a vessel structure pattern detector (SPD) work together based on the detected seed point to extract vessel segments or branches one at a time. An automatic 3D segmentation of the coronary arteries, based on mathematical morphology is presented by Bouraoui [BRB*08]. This method uses an *a-priori* anatomic knowledge related to the coronary arteries, in particular their size, their position (near the heart surface), and their initial point (on the aorta). The coronary arteries origins are detected using the fact that circular objects on the wall of the aorta are coronary arteries. Then region growing is used to proceed with coronary arteries segmentation.

2.2.3. Discussion

In this section, we presented different approaches for the aorta and coronary arteries segmentation. Many of these methods require very high resolution of images. Some of the above methods need manual interaction. In our case, we have two data sets of input images. One data set contains the complete aorta, and the second data set contains coronary arteries along with that part of the aorta near coronary arteries. Currently, there is no direct approach that automatically segments aorta and coronary arteries. In our approach,*we will be using fast marching method used in the work of Deschamps et al. [DC02] for the aorta and coronary arteries segmentation. For seed point selection, the concept presented in Kovacs [KCA*06b, KCA*06a] will be applied with some modification. Combining these*

different approaches will enable us to develop a fully automatic segmentation algorithm for the aorta and coronary arteries.

2.3. Arteries Skeletonization

The extraction of arteries' centerlines is an important step for the quantification of stenosis, topological representation, virtual endoscopy and visualization of the vascular network. Skeletonization is a process for reducing foreground regions in a binary image to a skeleton that preserves the extent and connectivity of the original region while throwing away most of the original foreground pixels. Thinning of binary images is an iterative process which erodes an object layer by layer until only a skeleton of the object remains. There have been many algorithms for creating a skeleton from a binary image. Some are very general, and some are specific to arteries. Here we give a review of algorithms that are used for creating centerline of the image contents. Benoit et al.[AAE*10] presented a thinning algorithm based on translated distance transform. It adapts an existing distance driven homotopic algorithm to perform skeletonization. A 3D thinning algorithm is proposed by Ma and others [MS96]. They propose a connectivity preserving fully parallel 3D thinning algorithm. They have described the sufficient conditions to prove a 3D thinning algorithm to be connectivity preserving. Kriete et al. [KS96] proposes a method that uses the gravity point of the vessel to guide the medial axis tracking process. An algorithm, preserving the topological and geometrical condition is presented by Lee et al. [LKC94]. It extracts the medial axis from 3D binary images. A coronary arteries specific thinning algorithm is presented by Higgins el al. [HSKR96]. This algorithm uses a series of image processing filters that involves user interaction. Egger et al. [EMGF07] have presented an algorithm that creates an initial centerline based on two user defined start and end points. For curved vessel structures, this initial centerline is computed by Dijkstra's shortest path algorithm. The start and the end point are directly connected for linear vessel structures. Thereafter, this initial path is aligned in the blood vessel that results in the vessels centerline. A topologically invariant skeletonization is presented by Bouix [BS00] and Malandain [MBA93]. This method uses segmented images. It first computes the distance transform [Bor84] of the object. In the next step, the divergence of the distance transform gradient is computed. Then the image is thinned by removing the simple points ordered by decreasing divergence. In the method presented by Eberly [EGM*94], the sub-voxel centerlines is extracted as ridges [EGM*94] of the image intensity. In this method, the gradient and the Hessian matrix is used to interpolate the zero-crossings of the gradient vector in the cross-sectional directions. A Multi-scale centerline detection algorithm is based on the work of Lindeberg [Lin96] and Krissian [KMA*00]. This method uses an integration of the gradient information and the circles of radii in the cross-section and finds points located at equal distance from the contour. A cluster based algorithm is presented by Ferchichi et al. [FW06]. This algorithm extracts the centerlines of 2D and 3D objects, based on clustering. The algorithm computes the centerline from all points of the object in order to remain faithful to the structure of the shape. The idea is to cluster a data set constituted of the points composing the object and their relative distance transforms. The centerline is derived from the set of computed clusters. In the work of Krissian [KMA*00] different centerline extraction algorithms are compared. In this survey, three methods i.e., Topological invariant

	Under 10 kg	10-20 kg	Over 20 kg
Needles	22 gauge Angiocath, 20 gauge Longdwel	20 gauge Potts, 18 gauge Longdwel	18 gauge Potts
Wires	.018 inch	.025 inch	.035 inch
Catheters	0.038-.041 inch (diameter)	.047-.055 inch (diameter)	.062-.066 inch (diameter)

Table 2.1.: Recommended needles, wires and catheters based on patient's weight.

skeletonization, Subvoxel gradient zero-crossings and Multi-scale centerline detection are compared and the strong and weak points of every method is given.

We tested different algorithms on 3D MR and CT images. Among these algorithms, the one presented by Lee [LKC94] was very fast and was able to successfully create the 3D skeleton of the aorta and coronary arteries. Therefore, in our project, we selected this thinning algorithm.

2.4. Non-image Processing Based Catheter Selection

2.4.1. Introduction

In medical literature there exist approaches for catheter selection that are not patient-specific. Literature related to optimal catheter selection discusses the general concepts about the shape of the aorta and coronary arteries and suggestions about suitable catheters.

2.4.2. Literature About General Anatomies and the Recommended Catheters

In the work of Schneider [Sch03] on catheter selection, a detailed study of different types of catheters has been presented. In this work, the different choices of guidewires and guidewire handling techniques have been discussed. He explains how catheters and guidewires are different from each other (see Figure 2.4) but he presents the very general conditions and the recommend catheters. A study about catheter selection in infants and children is presented by Kirks and others [KFHN76]. They have presented the results of their study related to needles, wires and catheter selection in infants and children. They have given a guide for catheter selection, flow rates, and contrast dosage for abdominal angiography in the pediatric patient. The selection of needle, guidewire, and catheter for pediatric angiography is based on the weight of the patient (see Table 2.1) [Sch03]. The study of Kimbiris et al. [KISB78] is a clinical study of the anomalous origin of the coronary arteries. Although the objective of the study was not the catheter selection problem, this study gives an idea of the challenges of selecting an optimal catheter. The study shows that these anomalous cases are also needed to be considered when selecting a catheter. Brinkman and others [BBN*94] have published results of a study on the variability of human coronary artery geometry. They have described a computer-based system to mea-

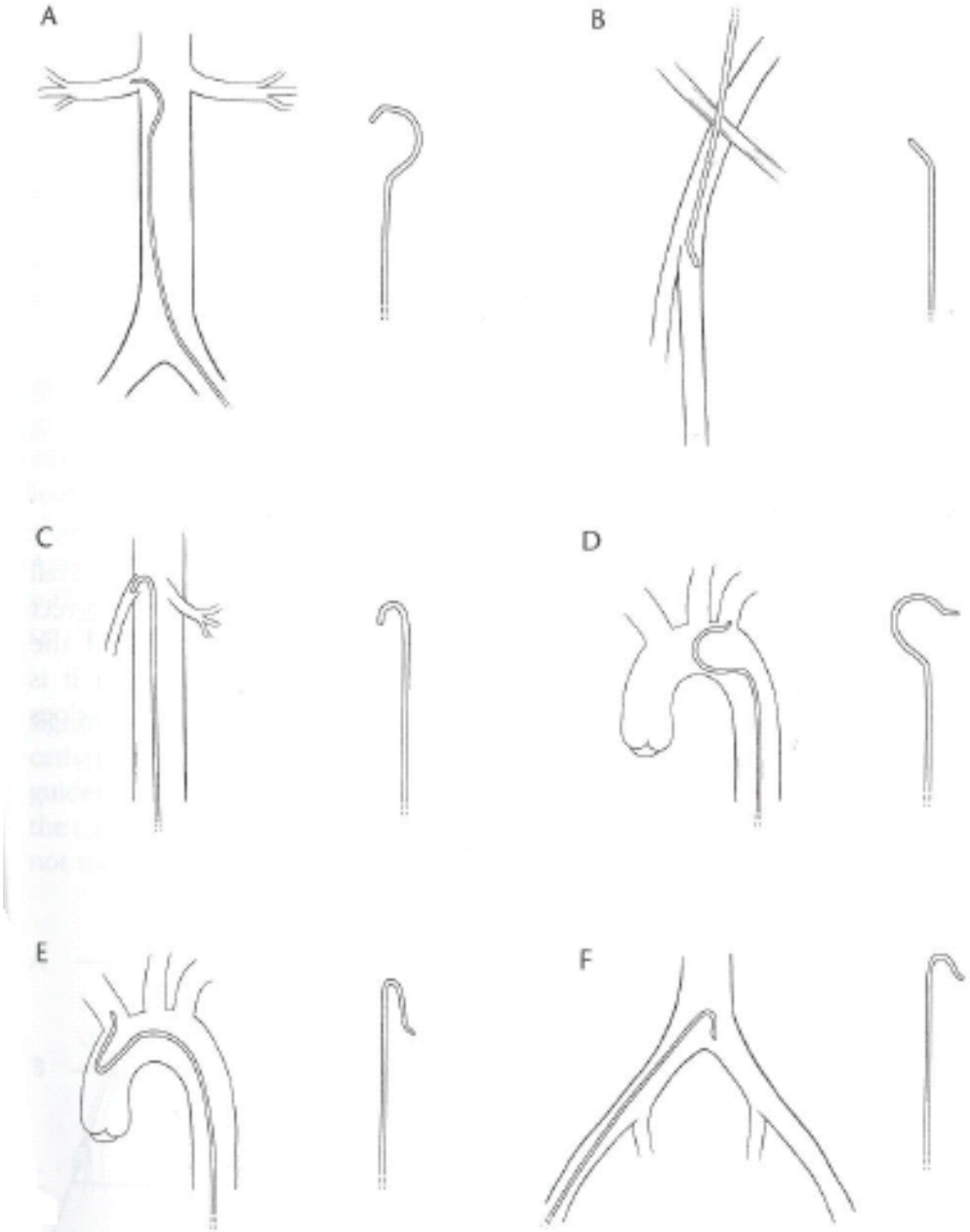

Figure 2.4.: Catheters' variation: A cobra catheter is used for renal artery catheterization (A), A Berenstein catheter is uded for cannulation of the superficial femoral artery (B), A tightly curved hook-shaped cather is used for catheterization of the visceral arteries (C), A headhunter catheter can be used to enter the branches of the aortic arch (D). A Simmons catheter is used to cannulate the carotid and innominate arteries (E), A shepherd'hook catheter is used to cross the aortic bifurcation (F) [Sch03].

sure the geometric parameters of arteries from angiograms. They have focused on the distribution of the geometric parameters of the left anterior descending coronary artery (LAD) and its first two major branches. The derived parameters include the angle between the left circumflex artery and the LAD; the angles between the LAD and its early diagonal and septal perforator branches and distances between branch points. No relation between geometric parameters and age or gender was seen. This study is not done for best catheter selection but it gives us an idea about the geometry variation that is needed to be considered during the catheter selection process. A general discussion about the guiding catheter selection for the right coronary artery angioplasty is given by Myler [MBCS90]. In this study they point out several parameters about the right coronary artery and catheters (see Figure 2.5 and Figure 2.6). They consider right coronary artery angle and the height of the right coronary artery ostium and the degree of anterior or posterior orientation. The recommendations in this study are not patient-specific and more than one option is suggested. This study leads to the idea of a patient-specific catheter selection by first computing patient-specific parameters and then select a catheter based on these parameters. Guiding catheters for right coronary angioplasty are shown in Figure 2.6. Voda and others [Vod92] present their study about catheter selection for left coronary artery. In this study, different geometric parameters have been pointed out that are important for catheter selection. Some of these parameters are the angles of the coronary arteries with the aortic wall, angle of left coronary arteries and the amount of back up support (see Figure 2.7). The study is not about patient-specific catheter but give us an idea about the important parameters that should be considered for patient-specific catheter selection for the left coronary artery. The study of Sarkar et al. [SSK09] is related to catheter selection for coronary angiography and intervention in an anomalous right coronary artery. In this study, a series of catheters have been tested to know an optimal catheter. They have tested 79 catheters on 24 patients which represent an average of three catheters per patient. This study is again a general recommendation.

2.4.3. Discussion

Literature related to optimal catheter selection discusses the general concepts about the shape of the aorta and the coronary arteries and suggestions about suitable catheters, but it lacks discussion about patient specific catheter selection. In the approaches presented above, the discussion is very generic and these approaches do not help to avoid the process of trying different catheters until a suitable placement of catheter is achieved. To the best of our knowledge, no one has suggested a patient-specific imaging-based optimal catheter selection before.

2.5. Geometric Parameters Computation from Image Data and Catheter Selection

2.5.1. Introduction

Quantification of the different parameters from the image data is very important for planning and diagnosis. Diameter of the aorta and coronary arteries, curvature of the aorta, and curve angles of the

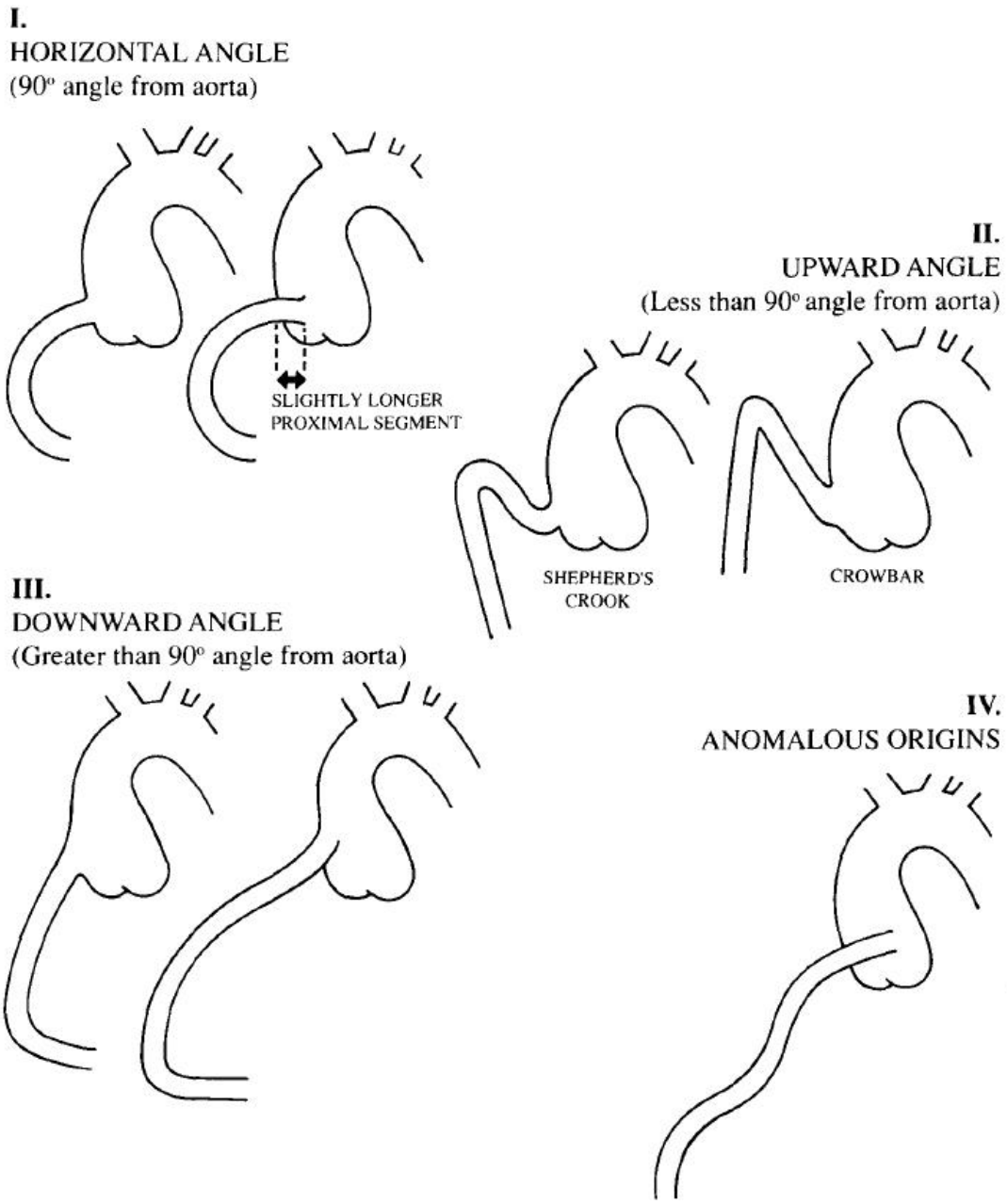

Figure 2.5.: Identifying different anatomies of the coronary arteries [MBCS90].

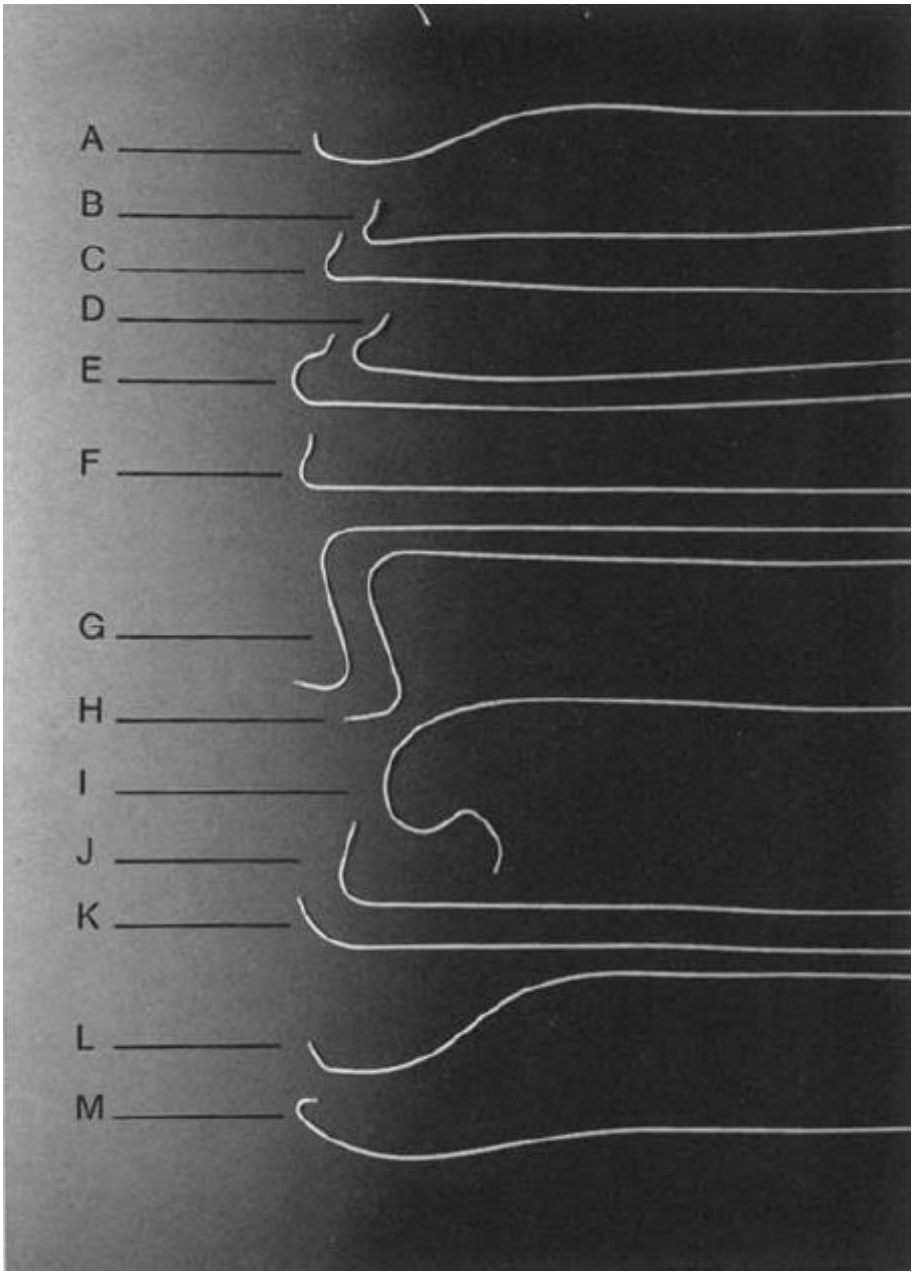

Figure 2.6.: Guiding catheters for right coronary angiography [Sch03]. A: Judkins femoral right. B: Amplatz R1. C: Amplatz R2. D: Amplatz L1. E: Amplatz L2. F: Wiliams L-R. G: Arani double loop (75^0). H: Arani double loop (90^0). I: Block short tip. J: El Gamal coronary bypass. K King multipurpose. L Coronary bypass R1. M: Internal mammary artery

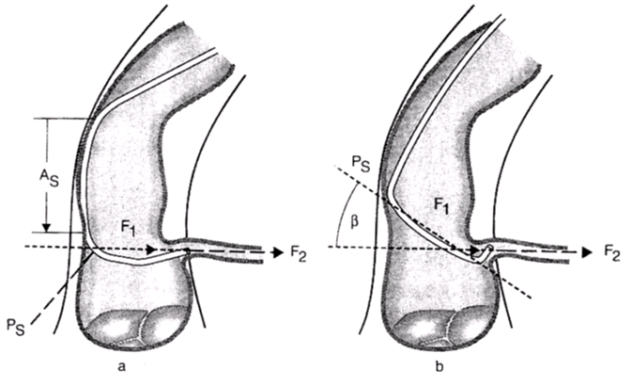

Figure 2.7.: Showing an optimal catheter for left coronary arteries using Voda catheter [Vod92].

coronary arteries are very important for the treatment. These measurements are also important for selecting an optimal catheter. In this Section, we will discuss the different approaches that are used to quantify these different parameters from the image data.

2.5.2. Geometric Parameters' Quantification

In the work of Rubin and others [RPJN98] a semiautomatic method is used for quantifying diameter and curvature of the aorta and its branches in CT data. A discriminative learning based Patient-specific Modeling and Quantification of the aortic and mitral valves in 4D cardiac CT and TEE is presented by Ionasec et al. [IVG*10]. A study for finding the coronary arteries ostia and the related objects for the aortic valve implantation is done by John et al. [JLZ*10]. They have used Marginal Space Learning (MSL) algorithm. Zheng and others [ZJL*10] have presented an algorithm that is able to find eight important aortic valve landmarks (three aortic hinge points, three commissure points, and two coronary ostia) are also detected automatically (see Figure 2.8). An approach given by Kiviniemi [KSK*04] is presented where the coronary artery diameter can be assessed reliably with transthoracic echocardiography. The study of Brinkman [BBN*94] describes a computer-based system to measure the geometric parameters of arteries from angiograms. The back projection technique was used to define the vessel axes in 3-D space. They present results of 30 cases, focusing on the distribution of the geometric parameters of the left anterior descending coronary artery (LAD) and its first two major branches. The derived parameters include the angle between the left circumflex artery and the LAD; the angles between the LAD and its early diagonal and septal perforator branches; distances between branch points. According to their study, no relation between geometric parameters and age or gender was seen. A commercial tool by Philips called HeartNavigator [Phi12] (see Figure 2.9) is used for automatic segmentation of the aorta and coronary arteries. This tool identifies the different parameters and provides measurement of these parameters.

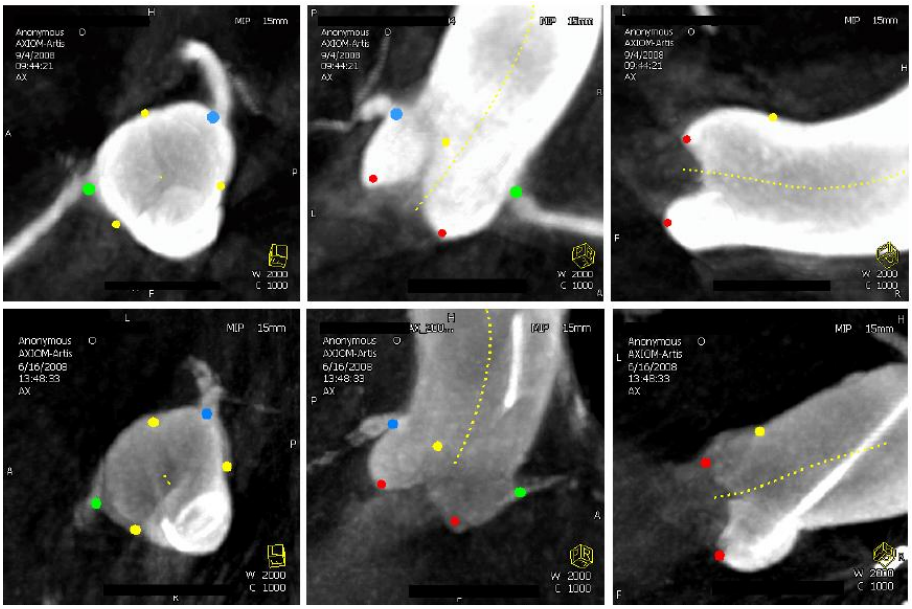

Figure 2.8.: The aortic valve landmark detection with red dots for the hinge points, yellow for the commissure points, blue for the left coronary ostium, and green for the right coronary ostium [IVG*10].

2.5.3. Discussion

We have seen that in the literature there are some semiautomatic approaches for computing parameters from the image data. There are also approaches for the patient-specific quantification of some parameters like the aortic valves and mitral valves landmark. These approaches lead us to the concept of patient-specific parameters' quantification and towards patient-specific catheter selection.

2.6. Catheter and Guidewire Simulation Approaches

2.6.1. Introduction

In previous section, we discussed that there exist approaches in the medical literature that discuss the catheter selection in a general way but these are not image processing based approaches. Then in Section 2.4 we discussed that in the medical imaging literature there are some approaches for computing geometric parameters but the goal of these approaches are not catheter selection. In this section, we extend our discussion and want to explore the literature related to catheter and guidewire simulation. Catheter simulation is an active research area and many training systems for catheter simulation are available. Although these training systems are not dealing with the problem of best catheter selection,

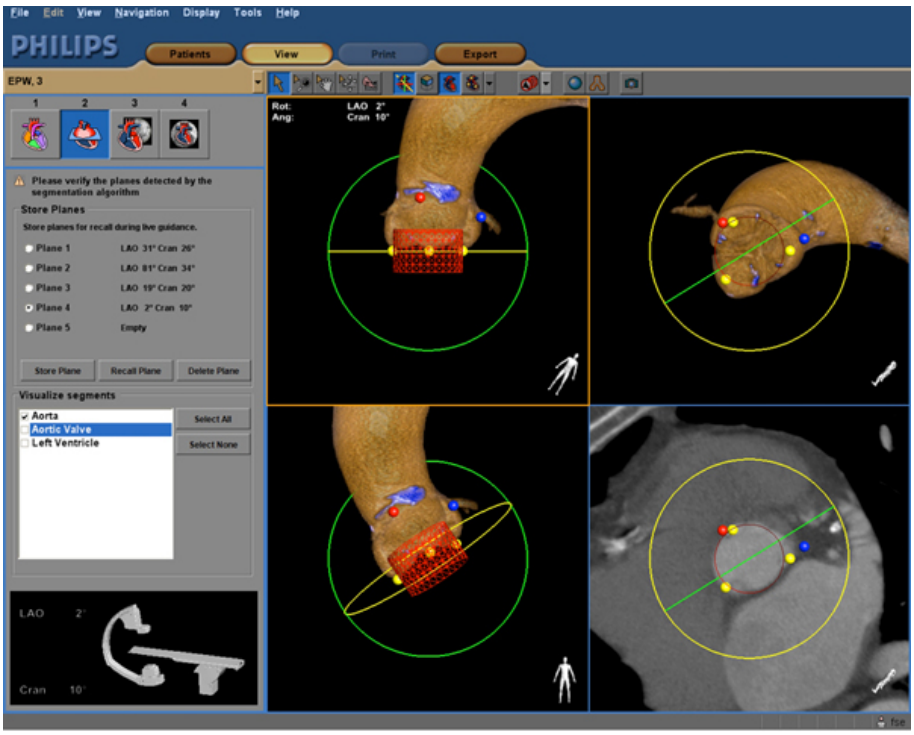

Figure 2.9.: Heart navigator identifies different landmarks like ostia, computing the aorta radius and finding aortic valves [Phi12].

these simulation strategies can be used for best catheter selection. In this section, we will present the different systems that are available for catheter simulation.

2.6.2. Catheter and Guidewire Simulation Systems

2.6.2.1. The 'Dawson-Kaufman' Interventional Radiology Simulator

One of the earliest training systems called Dawson-Kaufman simulator [Meg96] is developed by HT Medical Inc. This system is used for catheter navigation in the abdominal aorta. It is used for practicing angioplasty and other procedures (see Figure 2.10). This system uses a video monitor that duplicates the black and white X-ray images of a fluoroscopic screen. This simulator also incorporates tactile feedback so that physicians manipulating instruments sense the interaction with the vessels. The catheter movement requires longer time than the desired real-time response.

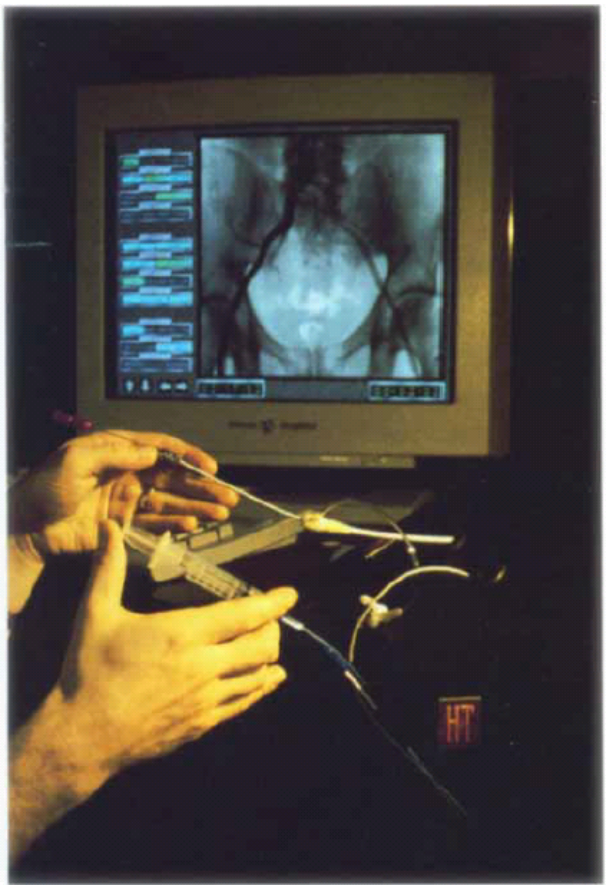

Figure 2.10.: The 'Dawson-Kaufman' Medical interventional radiology simulator. The haptic interface is shown with an example of the computer generated X-ray display. [Bn97]

2.6.2.2. daVinci

A vascular catheterization simulator called daVinci [AR98] is a training system where a catheter has been modeled as a finite element system. This system provides the interventional radiologist a user-friendly image based environment to augment training, enhance planing and design interventional product and devices. It provides real time simulated navigation of catheters in both 2-D and 3-D models of the vessels (see Figure 2.11).

2.6.2.3. Interactive Interventional Cardiology Simulation System (ICard)

The Kent Ridge Digital Labs (KRDL) Singapore have been working on a training system for medical students which is called interventional cardiology simulation system ICard[WCL*98]. It is designed to

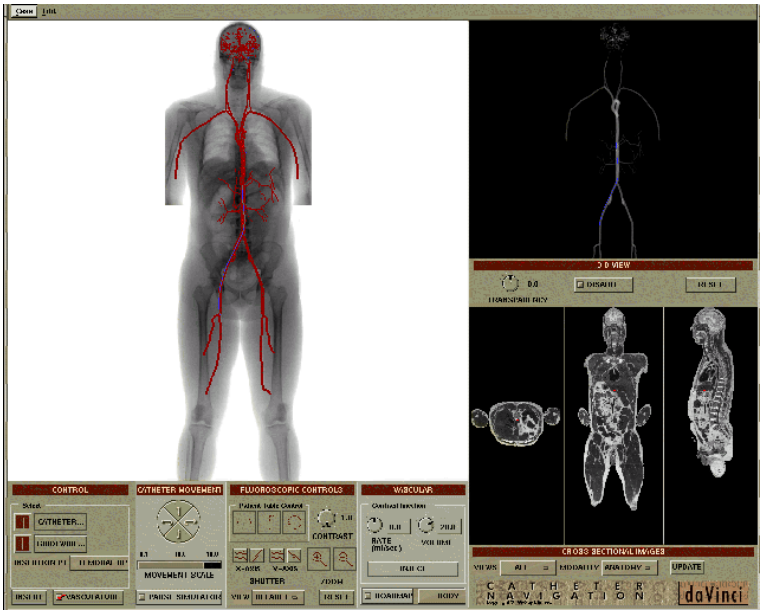

Figure 2.11.: User interface of daVinci. The left window provides a 2D fluoroscopic image view, the upper right window displays a 3D geometric view of vasculature; the lower right window gives the cross sectional image views relative to the catheter tip position. [CNW*12]

enable medical students or physicians to familiarize themselves with the techniques of interventional catheterization procedures. This system provides three-dimensional (3-D) views of the blood vessels and fluoroscopic images for real-time visualization of the catheter position. The 3-D human vasculature is created from image data and is represented with a central line hierarchy model. Finite element methods are used to model the interaction between the guidewire, catheter and arteries.

2.6.2.4. The Neuroradiology Catheterization Simulator (NeuroCath)

The neuroradiology catheterization simulator called NeuroCath [NC01] is a Finite Element Method based physical model with haptic apparatus that gives the sense of touch during intervention planning and training. The vasculature is based on patient specific image data.

2.6.2.5. Interventional Cardiology Training System (ICTS)

Interventional Cardiology Training System (ICTS) [CDM*00] is developed by the Medical Application Group at the Mitsubishi Electric Research Lab and the Center for Innovative Minimally Invasive Therapy (CIMIT) and the Massachusetts Hospital. The system consists of a simulation engine and an instructional system. The geometrical modeling is based on data from the Visible Human Project

(VHP) [Uni11]. The anatomy is modeled by polygonal representations based on the data from the VHP. The catheter and guidewires are represented as multi-body systems as a set of rigid links connected by joints. The contact forces between the catheter and arteries are determined according to the stiffness, damping and friction of the vessel wall. To determine the position and orientation of the multi-body system after an action has been performed on the instrument, all forces (internal and external) are evaluated at each link. A numerical integration is subsequently used to calculate the velocity and positions of the links (see Figure 2.12).

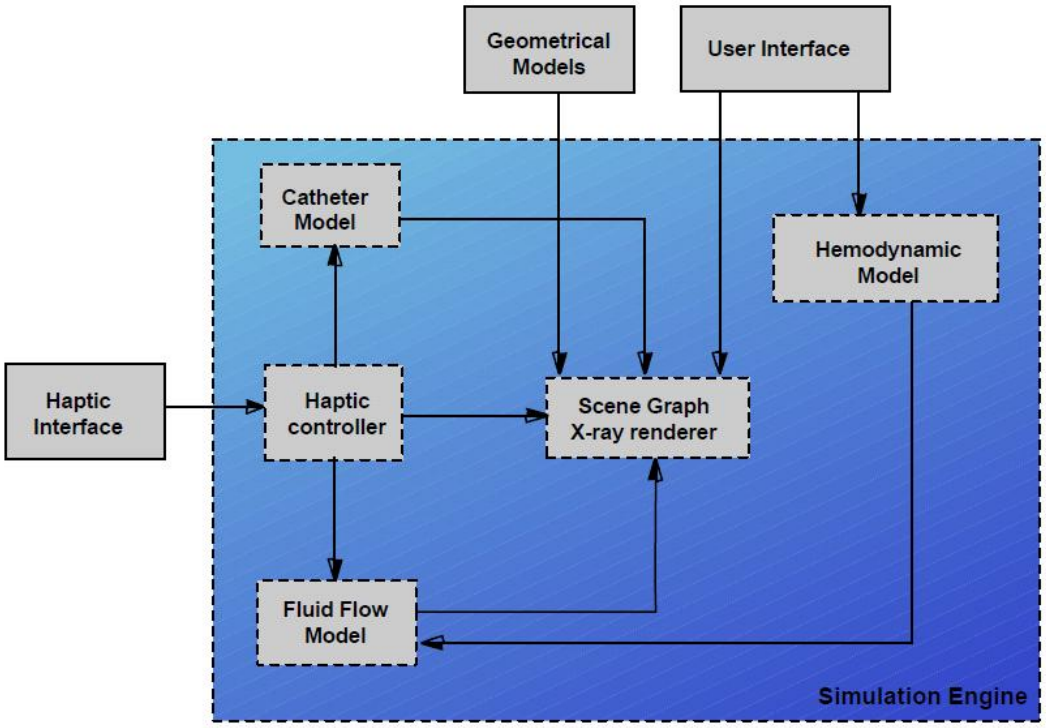

Figure 2.12.: Interventional Cardiology Training System (ICTS): Relation between the different components of the simulation system [CDM*00].

2.6.2.6. Neuroradiology Simulation

Duriez et al. [CDL*05] proposes a catheter model based on three dimensional beam theory. A real time non linear deformable beam model resulting in an accurate simulation has been introduced. The system is based on a real-time incremental Finite Element Model.

2.6.2.7. Catheter-guidewire Composite Model

A catheter-guidewire composite model is presented by Lenoir et al. [J. 06] that avoids the problems of handling the numerous contacts between the catheter and guidwire due to the fact that both devices are co-axial. It is a composite model that claims to realistically simulate a catheter, a guide wire or a combination of both. The main idea of this approach is to decompose the animation of the catheter/guidewire combination into a physics-based component and an animation component. The model is FEM based and dynamically adapts its material properties to locally described combination of both devices.

2.6.2.8. Mass Spring Based Models

Many people have also tried to design simulation models using mass springs. In the approach presented by Luboz et al. [LBGB09, LZL*10] a mass-spring model is used where the guidewire is modeled as a set of particles connected by stiff springs. The instrument is modeled as a hybrid mass-spring particle system while the vasculature is a triangulated surface mesh segmented from patient data sets. However, in these systems they have restricted their modeling only to guidewires. In Figure 2.13 guidewires are represented as particles connected by spring forces.

Another spring based model is presented by Takashima et al. [TOY*09]. In this system the guidewire model is composed of viscoelastic springs and segments. The proximal part of the guidewire model is constrained by the guidewire model, which is fixed and assumed to be a rigid tube. The blood vessel model is a circular elastic cylinder, whose shape is defined by the centerline and the radii. Collisions between the guidewire model and the blood vessel model are calculated and the contact forces are determined according to the stiffness of the vessel wall.

Another simulation system for training purposes is presented by Alderliesten et al. [AKN04]. The catheter is modeled as a set of joints and these joints are connected by straight, non bendable segments using spring forces. An algorithm for simulating the propagation of a guidewire within a vascular system, based on the principle of minimization of energy, has been developed. Both longitudinal translation and rotation are incorporated as possibilities for manipulating the guidewire. Two types of energies are introduced: internal energy related to the bending of the guide wire, and external energy resulting from the elastic deformation of the vessel wall. Mass spring models are faster than FEM but these are not suitable for modeling guidewires and catheters because these devices are not compressible and cannot be stretched out and preserve their length under stress. Mass spring models are better for modeling soft tissue deformation but not good for modeling catheters and guidewires.

2.6.3. Discussion

We discussed about the different techniques available for the catheter and guidewire simulation. We showed that the catheter is modeled using FEM or mass spring models. The systems that have used FEM models include the work of HT Medical Inc. [Meg96], daVinci [AR98], ICard[WCL*98], Duriez et al. [CDL*05], and NeuroCath [NC01]. The spring mass models are from Lenoir et al. [J. 06],

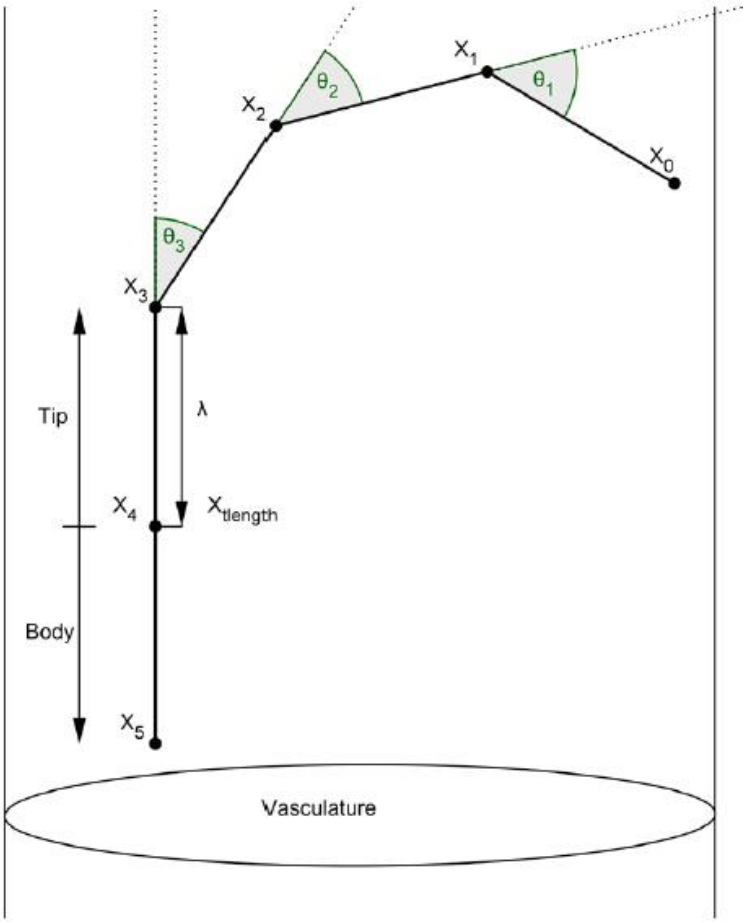

Figure 2.13.: Mass Spring Model: Particle representation of the guidewire [LBGB09, LZL*10]

Alderliesten et al. [AKN04], Lauboz et al. [LBGB09, LZL*10], Takashima et al. [TOY*09] and [LGW*12]. FEM based models are slow but are good in representing the physical behavior of the system. Spring based models are faster than FEM but these are not suitable for modeling guidewires and catheters because these devices are not compressible and cannot be stretched and preserve their length under stress. Mass spring models are better for modeling soft tissue deformation but not good for modeling catheters and guidewires. The people who have used spring models have avoided modeling the catheter and have focused only on the guidewire. Using an FEM based approach, one can easily model the different properties like cross-sectional area, cross-section moment of inertia, polar moment of inertia, solid and hollow devices of various cross-sectional geometries and mechanical properties.
The purpose of all these systems is to train young cardiologists by using virtual environment instead of real patients. These training systems help to familiarize them with the techniques of interventional

catheterization procedure. However, these systems are still far from the real environment. Moreover, these systems do not handle the problem of patient-specific optimal catheter selection. In our work we will model catheters and guidewire using FEM based modeling due to its capability of representing the physical behavior of these instruments.

2.7. Summary

In this chapter, different approaches related to an image processing based catheter selection problem were presented. The literature was reviewed for the image segmentation and skeletonization approaches. Medical literature was reviewed for finding non image processing based approaches and medical imaging literature was reviewed for tracing any image based approach for optimal catheter selection.
We first studied the different approaches for the aorta and coronary arteries segmentation. Many of these methods require very high resolution of images. Some of the segmentation methods need manual interaction. *It was found that currently there is no direct approach that automatically segments the aorta and the coronary arteries. However, it was concluded that the work of Deschamps et al. [DC02] about aorta segmentation that used Fast Marching Method can be used with some modification. For seed point selection the work of Kovacs [KCA*06b, KCA*06a] was found helpful. It was concluded that combining these different approaches will enable us to develop a fully automatic segmentation algorithm for the aorta and the coronary arteries*. For creating centerline extraction of the segmented images, we tested different algorithms on 3D MR and CT images. Among these algorithms, the one presented by Lee [LKC94] was very fast and was able to successfully create the 3D skeleton of the aorta and coronary arteries. Therefore, it was decided to use this algorithm for creating the centerline. In the literature review about geometric parameters, it was found that there are some semiautomatic approaches for computing some parameters from the image data. There are also approaches for the patient-specific quantification of some parameters like aortic valves and mitral valves landmark. *In Chapter 3, we will present a completely automatic method for the computation of geometrically important parameters*. It was also found that there is no approach that is used for suggesting patient-specific catheter. However these approaches lead us to the concept of patient-specific parameters quantification and towards patient specific catheter selection. *Defining an image processing based patient-specific model will be another contribution of this thesis*. Then we discussed about the different techniques available for the catheter and guidwire simulation. We showed that the catheter is modeled using FEM or mass spring models. FEM based models are slow but are good in representing the physical behavior of the system. Spring based models are faster than FEM but these are not suitable for modeling guidewires and catheters because these devices are not compressible and cannot be stretched and preserve their length under stress. Mass spring models are better for modeling soft tissue deformation but not good for modeling catheter and guidewire. The people who have used spring models have avoided modeling catheter and have focused only on guidewire. Using an FEM based approach, one can easily model the different properties like cross-sectional area, cross-section moment of inertia, polar moment of inertia, solid and hollow devices of various cross-sectional geometries and mechanical properties.

Module	What is being done	Novelty/Extension
Segmentation	Many semiautomatic approaches are available	Extending the current approaches for complete Automatic segmentation
Skeletonization	The current approaches can be used	–
Parameters estimation	Manual approaches are available	Automatic computation approach is needed
Non image processing based catheter selection	General approaches are available	–
Image processing based catheter selection	No available approach	Need new approach
Simulation based catheter selection	Catheter simulation for training purposes are available	Need to adapt the current approaches for catheter selection

Table 2.2.: A summary of research areas where we need extension or we need new approaches

The purpose of all these simulation systems is to train young cardiologists by using virtual environment instead of real patients. These training systems help familiarize them with the techniques of interventional catheterization procedure. However, these systems are still far from the real environment. Moreover, these systems do not handle the problem of patient-specific optimal catheter selection. In our work, *we model catheters and guidewire using FEM based modeling due to its capability of representing the physical behavior of these instruments*. In Table 2.2 we have summarized what has been done and what is needed to be done or extended. For *segmentation*, we will extend the current approaches and will present a completely automatic segmentation scheme. For *geometric parameters computation*, we will present a new automatic approach. Similarly, *a novel model for the catheter selection* will be defined. For simulation, the existing strategies will be adopted for the catheter selection problem.

3. An Image Processing Based Patient-Specific Model for Optimal Catheter Selection

3.1. Introduction

In this chapter, we present our concepts of an image processing based catheter selection model. The basic idea of this approach is to obtain MR/CT images before starting angiography. From these images, the patient arteries are segmented and some geometric parameters are computed from the segmented images. At the same time, geometric parameters are computed from the available catheters. A model is developed, which is based on these parameters from the patients' image data and parameters from the catheters. This model reduces the number of catheter choices. In the next step, the reduced number of catheters are simulated and the most optimal catheter is obtained. A flow chart of the procedure is given in Figure 3.1. This chapter is organized as follows:
The first step of our image processing based patient specific-catheter selection procedure is the segmentation of the aorta and coronary arteries. Our method about segmentation is presented in Section 3.2. The next step is the skeletonization and centerline extraction as well as geometric parameters computation from the patient's image data. These concepts are presented in Section 3.3. In Section 3.4, models are presented that reduce the large set of catheters choices to few choices. Different models are developed for right coronary angiography, left coronary angiography and for angiography where the coronary arteries' shape and origin deviate from the normal pattern. In Section 3.5, our simulation strategy is presented where the reduced number of catheters are simulated that results in a final suitable catheter recommendation. At the end, a summary of the chapter is given.

3.2. Arteries Segmentation

3.2.1. Introduction

The first step of an image processing based catheter selection model is segmentation. The imaging protocol used by our clinical partner dictates that the procedure has to be performed on special MRI data that is acquired prior to coronary angiography. The coronary arteries are much smaller and higher resolution images are needed to get the detailed information while the aorta is much bigger and it would take too much time to get the information with the same resolution as for coronary arteries. Therefore, to image the aorta, low resolution images are obtained. The resolution in the aorta is low but still information is obtained in less time. So one set of images contains the complete aorta but with

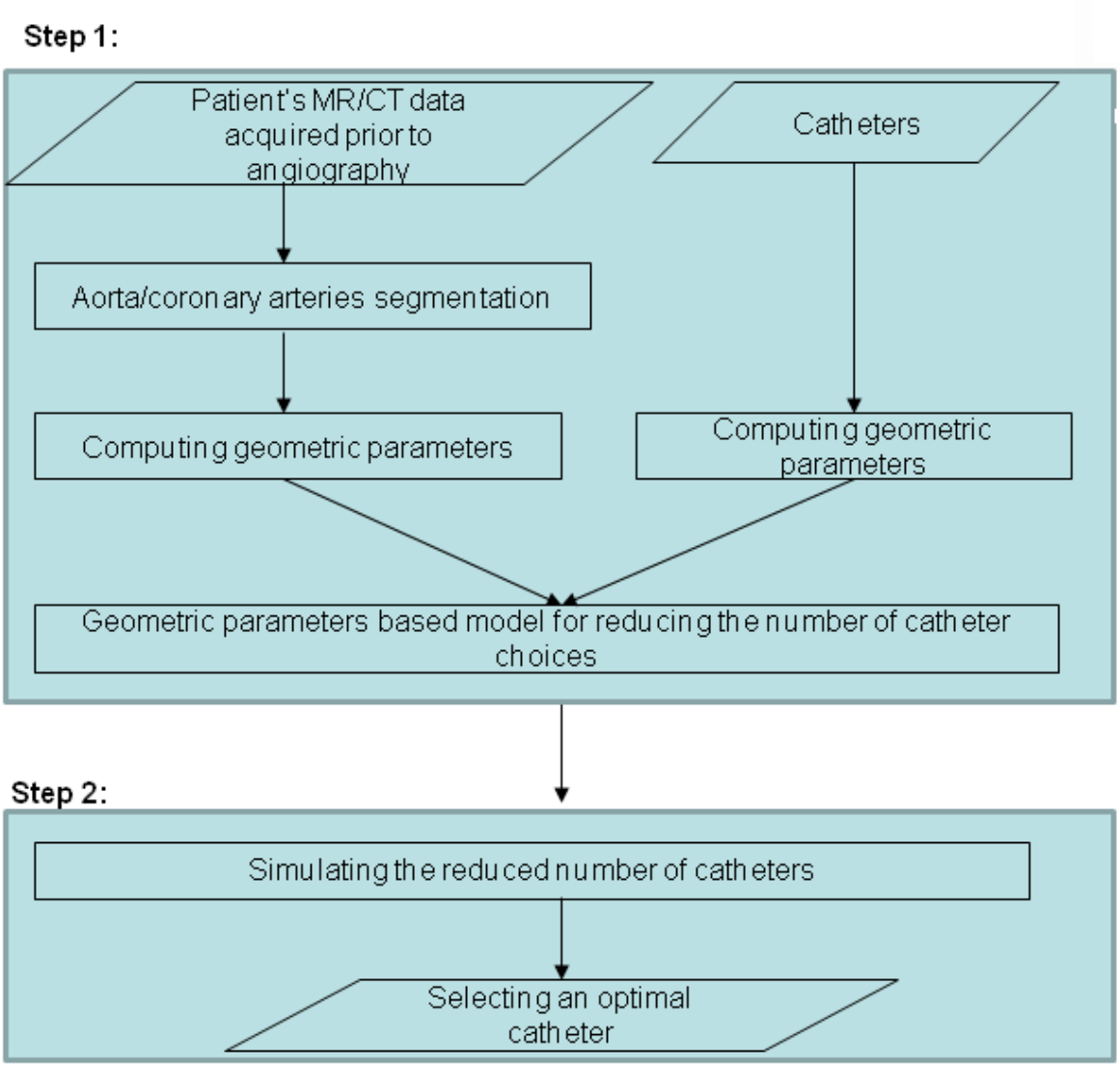

Figure 3.1.: A two step approach for finding an optimal catheter.
Step 1: Geometric parameters based approach for reducing the number of catheter choices.
Step 2: Simulation based approach for finding the final selection using the reduced number of catheters.

low resolution ($0.83 \times 0.83 \times 1.5\, mm^3$) while the other set contains detailed high resolution images ($0.68 \times 0.68 \times 0.5\, mm^3$) of the coronary arteries as well as the aorta in this region. Our goal is to obtain from these two data sets a single patient-specific model of the aorta and the adjacent coronary arteries arising from the ascending part of the aorta while masking the other arteries (e.g. subclavian and carotid). Then we have to derive a set of geometrical parameters. For this, the first step is to segment the relevant anatomical structures, then fuse the regions of both data sets and finally generate a skeleton of the vascular structures. The standardized image acquisition protocol as well as our developed methods allow a fully automatic segmentation as well as a computation of the geometrical parameters. We first register these arteries, then segment the aorta and coronary arteries and get a final combined model. The different steps of getting a patient-specific model are shown in Figure 3.2.

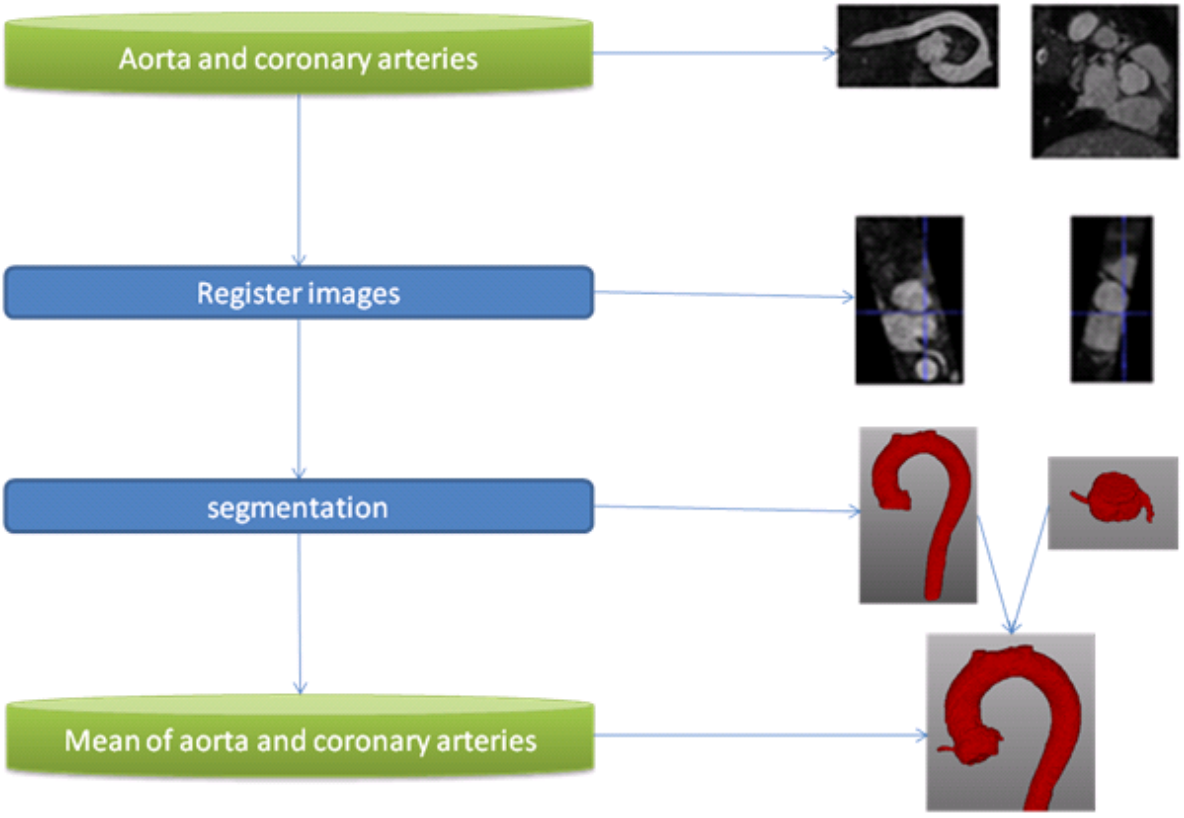

Figure 3.2.: Segmentation pipeline.

3.2.2. Aorta Segmentation

The segmentation of the aorta in the low resolution image data is performed in a slice-wise manner. We combine a Hough transform [Bal81] with a *Fast Marching Method* (FMM) [Set99]. In a pre-processing step, different filters from the ITK [Kit12, PM90b] have been used (see Figure 3.3). The image data is rescaled and smoothed with an anisotropic diffusion filter. Gradient magnitude filter and a sigmoid filter is applied to the input images.

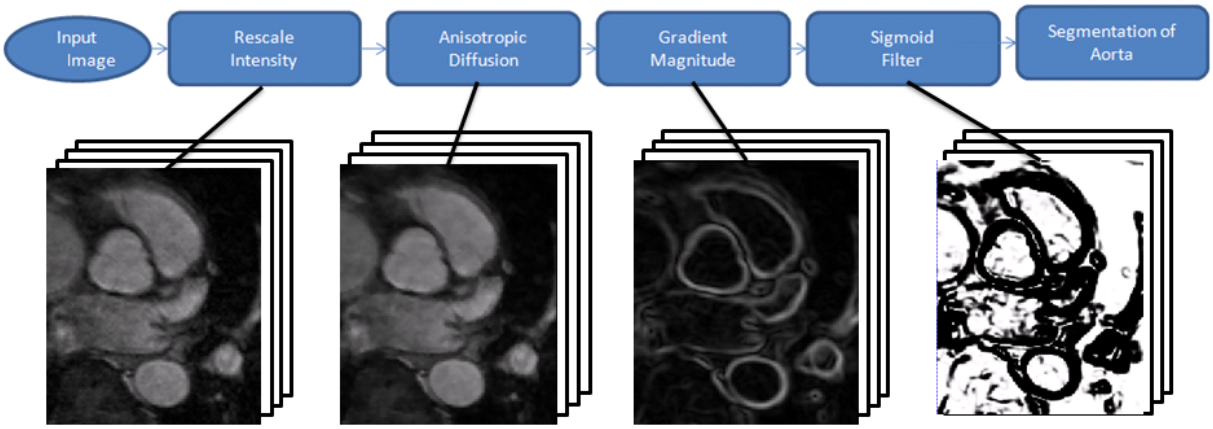

Figure 3.3.: Preprocessing of the aorta.

An initial start point for the FMM is found automatically by searching for circles with the strongest Hough peaks in the gradient magnitude filtered image slices. This approach has some similarities to the work of Kovács et al. [KCA*06b] but in contrast to their method, we start from the middle slice of the stack of image data and search in 10 % of the neighboring slices for three circles with the strongest Hough peaks (see Figure 3.4). Two of these represent the ascending and descending aorta, respectively. The third one is another more or less circular structure with varying location over the different slices. Searching for three circles guaranties that the two parts of the aorta will be found in each slice. In the next step, the circles in neighboring slices are combined to cylindrical shapes. There, two cylinders which are the largest ones emerge. The one with the largest diameter represents the ascending aorta close to the aortic root, the other one the descending aorta. The center of the latter one defines the starting point for the FMM based segmentation (see Figure 3.5). Starting at this position, the sigmoid filtered image slices are segmented stepping down to the descending aorta. An FMM is applied to each slice and the center of gravity (CoG) of the segmented region is propagated to the next slice as starting point for the FMM. Similarly, the algorithm steps upwards along the descending aorta until the size of the segmented region abruptly decreases. This avoids the inclusion of subclavian and carotid arteries into the segmentation. A few slices below, the size of the segmented region has been abruptly increased; being the position at which ascending and descending join. For the left half of the segmented region in this slice, the CoG is computed and serves as a start point for the segmentation of the ascending aorta. This part is segmented the same way as the descending aorta by stepping down towards the

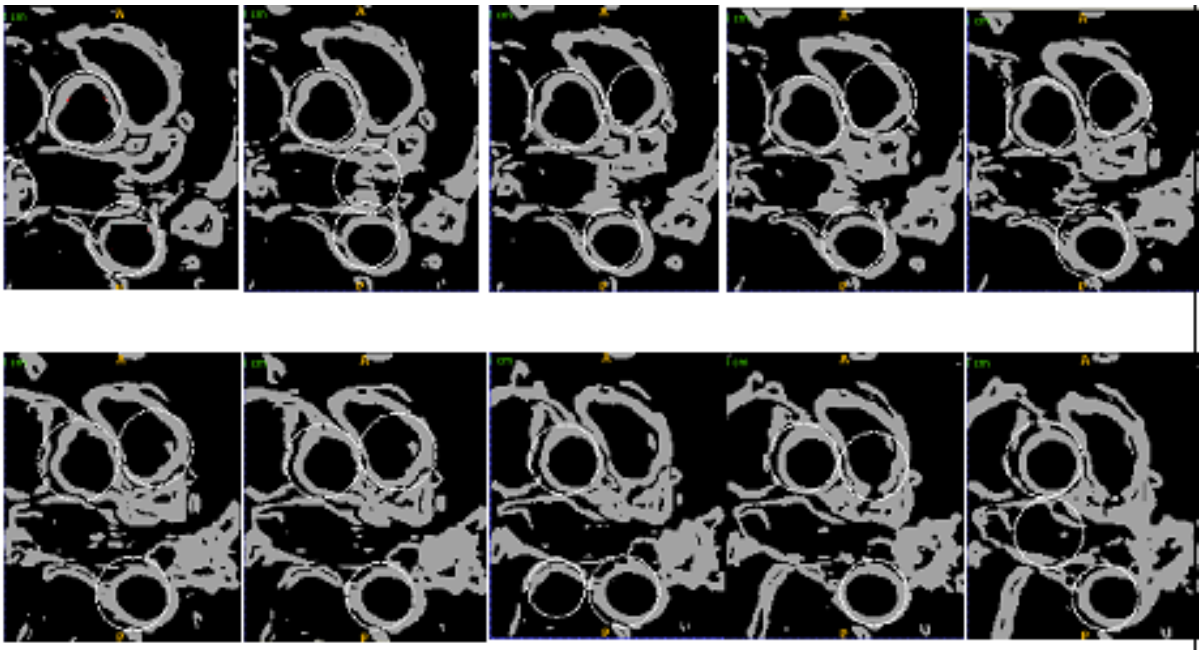

Figure 3.4.: For seed point selection, the aorta is searched for three circles with the strongest Hough peaks. Two of them represent the ascending and descending aorta, respectively. The third one is another more or less circular structure with varying location over the different slices. Searching for three circles guarantees that the two parts of the aorta are found in each slice.

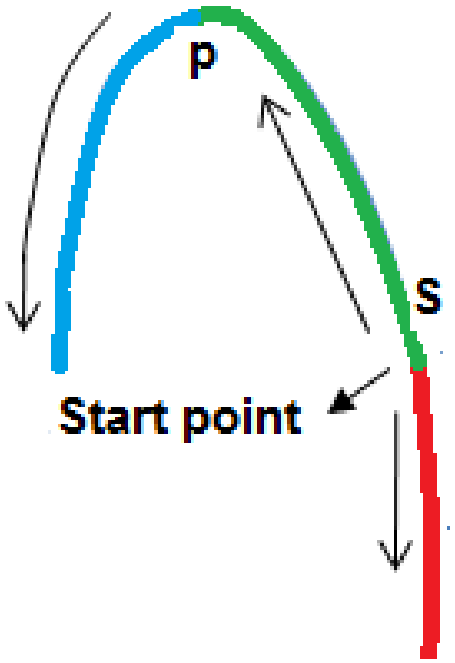

Figure 3.5.: Aorta segmentation: For the red segment, segmentation is started at seed point S, FFM is used at each slice downwards, the center of gravity (CoG) of the segmented region is propagated as the a start point for the next slice. For the green segment, the same is repeated in upwards direction until the size of the segmented region abruptly decreases (point P). Ascending aorta: For the blue segment, segmentation starts at point P, the same procedure is repeated in downwards direction until the size of the segmented region abruptly increases which occurs just below the aortic valves.

aortic valves. The segmentation is stopped in case the size of the segmented region abruptly increases, occurring just below the aortic valves. The complete segmentation steps are shown in Figure 3.6.

3.2.3. Coronary Arteries Segmentation

Coronary arteries segmentation is not as simple as the aorta segmentation. Here we need to apply FMM in 3D due to the fact that sometimes parts of the coronary arteries are not directly connected to the aorta on the same slice. We also consider a special procedure for a fast and automatic seed point selection for the coronary arteries. Preprocessing is the same as in the low resolution one (see Figure 3.7) and in addition, two *vesselness filtered* [FNH*99] image data sets are created.

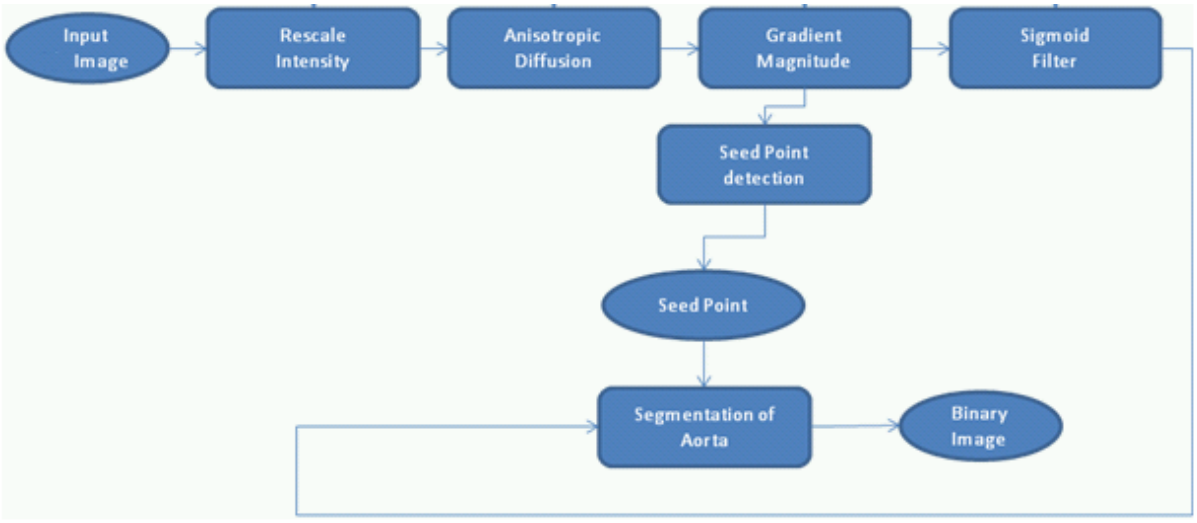

Figure 3.6.: Aorta segmentation steps.

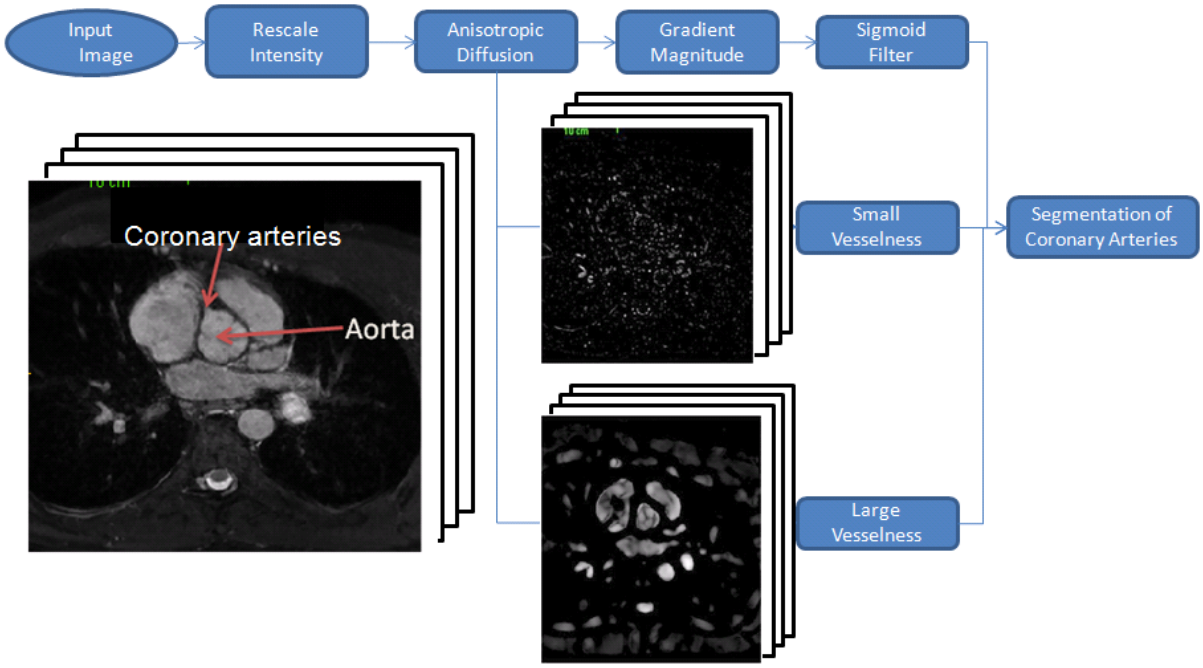

Figure 3.7.: Preprocessing of the coronary arteries.

3.2.3.1. Seed Point for Coronary Arteries Segmentation

In order to initialize it, we first perform a rigid registration of both data sets employing a *Mean Squares Metric* and upsampling the low resolution data set to the voxel sizes of the high resolution one. We restrict the low resolution data set to 3 cm lying above the aortic valves, whose position is known from the whole aorta segmentation described in Section 3.2.2. This increases the speed and robustness of the registration. Once the alignment is done, the CoG of the aorta region already segmented in the low resolution data set and having an overlap with the high resolution data set, is taken as a start point. We explicitly segment the high resolution data set instead of simply transferring the segmented region from the low resolution data set since we need an accurately delineated aorta in the region of the coronary arteries' ostia.

3.2.3.2. Coronary Arteries Segmentation

For enhancing the structure we are looking for, vesselness filters can be used with proper smoothing of the Hessian matrix. We set $\sigma = 1$ for highlighting the coronary arteries (see Figure 3.8 (a)) and $\sigma = 4$ for the aorta (see Figure 3.8 (b)). These two data sets represent additional input for the segmentation.

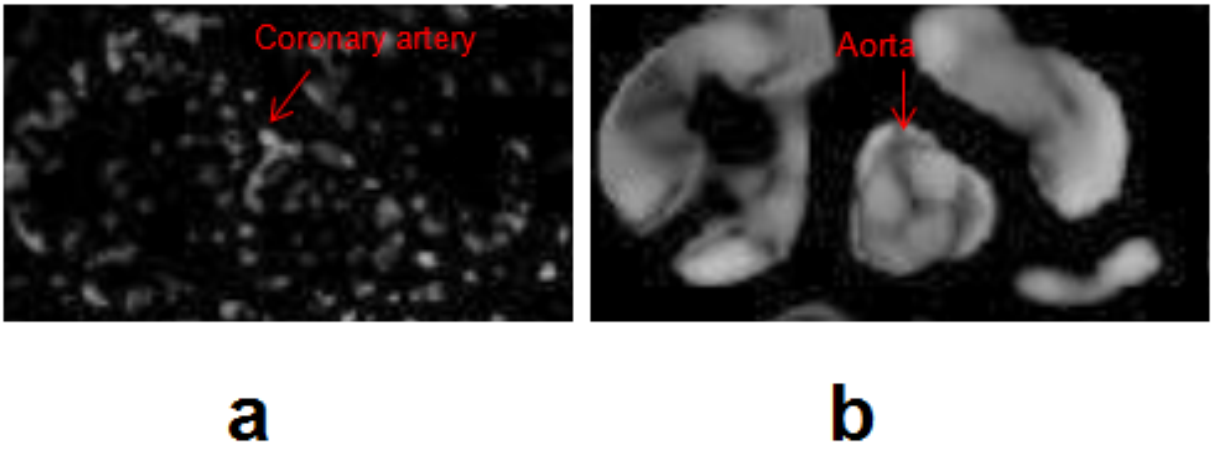

Figure 3.8.: Vesselness filter applied to the high resolution data set. For vesselness we set $\sigma = 1$ for highlighting the coronary arteries(a) and $\sigma = 4$ for the aorta (b).

The aorta and the coronary arteries are extracted in two steps, each of them employing one of the vesselness filter output image data sets. First, the one with $\sigma = 4$ is multiplied voxel-wise with the sigmoid filter's output. Then, an FMM based slice wise segmentation is performed up and down the aorta. Afterwards, the vesselness filtered image data with $\sigma = 1$ is added voxel-wise to the output of the FMM and the FMM is run again – but in this case in 3D. This two steps segmentation extracts in addition to the aorta the coronary arteries being the only small structures which are directly connected to the aorta. The complete segmentation steps are shown in Figure 3.9.

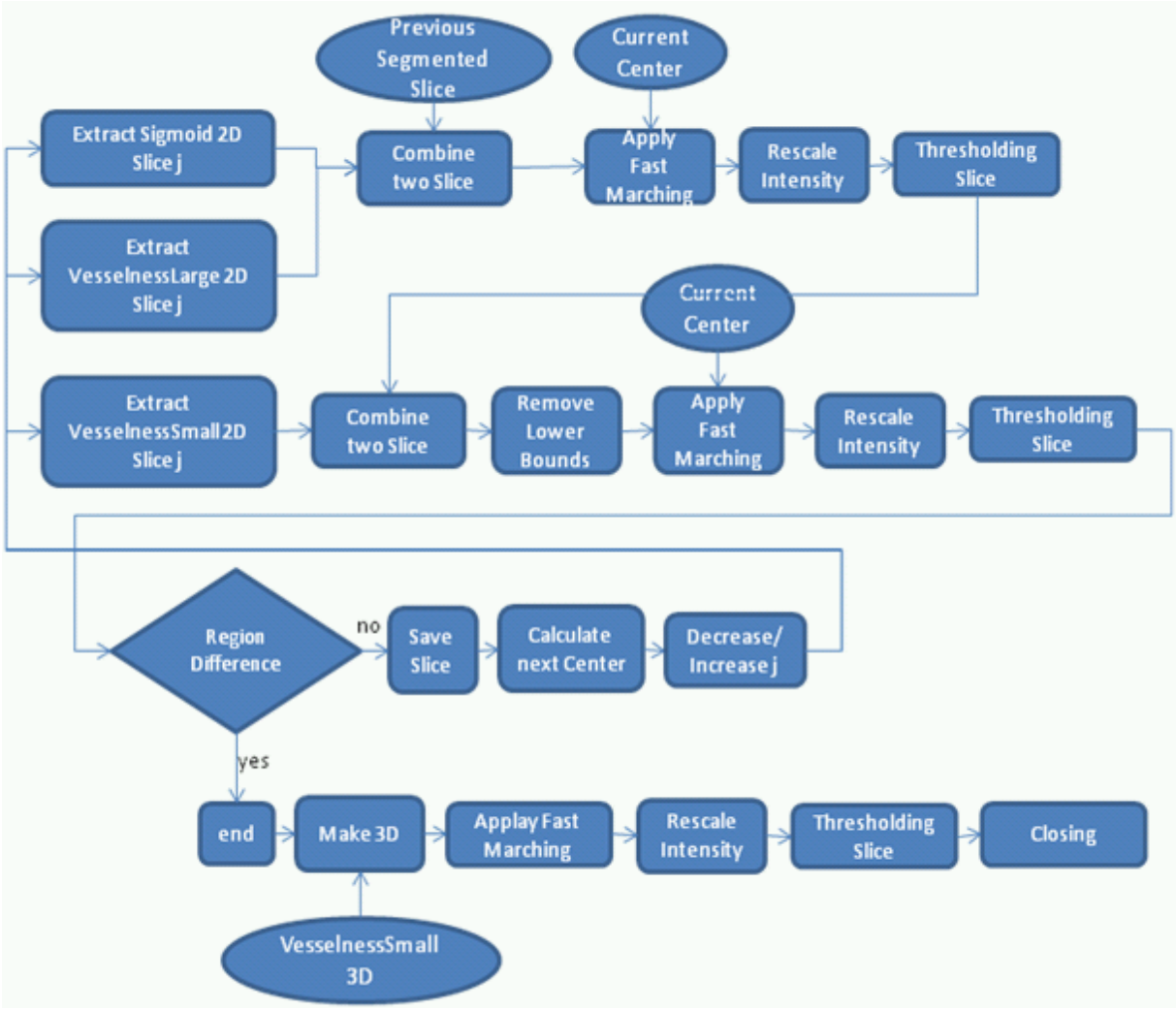

Figure 3.9.: Coronary arteries segmentation.

3.2.4. Fusion of the Aorta and Coronary Arteries

We have explained in Section 3.2.1 that the imaging protocol demands for obtaining a model from two different sets of image data. One set is low resolution aorta and the second set is high resolution coronary arteries. A straightforward fusion of the two images is not possible because both image sets do not cover the same area. Both images share only small common area near the coronary arteries valves. Due to the blood circulation, the size of the aorta and coronary arteries varies and due to the breathing effect, the heart chambers in both images do not remain constant. We solve this problem by roughly cutting the shared area from both images, first applying rigid registration on these sub images and then applying the registration parameters to the whole image. The rigid registration roughly aligns both images and after that we apply deformable registration. Once, both image data sets are registered then the aorta and coronary arteries are segmented using the algorithm described in Section 4.2. Both images are then fused after segmentation. For the fusion, a filter is created that takes the two segmented images as input and applies a voxel-wise mean computation. For regions where both data sets do not overlap i.e., for one data set there is no information at that voxel position, only the information from the second data set is used without computing the mean.

3.2.5. Discussion

We presented segmentation and fusion of specially acquired MR data of the aorta and coronary arteries where both images share only small common area near the coronary arteries' valves. The seed point definition as well as the segmentation and registration process is completely automatic. The data is registered before starting the segmentation and then this registration process helps us to find a seed point for coronary arteries from the segmented aorta. As a result, we get an automatic segmentation process for a complete model of the aorta and coronary arteries. This model is then used to compute the geometric parameters from the 3D segmented data. In the next step, we discuss the skeletonization and geometric parameters computation.

3.3. Geometric Parameters' Computation

3.3.1. Introduction

Extraction of the arteries' centerlines is an important step for the quantification of stenosis, topological representation, virtual endoscopy, visualization of the vascular network and catheter simulation. We need the arteries' skeleton for developing a catheter selection model. Different parameters such as, the arteries centerline, coronary arteries angle, position of the two ostia, tips of the coronary arteries and position of the aortic valves are needed for this process. In this section, we describe our automatic procedure for extracting this information from the segmented images.

3.3.2. Clinically Important Geometric Parameters

Centerline Extraction

Centerline extraction is the initial step for computing the different geometric parameters. The algorithm presented by Lee [LKC94, MS96] is able to successfully create a skeleton of 3D images. We have used this algorithm for creating centerline of the aorta and coronary arteries.

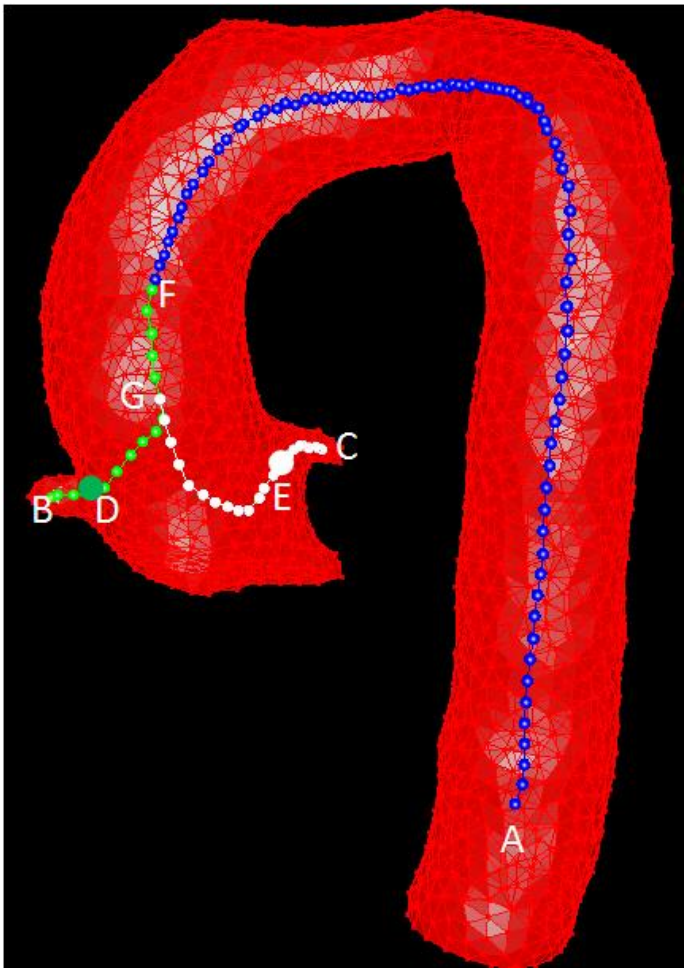

Figure 3.10.: Centerline extraction and marking right and left coronary arteries curves.

Aorta and Coronary Arteries Diameter

For computing the diameter of the aorta and coronary arteries, a plane, normal to each of the cen-

terline's points is created. Along that plane, the averaged distances of the points lying on the surface of the segmented region are determined, providing values for the aorta as well as the coronary artery diameters.

Coronary Arteries' Tip Points

To extract the coronary arteries tip points B and C in the skeleton image (see Figure 3.10) we perform a search using the axial view. We start searching the slices from bottom to top and search the first slice with a non zero pixel. The position of the pixel at the first non-zero slice (point A in Figure 3.10) is selected as starting pixel point. Then we try to find the tip of the right coronary artery (point B in Figure 3.10). This is done by iteratively searching non-zero neighbor pixels and selecting the pixels with minimum X indices. These conditions compel the search-pointer to follow the main aorta (see Figure 3.10, blue curve) and then enter into the right coronary artery (see Figure 3.10, green curve). To compute the left coronary artery tip point C, the same procedure is repeated but this time selecting the next pixel with maximum X. This condition compels the search-pointer to follow the main aorta and then enter into the left coronary artery (see Figure 3.10, white curve).

Coronary Artery Ostium

For finding the ostium of the right coronary artery, we start from the right end point B of the skeleton (see Figure 3.10), compute the diameter of the right coronary artery at this point, move to the next point on the skeleton and compute the diameter. The process is proceeded to the next points by calculating the ratio between current value of the diameter and the previous one. We determine the skeleton point where this ratio exceeds 2.0 indicating that this point is already inside the aorta. This point D is considered as the ostium of the right coronary artery. Similarly, we find the point E as the ostium of the left coronary artery.

Coronary Artery Curve

The coronary arteries' skeleton part and half of the ascending aorta skeleton is considered as coronary arteries' curve. In Figure 3.10 the right coronary artery is shown as green curve and the left coronary artery as white curve.

Coronary Artery Angle

For the computation of the angles of both coronary arteries with respect to the aorta, the coronary arteries' curves are projected onto a 2D plane. The projection planes are different for the left and right curves. For the right curve, the projection plane is created from points B, G, and F (see Figure 3.10) and for the left curve the plane is formed from points C, G, and F. The curve angles are computed after these projections.

Aortic Valves Position

The aortic valve position which has already been estimated during the segmentation of the whole aorta is refined. For this, the intensities in the low resolution data set within the segmented area in the slices which are close to the estimated valve position, are considered. The valves appear as darker structures compared to the aorta lumen. Thus, by stepping upwards from the slice containing the initially estimated aortic valve position we search for the first slice where the mean intensity within the segmented region increases by a factor of 1.5 and consider the slice just below as the position of the aortic valves.

Distance of the Ostium from the Aortic Valves

Having determined the aortic valves position H (see Figure 3.11), we can finally calculate the distance from the valves to the ostium E. This final parameter provides information whether the coronary arteries have a higher take-off, a lower take-off or a normal one. This is especially important in order to decide for or against a so-called *Amplatz* catheter. The set of computed geometrical parameters are displayed in Figure 3.11.

3.3.3. Discussion

Using the image data, all the above parameters are computed automatically. These parameters are of great help for the cardiologist to investigate different treatment and diagnoses. Finding the diameter of the aorta helps to know about stenosis and aneurysm. Diameter of the coronary arteries helps to know whether the artery has become thin or not. The position of the coronary arteries' ostium and its distance from the aortic valves helps to know whether the coronary arteries have a high takeoff or a low takeoff. Similarly, the angle of the coronary arteries with the aorta, helps to know whether the takeoff is horizontal, inferior or superior. In our work, these parameters provide the basis for geometric parameters based models. In the next section, based on these parameters, we present our image processing based catheter selection models.

3.4. Image Processing Based Catheter Selection Models

3.4.1. Introduction

In this section, we present image processing based patient-specific models for selecting optimal catheters. First, we discuss the general guidelines from the medical field for best catheter selection. These guidelines are about different anatomies and the related suitable catheters. Based on these guidelines, we define different parameters related to the patient's image data and parameters for the catheters. Catheter optimality condition for the left and the right coronary angiography are different, and therefore, we develop separate models for each. Similarly, coronary arteries have also anomalous cases and again the optimality condition for catheter selection changes. So we have a third model for coronary angiography

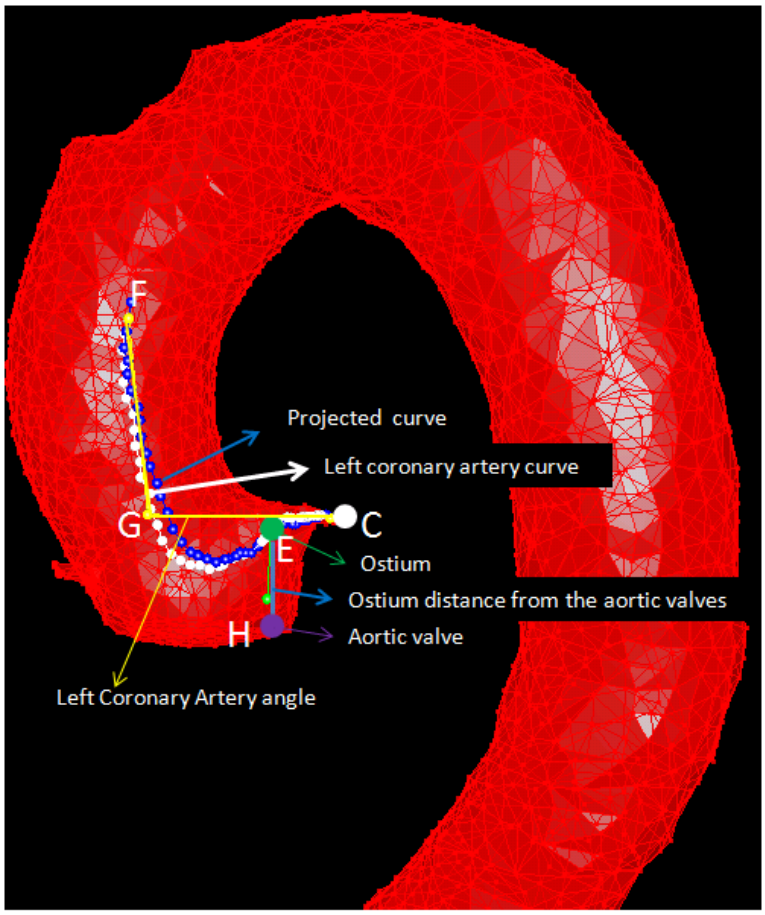

Figure 3.11.: The set of computed geometric parameters illustrated for the left coronary artery.

where the arteries have a high takeoff. These models will enable to restrict the catheter choices from a large set and will help cardiologists, especially the inexperienced ones, to have a catheter suggestion before starting angiography.

3.4.2. Model for the Right Coronary Angiography

We present a catheter selection model for the right coronary angiography. In this section, we will consider angiography where the coronary arteries are normal and there is no deviation from the normal anatomy. Sometimes, due to different aortic diseases like aneurysm or stenosis, the aorta diameter deviates from its normal shape. If the aorta diameter is in the range of 3.5 *to* 4.0 *cm*, then such aorta is called a normal aorta otherwise it is either dilated or narrowed (see Figure 1.4).

The most important parameter for the right catheter selection is the takeoff of the coronary arteries. If the coronary artery departs from the aorta at an abnormally high distance above the aortic valve, then such takeoff is called a high takeoff (see Figure 4.22(c)) and this situation demands for special consideration during catheter selection. Another takeoff is called horizontal takeoff where the coronary artery departs at right angle to the ascending aorta (see Figure 4.22(d)). A takeoff that makes an angle less than 90 degrees is called an inferior takeoff (see Figure 4.2(a)) and a takeoff with an angle greater than 90 degrees is called a superior takeoff (see Figure 4.2(b)). We have to consider these variations during catheter selection. Clinically, it is confirmed that a catheter placed along the aorta and coronary arteries centerline is an optimal catheter (see Figure 3.12). Keeping in mind these guidelines from the clinic, we define a model for right coronary arteries.

3.4.2.1. Catheter Selection Model

For our catheter selection model, the prerequisites are the segmented images of the aorta and coronary arteries as well as information about the geometry of the catheters. Our model can be defined as follows:

We consider the curve of catheters (see Figure 3.14) and the curve formed by the aorta and RCA (see Figure 3.15 (c) yellow curve). We compute the Curve Length (CL) and Curve Angle (CA) of the available catheters and CL and CA of the patient's RCA and suggest a catheter with closest CL and CA with respect to the patient's RCA. In Figure 3.13, the optimal catheter selection procedure is shown.

Catheter's Curve Angle Computation

Computing CA of catheters is straightforward. We extract the centerline of catheters and compute the CA and CL. For this, we consider one point (point A in Figure 3.14) at the tip of the catheter and a second point (point C in Figure 3.14) at a position above the catheter's curve. We create a line, starting from the point A and passing through the point B. Another line starting from the point C and passing through the point D is created. We find the intersection point P and compute the angle between the points A, P and C which is the CA of the catheter. We then compute the CL of the catheters. For simplification, we consider half of the CL of catheter and half CL of RCA. The half CL is further simplified to the length between the tip of the catheter and the point at its maximum curvature. We call this length the *Catheter Half Curve Length* (CHCL)and compute CA and CHCL of all the catheters in this way.

Artery's Curve Computation from the Patient's Image Data

A series of steps are needed for computing CA of the RCA. We need to segment the aorta and the RCA, get the centerline, find the RCA curve and then compute the CA of the RCA. The algorithm for optimal catheter computation is independent of the segmentation schemes and any segmentation scheme that extracts the aorta and the coronary arteries can be used. For this work, we use image data where the aorta and the coronary arteries have been segmented. In the next step, we extract the

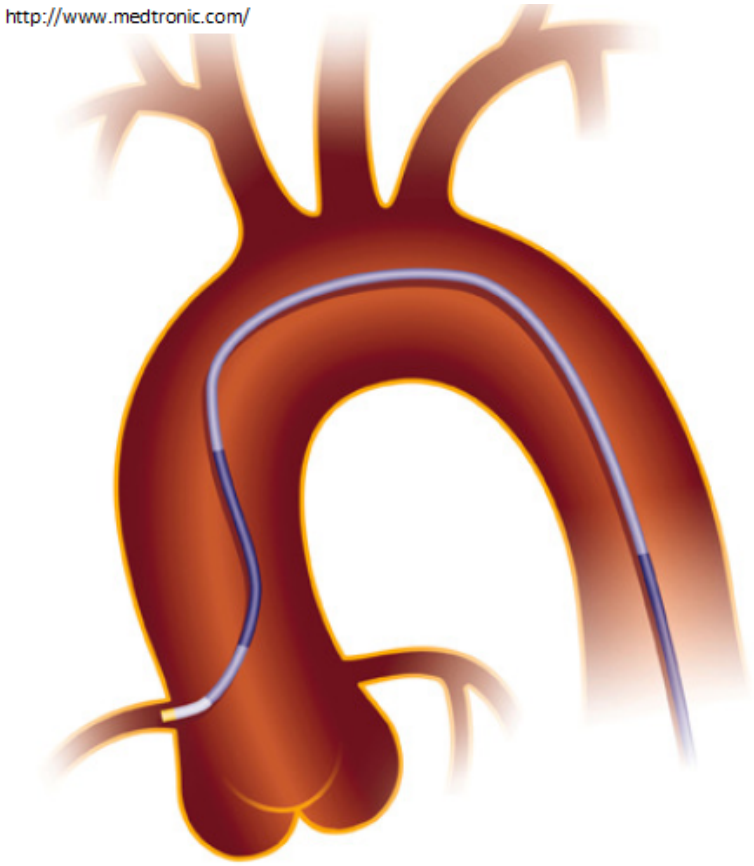

Figure 3.12.: Catheter placed along the aorta and the coronary arteries' centerline is an optimal catheter for the right coronary artery with normal takeoff.

centerline of segmented images (see Figure 3.15 a). We have used the *Binary Thinning Image Filter algorithm for 3D images* [Hom07] for the centerline extraction. To extract the RCA curve in the skeleton image, we perform a search using the axial view. We start searching the slices from bottom to top and search the first slice with a non zero pixel. The position of the pixel at the first non-zero slice (point A in Figure 3.15 (b)) is selected as starting pixel point. Then we try to find the tip of the RCA (point B in Figure 3.15 (b)). This is done by iteratively searching non-zero neighbor pixels and selecting the pixels with minimum X indices. This condition compels the search-pointer to follow the main aorta and then enter into the right coronary artery (green line in Figure 3.15 (b)).

In the next step, we find the path (red curve in Figure 3.15 (b)) from the tip of the RCA to the tip of the Left Coronary Artery (LCA). We start the search from point B and search the neighbor non-zero pixels and select the pixels with maximum Z and X indices. These conditions compel the pointer to reach to the tip of the LCA (point C in Figure 3.15 (b)). In the third step, we start again from the point

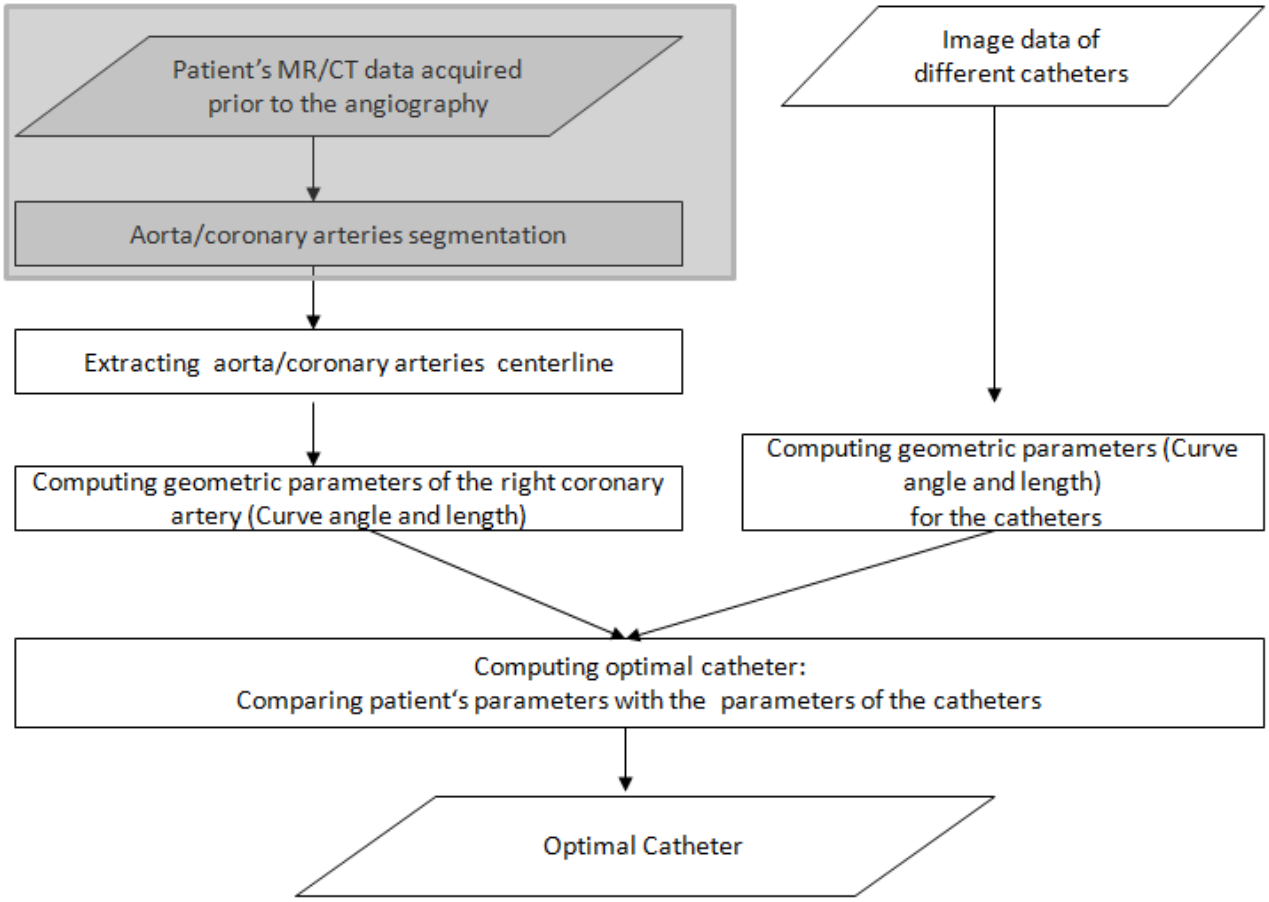

Figure 3.13.: Optimal catheter selection for the right coronary artery.

B and explore neighbor pixels checking if a pixel belongs to the green and the red curve. If a pixel does not belong to the red curve then it is marked as a branching point of the RCA (point D). Then we follow the green line in upward direction untill half of the ascending aorta and extract the yellow line as the RCA curve.

The RCA is extracted from the 3D images and we have to reduce the dimension to 2D in order to allow a comparison with the 2D catheters. Therefore, we project the RCA curve onto a 2D plane. The projection plane is the plane formed from points B, D and E. After reducing the dimension of the RCA, the next step is to compute the CA. We consider the two points $\bar{B}$ and $\bar{E}$ (see Figure 3.15 (c)). The point $\bar{B}$ is obtained by averaging the index of five pixels starting from the point B along the curve and the point $\bar{E}$ is the averaged index of the five pixels along the curve starting from the point E towards the point B. We then create a line starting from the point B and passing through the point $\bar{B}$ and a line starting from the point E and passing through the point $\bar{E}$. Then we project these lines on the plane

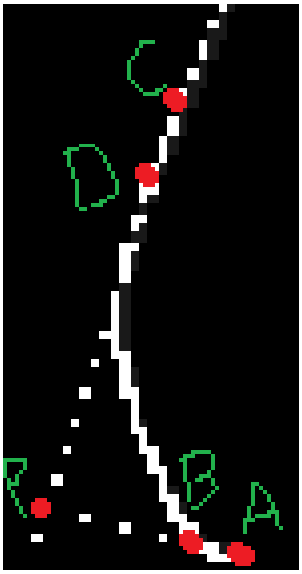

Figure 3.14.: Catheter's curve angle computation.

formed from the points B, D, and E. We find the intersection point P between these two lines. Then we compute the angle between the points B, P and E which is the CA of the the RCA.
In case of the catheter, we simplified the CL of the catheter to the length between the tip of the catheter and the point at its maximum curvature. Here too, we simplify the CL of the RCA to the distance between points B and D and call it Right Coronary Artery Half Curve length (RCAHCL). Now we have computed the CA of the catheters, CA of RCA, CHCL and RCAHCL.

Optimal Catheter Selection

After computing parameters for all the catheters and for the given patient's image data, our next step is to define a quantitative measure for the optimal catheter selection. We propose the following cost function. The optimal catheter is given as the minimum of all the costs CC_i computed for all considered catheters i.

$$OC = \arg\min_i \{CC_i\} \tag{3.1}$$

where i is the i^{th} catheter and

$$CC_i = a\sqrt{\left(\frac{1}{N_{CL}}\left((CHCL)_i - RCAHCL\right)\right)^2} + b\sqrt{\left(\frac{1}{N_{CA}}\left((CA)_i - RCACA\right)\right)^2} \tag{3.2}$$

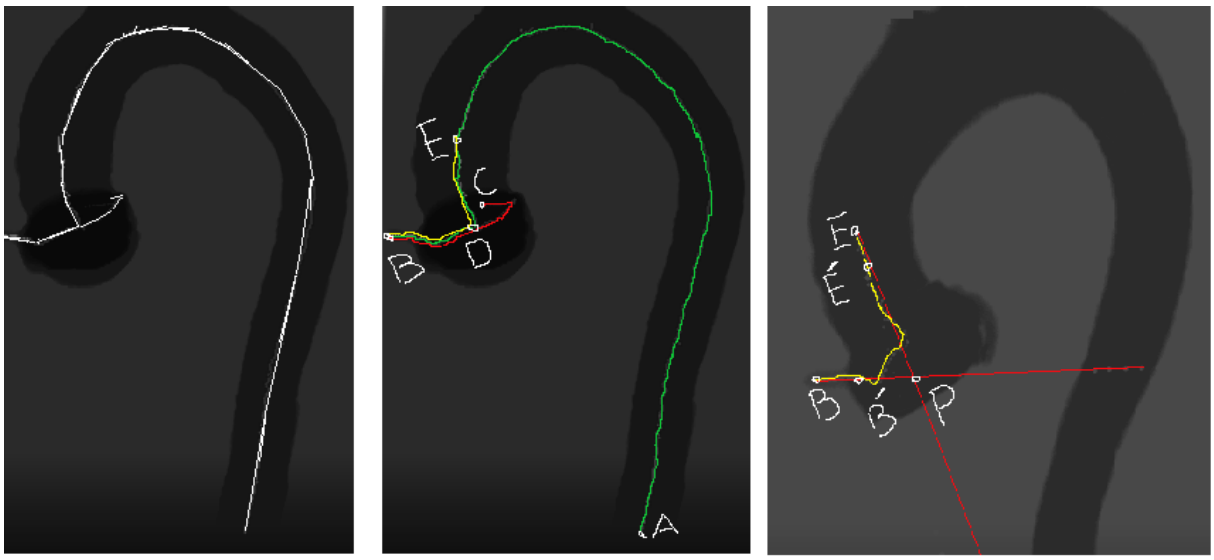

Figure 3.15.: Right coronary artery curve computation.

where N_{CL} and N_{CA} are the normalization factors for the curve length and curve angles, respectively. Coefficients a and b are weights assigned to each term of the formula. The strongest criteria for the catheter selection should be the best matching of CHCL and RCAHCL. The best match of this parameter will guarantee that the catheter has a suitable CHCL for the given patient geometry. These weights however, are heuristic values derived from the importance of each parameter. In Chapter 4, we will discuss how to select optimal values for these parameters.

3.4.3. Model for the Left Coronary Angiography

Catheter selection for the left coronary angiography is not as straightforward as for the right coronary angiography. During left catheter selection many factors are needed to be satisfied. We need to consider the different types of coronary artery's takeoff, size of the aorta, length and diameter of the ascending aorta and backup support for the catheter. The most important parameter for the left coronary angiography is the length of the catheter segment between the two curves of the catheter (see Figure 3.16). This segment should be long enough to reach the ostium of the left coronary artery.

The next important parameter is the takeoff of the left coronary artery. The takeoff can be either superior, inferior or lateral. The catheter having a suitable tip angle is to be selected. If the catheter tip is not coaxial then the tip can damage the artery (see Figure 3.17 (a)). A third important parameter is the backup support provided at the contralateral wall of the aorta. The stability of the catheter depends on the amount of backup. For example, in Figure 3.18 (a), the backup is provided at one point where

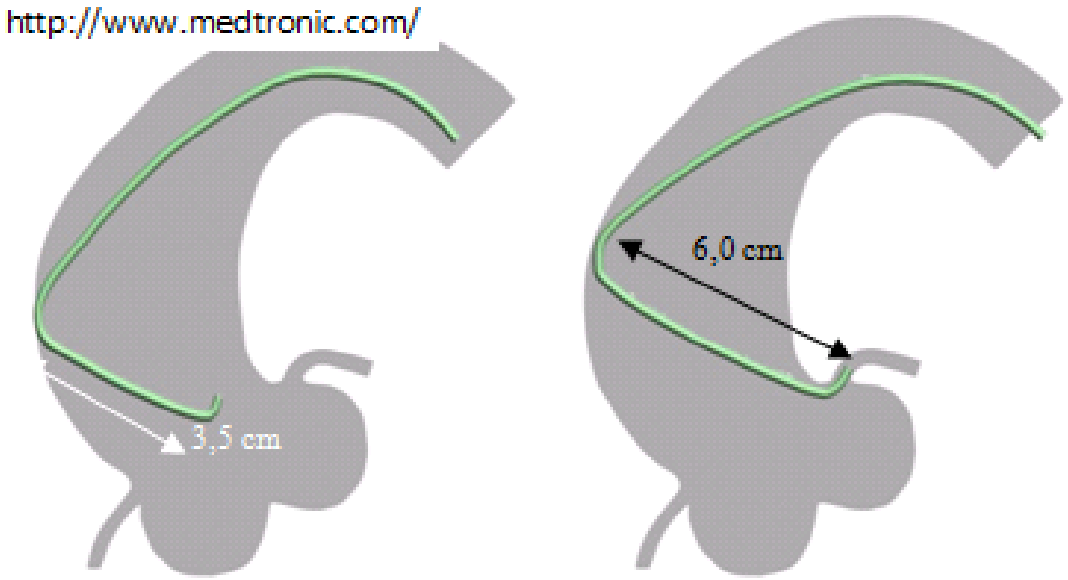

(a) Catheter is too small and does not reached the ostium. (b) Catheter length is enough, it reaches the ostium and has coaxial placement in the ostium.

Figure 3.16.: The length of the catheter segment between the two curves plays an important role in the catheter selection decision.

as in Figure 3.18 (b), there is sufficient backup at the contralateral wall, guaranteeing a more stable placement of the catheter.

Clinically, it is confirmed that a catheter is said to be ideally placed when it has coaxial position in the coronary artery and has sufficient support at the contralateral wall of the aorta (see Figure 3.19). We consider these guidelines and present a catheter model for the left coronary angiography.

Our method can be described as follows:
We consider the angle and length of the two curves of catheters (green and yellow curves in Figure 3.20 (b)). We call the yellow curve *Catheter's Curve 1* (CC1) and the green curve *Catheter's Curve 2* (CC2). CC1L is the *length of CC1*. CC2A is the *angle of CC2*. The distance between CC1 and CC2 (white segment in Figure. 3.20 (b)) is referred to as the *Catheter's Straight Segment Length* (CSSL). From patient image data (see Figure 3.20 (a)) we consider the following parameters:

- The yellow curve is the *Contralateral Wall Curve* (CWC).
- The green curve as *LCA curve* (LCAC).
- The *length of CWC* (CWCL).
- The *angle of LCAC* (LCACA)

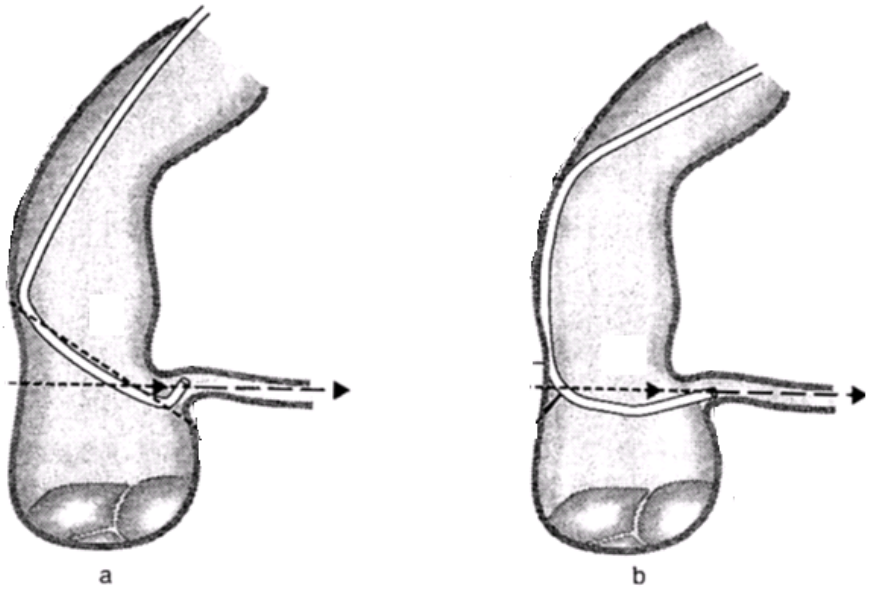

Figure 3.17.: , Risk of artery damage (a), Suitable placement with no chance of artery damage (b) [Vod92]

- The *distance between CWC and LCAC* (white line in Figure 3.20 (a)) is referred as the Aorta Cavity Length (ACL).

3.4.3.1. Catheters' Parameters Computation

Computing curve angles and lengths of catheters is straight forward. We take photos of the catheters and extract the centerline of the catheters. We then consider the two curves (yellow and green curves in Figure 3.21). The yellow curve provides back-up support at the contralateral wall of the aorta. The distance from point N to O is considered as CC1 Length (CC1L). Catheter's Curve 2 Angle (CC2A) is computed using points Q, Y and T. This angle has to be matched with the LCACA. The Catheter Straight Segment Length (CSSL) is the length between the points O and S which will be matched to the ACL.

3.4.3.2. Arteries' Curves Computation from the Patient's Image Data

Curves computation of the LCA is more difficult and is done as follows. We need to segment the aorta and LCA, get the centerline, find the LCACA, CWCL and ACL. We have described our automatic segmentation technique in our paper [FRWV11]. However, the algorithm for optimal catheter computation is independent from segmentation schemes and any segmentation scheme that extracts the aorta

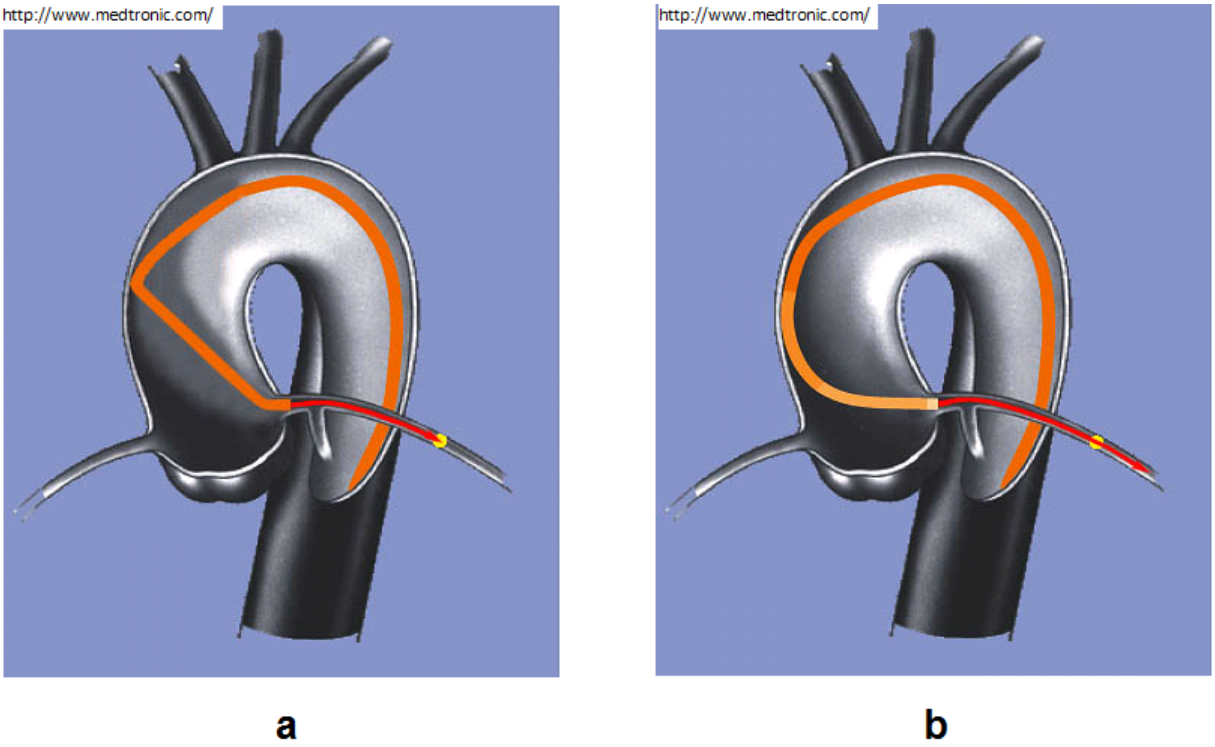

Figure 3.18.: Back up at only one point at the contralateral wall (a), Sufficient backup guarantees stable placement.

and the coronary arteries can be used. In Figure 3.22 (a) the segmented arteries and the centerline are shown. During left coronary angiography, the catheter follows the centerline inside the descending aorta and the aortic curve. It then follows the tangent path at the maximum curvature point of the aortic curve, hits the contralateral wall, moves along the contralateral wall and then bends towards the LCA. In Figure 3.22 (b) the green line shows such a path. Although the catheter may sometimes deviate from this path, we will show below that it will not have significant effect on our overall results. In Figure 3.22 (c) the different points that are used for the curves computation of the arteries are shown. Point A is the point where the aortic curve has maximum curvature. The Points B and $\bar{B}$ are the adjacent points of point A on the centerline. The catheter is supported by the contralateral wall in the area between the points C and D. The point C can be computed using the tangent line at point A. This tangent line can be estimated by a line that passes through the points B and $\bar{B}$. The tangent line is extended until it touches the contralateral wall. This point is marked as the point C. The point D can be computed in the same way using the points E and F. The point E is the branching point in the centerline. The Point F is the position of the LCA ostium and G is the tip of the LCA. The method to find points E and G are explained in our paper [RWV11a] and the ostium position in our paper [FRWV11].

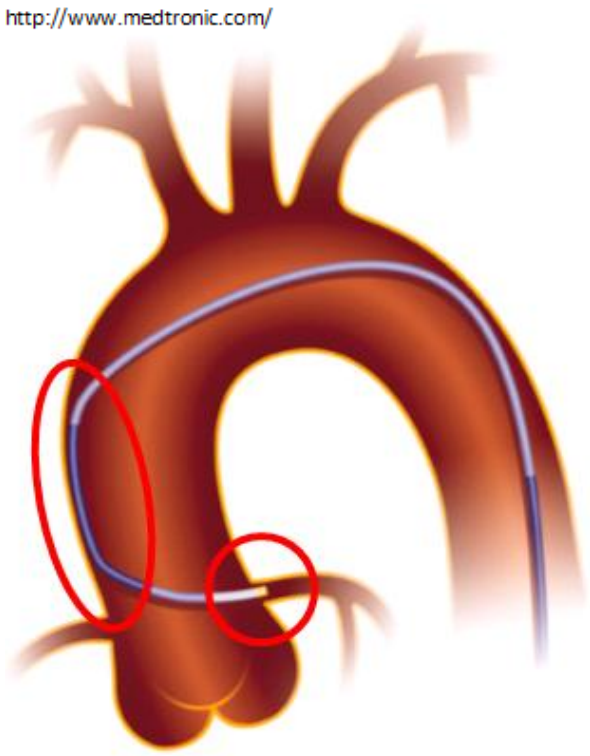

Figure 3.19.: Ideal position: During left coronary angiography the ideal position of the catheter is to have coaxial tip position and a stable backup support.

Contralateral Wall Curve Length (CWCL):
The CWCL is taken as the distance between point C and D in Figure 3.22 (c). This length shows the area where the catheter is touching the contralateral wall and gets backup support.

Left Coronary Artery Curve Angle (LCACA):
The LCACA is computed using the two green lines (see Figure. 3.22 (c)). First, we compute the intersection point F of these two lines and then the angle between the points E, F and G.

Aorta Cavity Length (ACL):
The most important parameter is the ACL, i.e. the length between the LCA branching point F and the point D. This length is compared with the CSSL. We want to emphasize that all these computations are done automatically.

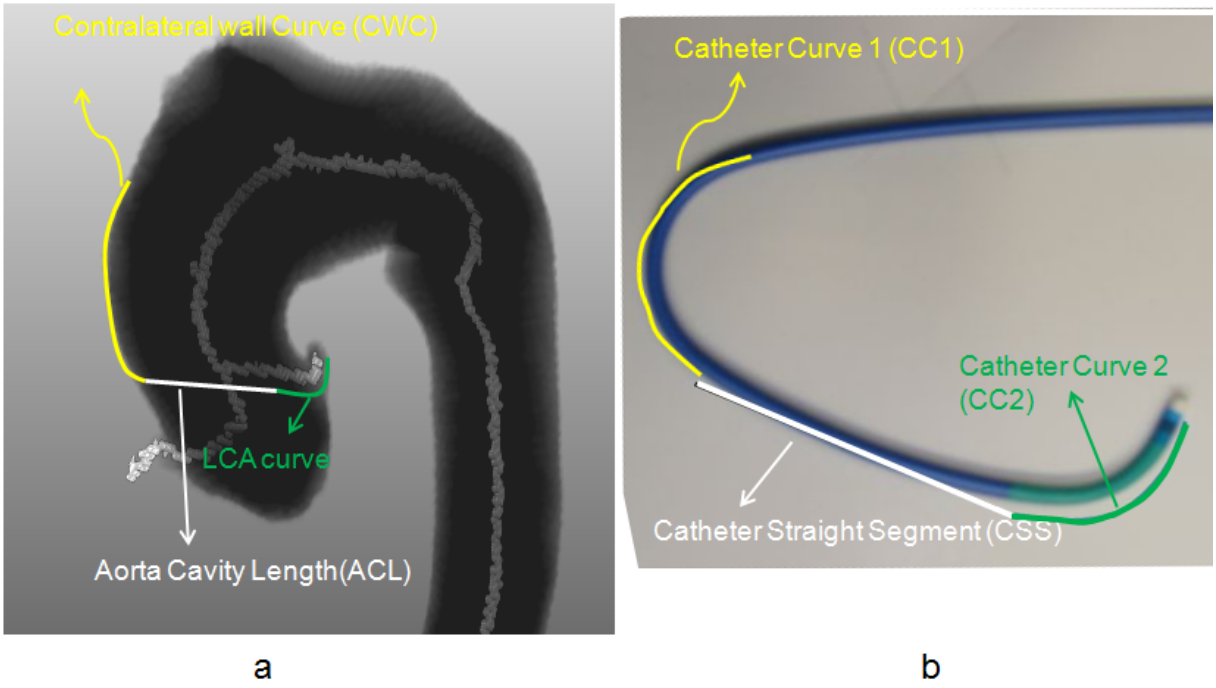

Figure 3.20.: Parameters for the arteries (a), parameters for the catheters (b).

3.4.3.3. Optimal Catheter Selection

After computing parameters for all the catheters and for the given patient's image data, our next step is to define a quantitative measure for the optimal catheter selection. We propose the following cost function. The optimal catheter is given as the minimum of all the costs CC_i computed for all the considered catheters i.

$$OC = \arg\min_i \{CC_i\} \tag{3.3}$$

where i is the i^{th} catheter and

$$CC_i = a\sqrt{\left(\frac{1}{N_1}\left((CSSL)_i - ACL\right)\right)^2} + b\sqrt{\left(\frac{1}{N_2}\left((CC2A)_i - LCACA\right)\right)^2} + c\sqrt{\left(\frac{1}{N_3}\left((CC1A)_i - CWCA\right)\right)^2} \tag{3.4}$$

Where N_1, N_2 and N_3 are the normalization factors and a, b and c are weights assigned to each term of the formula. The strongest criterion for the catheter selection is the best matching of CSSL and ACL and a is a weight coefficient for this term. The best match of this parameter will guarantee that the catheter has a suitable CSSL for the given patient's ACL. Therefore, highest weight should be given to

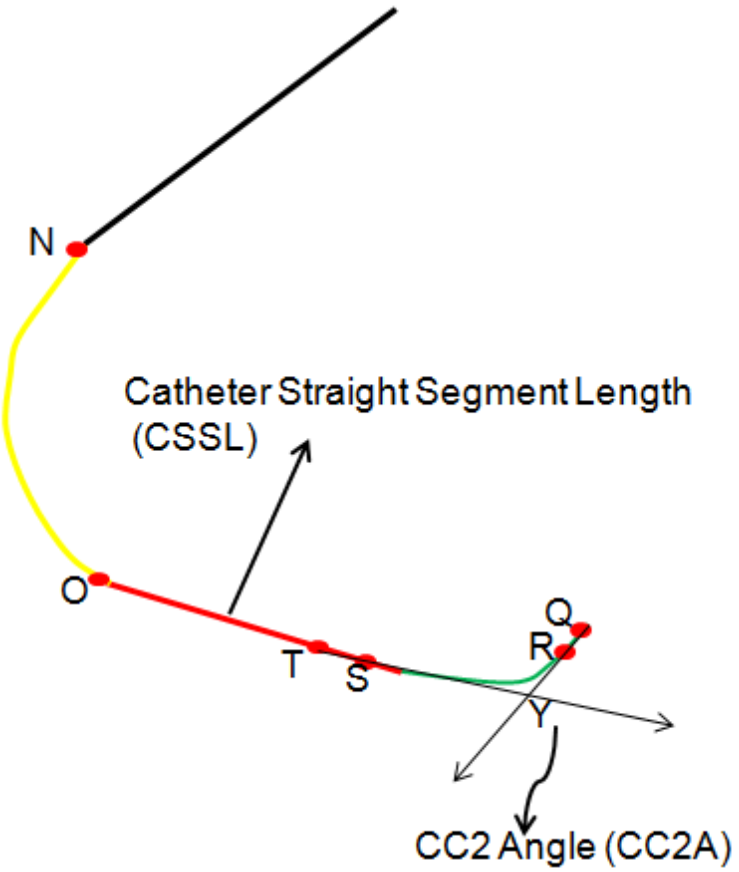

Figure 3.21.: Catheter's parameters computation.

a. The next important criterion for the optimal catheter selection is the difference between CC2A and LCACA. *b* is a weight coefficient for this term and it gets next highest value. The weight coefficient for the difference between CC1L and CWCL is *c*, representing the backup support. Backup support is important but before looking at this it should be assured that the catheter has already reached the LCA at the correct angle. Therefore, we give the smallest weight to *c*. In the next chapter, we will present experiments for finding optimal values for *a*, *b* and *c*.

3.4.4. Model for the Coronary Arteries with High Takeoff

In Section 3.4.2 and 3.4.3, we discussed catheter selection models for a normal left and right coronary artery. If the distance of a coronary artery's ostium is greater than 1.5 *cm* then such a takeoff is referred to as a high takeoff. In this case, the catheter is placed close to the aortic valves (see Figure 3.23) and the backup support is provided from the aortic valves as well as contralateral wall of the aorta. Special

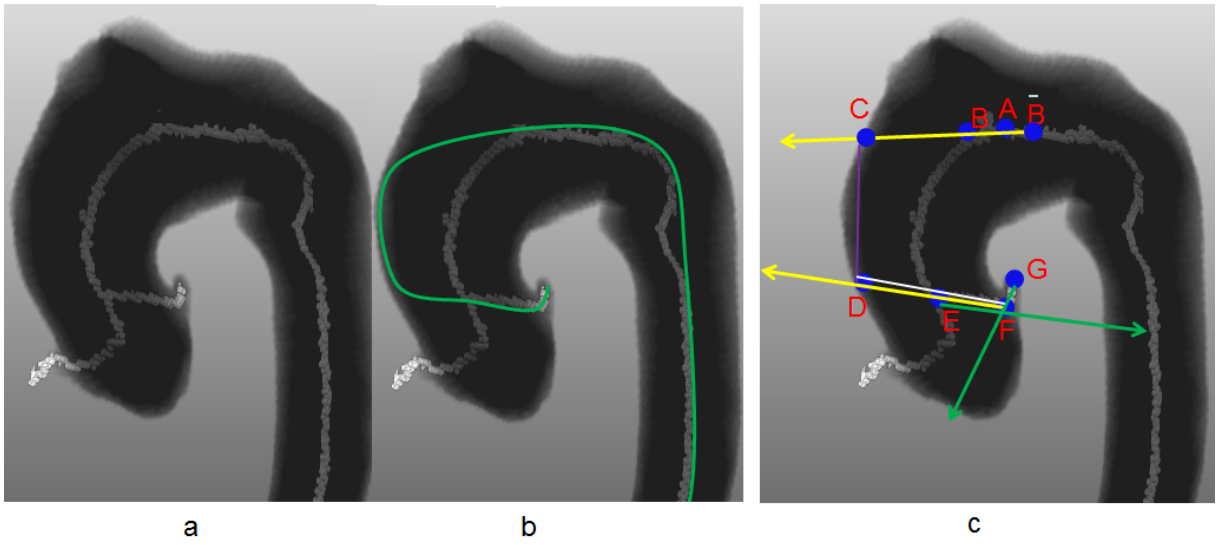

Figure 3.22.: Arteries' parameters computation.

catheters called *Amplatz* are used for this purpose. An amplatz right coronary catheter can be used to cannulate right coronary arteries with abnormal, usually, an inferior origin. An amplatz left coronary catheter is used to engage left coronary ostium which is difficult to cannulate with other catheters. An amplatz left coronary catheter is also used to engage high anterior right coronary arteries.

In order to compute the optimal catheter selection for the coronary arteries with a high takeoff we first compute the distance between the ostium and the aortic valves. In Figure 3.24, an optimally placed catheter is shown where the secondary curve of the catheter is positioned at the aortic valves, and the primary curve has co-axial position at the coronary artery curve. The secondary curve has enough depth to reach the coronary arteries, and the secondary curve has a width equal to the aorta diameter. If the width is smaller than the aorta diameter then the backup support will be loose at the aortic valves as well as at the contralateral wall. If the width is greater than the aorta diameter then it will be difficult to optimally place the primary curve inside the coronary artery. We use these parameters and compute an optimal catheter.

We compute coronary arteries' curve angle (CACA) (see Figure 3.25 (a) red curve), distance of the ostium from the aortic valves, i.e., the Ostium Height (OH) (see Figure 3.25 (a) violet line) and the aorta diameter (AD) near the ostium (see Figure 3.25 (a) blue line). We then consider catheters and compute Catheter's Primary Curve Angle (CPCA) (see Figure 3.25 (b) red curve), catheter's Secondary Curve Depth (CSCD) (see Figure 3.25 (b) violet line) and Catheter Secondary Curve Width (CSCW) (see Figure 3.25 (b) blue line). We compare CACA with CPCA, OH with the CSCD and AD with CSCW and suggest a catheter that is the closest to the patient's arteries geometry.

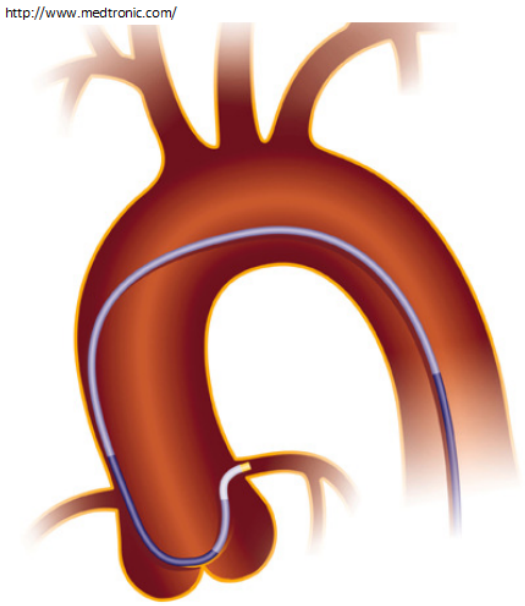

Figure 3.23.: Optimal placement using an amplatz catheter. Amplatz is able to deeply engage the coronary artery.

3.4.4.1. Catheter's Parameters Computation

In Figure 3.26 we have shown the different parameters used in our computation. The Amplatz catheter has two curves. We have marked the first curve in red color and named it Catheter's Primary Curve (CPC) and the second curve in green color and named it Catheter's Secondary Curve (CSC). The following parameters are computed for all the Amplatz catheters. We consider the primary curve angle and the secondary curve depth and width. We consider point R as the point of maximum curvature at CPC and point X as the point with maximum curvature at CSC.

Catheter Secondary Curve Width (CSCW): Line PQ is a tangent line at point X of CSC. We draw a line RS starting from point R and going parallel to line PQ. This line intersects CSC at point O. The distance between R and O is CSCW.

Catheter Secondary Curve Depth (CSCD): We draw a line XY, starting from point X and is being perpendicular to the tangent line PQ. Line XY intersects line RS at point M. The distance between X and M is CSCD.
Catheter Primary Curve Angle (CPCA): The angle of the catheter's primary curve is named as CPCA.

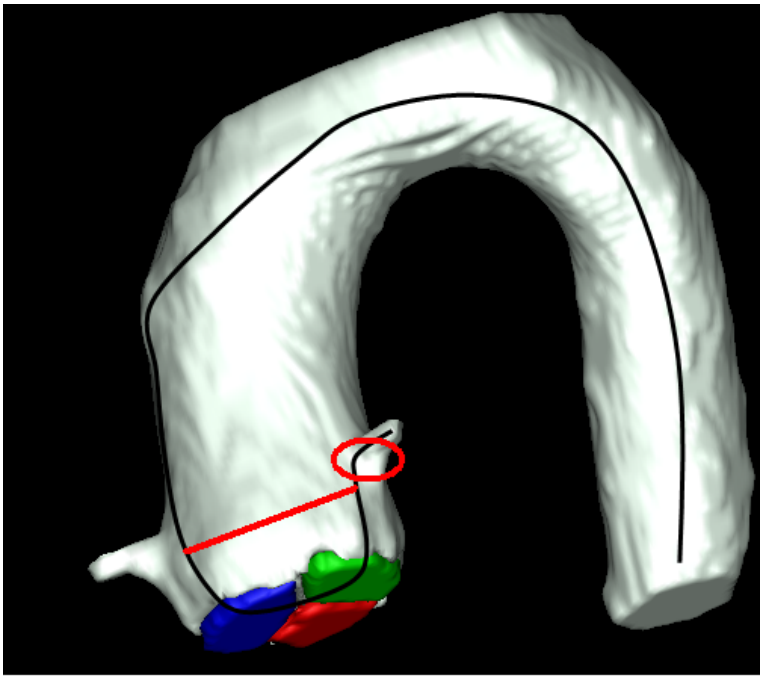

Figure 3.24.: Optimally placed catheter.

3.4.4.2. Geometric Parameters from the Patient's Image Data

For computing parameters from the patient's image data, the segmented arteries are obtained from the MR/CT data. Then the following parameters are obtained.

Ostia Height (OS): To compute the height of the ostium, we need to know the ostium position and the aortic valves. In Section 3.3 we have described how to find these parameters.

Aorta Diameter (AD): We are interested in the aorta diameter near the ostium. The details can be found in Section 3.3.

Coronary Artery Curve Angle (CACA): For computing the coronary arteries curve computation the method presented in section 3.4.2 and 3.4.3 is used.

3.4.4.3. Optimal Catheter Selection

Similar to models for right and left coronary arteries, here too, we define a quantitative measure for the optimal catheter selection. We propose the following cost function. The optimal catheter is given as the minimum of all the costs CC_i computed for all considered catheters i.

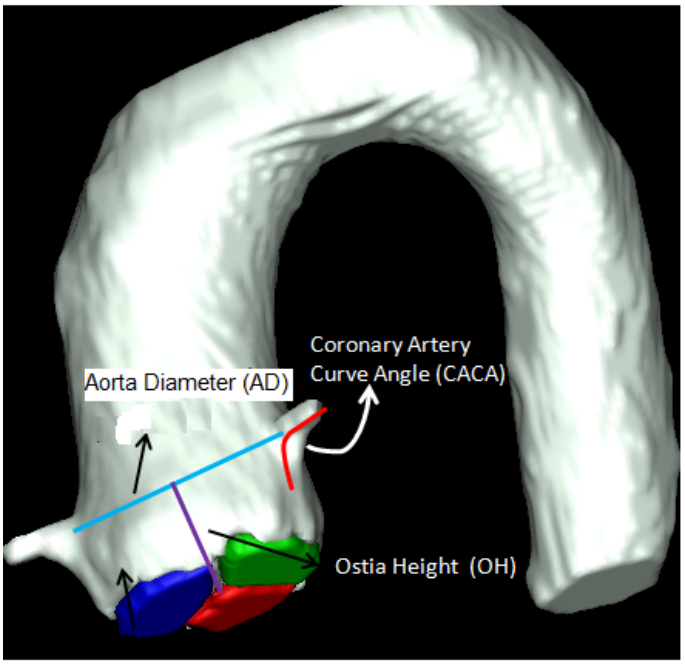

a

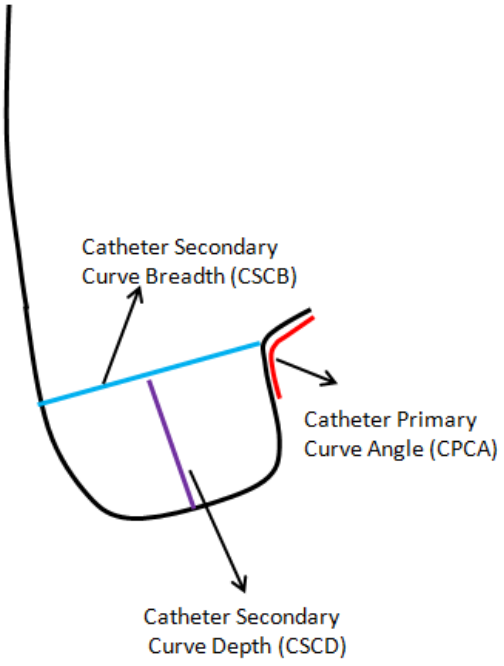

b

Figure 3.25.: Optimal catheter selection.

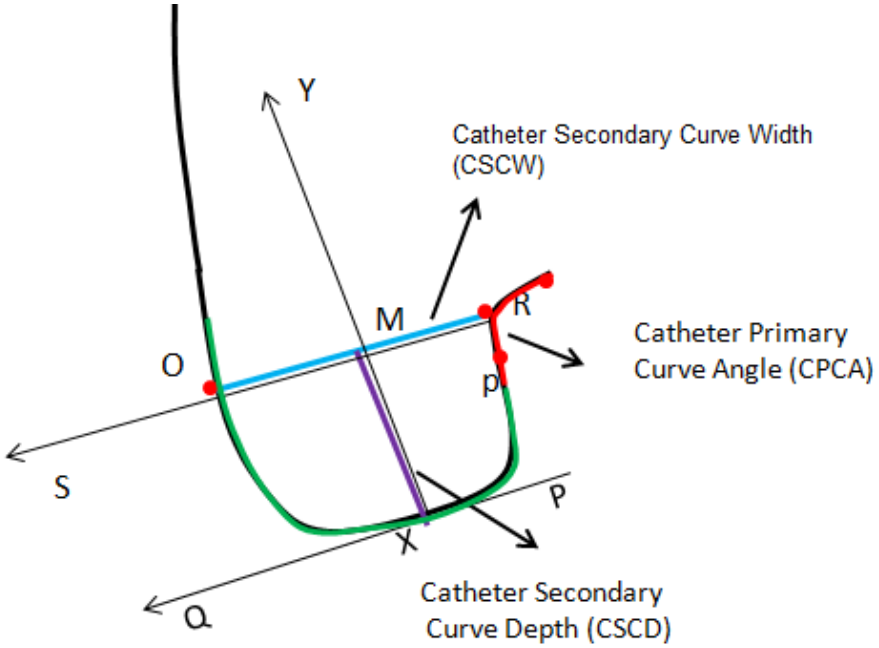

Figure 3.26.: Catheter parameters computation for Amplatz catheters.

$$OC = \arg\min_{i} \{CC_i\} \tag{3.5}$$

where i is the i^{th} catheter and

$$CC_i = a\sqrt{\left(\frac{1}{N_1}\left((CSCD)_i - OH\right)\right)^2} + b\sqrt{\left(\frac{1}{N_2}\left((CSCB)_i - AD\right)\right)^2} + c\sqrt{\left(\frac{1}{N_3}\left((CPCA)_i - CACA\right)\right)^2} \tag{3.6}$$

Where N_1, N_2 and N_3 are the normalization factors. We have given different weights to each term of the formula. The strongest criteria for the catheter selection should be the best matching CSCD and OH. The best match of this parameter will guarantee that the catheter has a suitable depth for the given patient geometry. Therefore, highest weight is given to this parameter. The next important parameter is the breadth which will guarantee tight placement of the catheter, and the third parameter will ensure a suitable angle. Selecting optimal values for a, b, c will be discussed in the next chapter.

3.4.5. Discussion

In this section, we presented different image processing based patient-specific models for best catheter selection. The objective of these models is to replace the conventional *trial and error* based catheter

selection procedure. We presented models for right coronary angiography, left coronary angiography and for angiography of an anomalous coronary arteries. These models will reduce the catheter choices from many to few and will make the job easier for inexperienced cardiologists. These models will also help to reduce the patient's exposure time to radiation. Our models still need to include further anomalous cases.

3.5. Simulation

3.5.1. Introduction

In Section 3.4 we presented different models for reducing the large number of catheter choices to few choices. There, for simplicity reasons, we have assumed catheters as rigid objects but in reality, the catheters may deform their original shape inside the patient's arteries. The original computations of the catheter's parameters may not remain the same when the catheters are inside the patient's arteries. Therefore, it is important to further refine decisions of our reduced number of catheters by simulating these inside the patient's arteries. This will help us to know the correct final position of the catheters. We will also be able to compare catheter's parameters before insertion thus providing correct information about the deformation of a catheter from its original shape. We will also simulate catheters other than our suggested catheters and will thus be able to know whether any catheter other than our suggested range, can also be part of an optimal catheters list. The simulation will help the cardiologists to visualize all the suggested catheters as well as his/her own choice of catheters and see the final placement.
For simulation, we will use patient-specific arteries' model that will be computed from the patient image data acquired prior to the intervention. The catheters and guidewires will be modeled using Finite Element Method (FEM). The reduced number of catheters will be simulated in a patient-specific arteries' model, final placement of different catheters will be obtained, and an optimal catheter will be suggested. The simulation will be implemented using the *Simulation Open Framework Architecture* (SOFA).

3.5.2. Catheter and Guidewire Simulation in Patient Specific Arteries Model

3.5.2.1. Arteries Modeling

For arteries' modeling, we need to segment the aorta and coronary arteries. We have described an automatic segmentation technique in our previous work [FRWV11]. However, the modeling algorithm is independent from segmentation schemes. Thus, any segmentation scheme that extracts the aorta and the coronary arteries can be used. A surface mesh is created from the segmented images using a series of VTK filters [SML06, Kit11] (see Figure 3.27 (a))

3.5.2.2. Catheter and Guidewire Modeling

The catheter is a flexible wire made of a rubber or plastic material and is used to transfer contrast agent to the location of interest. A guidewire is a flexible spring used to provide additional stiffness to the catheter and guide the catheter towards the location of interest. For details please look at Section. 1.3.2.

We model the catheter as flexible beams that bend when they collide with the internal walls of the arteries. We need different parameters for the model, for example, diameter, mass and modulus of elasticity (Young's Modulus). We consider diameter and length of the catheters. We then discretize the catheters and find the mass of each point. For this, we measure the mass of the whole catheter and then divide it by the number of discrete points. The essential parameter for the simulation obtained by direct measurement is the modulus of elasticity. We use the following beam deflection formula to compute the elasticity [Hib10].

$$\delta_{max} = P \cdot L^3 / 3 \cdot E \cdot I \tag{3.7}$$

Where δ_{max} is the maximum deflection, P is the applied force, L is the beam length, E is the modulus of elasticity and I is the second moment of inertia. For the second moment of inertia the following formula [Pil02] is used.

$$I = phi/64 \cdot ((OD)^4 - (ID)^4) \tag{3.8}$$

Where OD and ID is the outer and inner diameter of the catheter, respectively.

To compute δ_{max} in Equation 3.7 we take each catheter and divide the whole catheter into different small segments. The length of each segment is taken as one centimeter. We fix one end of the segment and apply a force of one Newton at the other end of the segment and measure the maximum deflection (see Figure 3.28).

To compute I in Equation 3.8, OD and ID are read from the catheter manual.
Catheters are modeled as triangulated surface meshes. Guidewires are modeled as one dimensional bendable beams. For catheters and guidewires, denser sampling is taken at the curved area and sparse sampling at the straight area.

3.5.2.3. SOFA Framework

Having created the models for the arteries and catheters, the next step is the simulation. We use the *Simulation Open Framework Architecture* (SOFA) [ACF*07][1] for simulation. SOFA is an open source framework used for real-time simulation. Based on an advanced software architecture, it allows creating complex and evolving simulations by combining new algorithms with algorithms already included in SOFA. It allows to modify most parameters of the simulation, i.e., deformation behavior, surface representation, solver, constraints and collision algorithms etc. It efficiently simulates the dynamics

[1] http://www.sofa-framework.org/

of interacting objects using abstract equation solvers. There are many collision models like *SphereModel, SphereTreeModel, CubeModel, TetrahedronModel, TriangleModel* etc. A number of ordinary differential equation (ODE) solvers are also available in SOFA.

3.5.2.4. Catheter's Simulation

In our algorithm, we have used different components of SOFA. The scene graph of our simulation is described as follows (see Figure 3.29):
Different segments of a catheter have different elasticity levels. Therefore, we model a catheter as a combination of these segments. The segments are connected using the *AttachConstraint* component. All the segments use *CGLinearSolver* component as linear solver and *CGImplicitSolver* component as ODE solver. Every segment uses its own *MechanicalObject* component for representing position and velocity coordinates. Similarly, each segment uses its own *BeamFEMForceField* component for beam finite elements representation. For topology representation, each segment uses its own *MeshTopology* component. Each segment uses the *LineModel* and *PointModel* components for the collision detection. For the arteries' representation, the *MeshLoader* component is used to load the mesh object file. *MechanicalObject* component is used for representing position and velocity coordinate. *OGLModel* component is used for visual representation. *TriangleModel*, *LineModel* and *PointModel* components are used for the collision detection. Velocity directions for the catheter are obtained from the centerline of the arteries (for details of the simulation, please see [RTWV12]).

We simulate different catheters and find the final position of the catheters. We want to see how closely these different catheters are placed along the clinically confirmed optimal path. For this, we divide the Optimal Path (OP) into N equidistant points. Similarly, we consider the final placement of the catheters after simulation and every catheter k is divided into N equidistant points. Then we compute the distance between catheter k and ACL.

$$distanceCatheter_k = \sum_{i=1}^{N} \left(\sqrt{(Catheter_{ki} - OP_i)^2} \right) \tag{3.9}$$

Where $Catheter_{ki}$ is the i^{th} point of catheter k and OP_i is the i^{th} point of OP. Since the points are in space so we can write this equation as

$$distanceCatheter_k = \sum_{i=1}^{N} \left(\sqrt{(X_{Catheter_{ki}} - X_{OP_i})^2 + (Y_{Catheter_{ki}} - Y_{OP_i})^2 + (Z_{Catheter_{ki}} - Z_{OP_i})^2} \right) \tag{3.10}$$

Where $X_{Catheter_{ki}}$, $Y_{Catheter_{ki}}$ and $Z_{Catheter_{ki}}$ are the x, y and z coordinates, respectively, of the i^{th} point of k^{th} catheter. X_{OP_i}, Y_{OP_i} and Z_{OP_i} are the x, y and z coordinates of the i^{th} point of OP respectively. The optimal catheter will be selected as the one with the closest distance to the centerline.

$$OptimalCatheter = \arg\min_{k} \{distanceCatheter_k\} \tag{3.11}$$

3.5.3. Discussion

In this section, we presented a simulation based technique for patient-specific optimal catheter selection. This work is an extension of our previous approach where we have developed models for reducing the catheter choices. In those models, we have not considered the deformable nature of catheters and also considered the arteries as rigid bodies. In this work, we simulate the catheters inside the arteries and consider its shape after deformation. We can also change stiffness of the arteries which helps to get more realistic final position of the catheters. The simulation takes more time as compared to simple parameters' computation but it considers the deformable nature of catheters as well as arteries. This work will help (especially) inexperienced cardiologists who try many catheters per patient.

3.6. Summary

In this chapter, we presented a concept of an image processing based patient-specific catheter selection. The model is able to replace the conventional *trial and error* based procedure. Using this model, the cardiologist will already get a recommendation about an optimal catheter for a given patient prior to the intervention. This model involves a series of steps like segmentation of the arteries from the patient images, skeletonization, parameters computation, reducing catheter choices and simulation. We presented a complete automatic scheme for segmenting the aorta and coronary arteries from the MR image data. Using the segmented arteries, we developed algorithms to compute different geometric parameters. These algorithms are completely automatic and the different parameters like centerline extraction, diameter of the aorta and coronary arteries, aortic valves, ostia of the left and right coronary arteries, angles of the left and right coronary arteries and distance of the ostia from the aortic valves are computed without user intervention. Using these parameters as well as parameters from the catheter, we developed different models for reducing the catheter choices. These models are developed for right and left coronary angiography as well as for angiography where the coronary arteries have abnormal takeoff. In these models, we have considered the catheters and arteries as rigid object which may lead to inaccurate results due to the fact that catheters deform inside the arteries. In order to compensate for this, we presented a simulation scheme which simulates the reduced number of catheters and final placement of different catheters are obtained after simulation. The simulation helps us to visualize the catheters' final placement inside the patient's arteries that give clear idea to the cardiologist how the different catheters will look inside the patient's arteries.

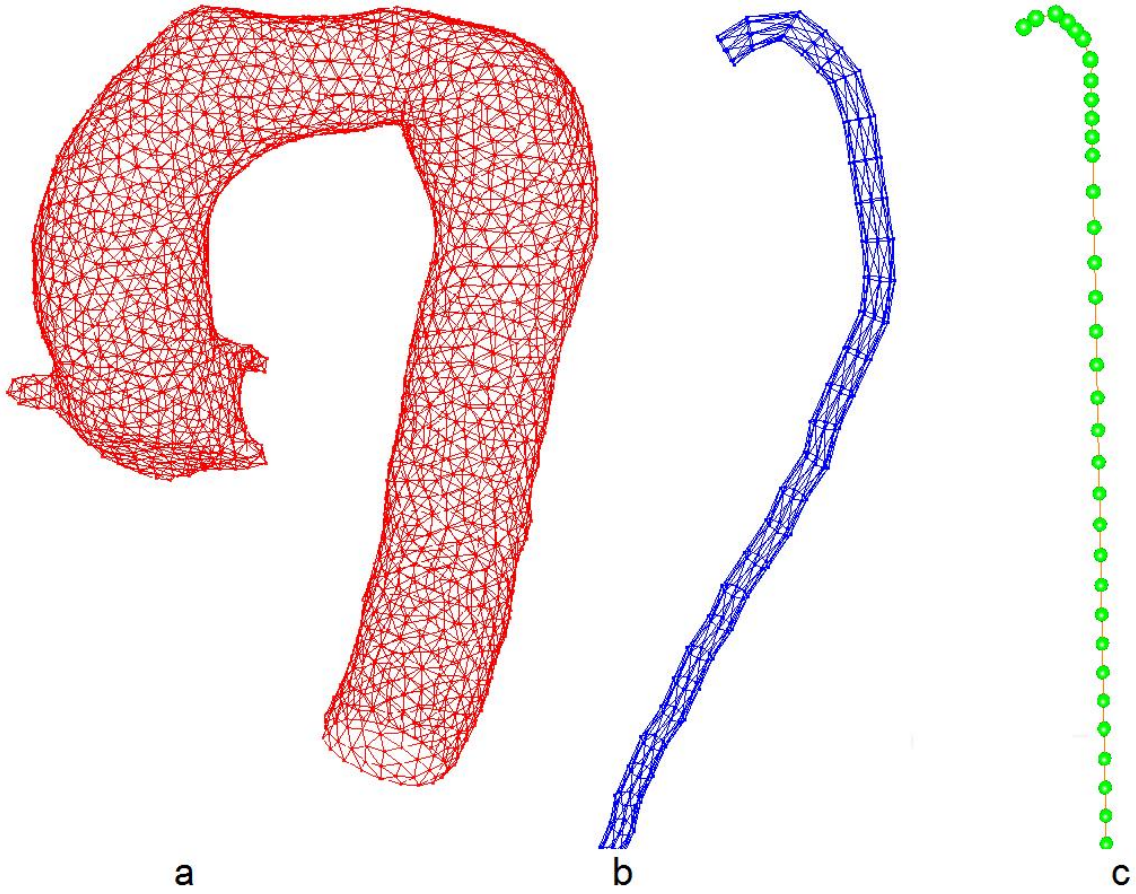

Figure 3.27.: The artery's surface mesh is created from the segmented images (a), For catheter modeling, the centerline is created from the photos of catheters and then the 3D catheter is created from the centerline using the diameter of the original catheter (b). Guidewires are modeled as one dimensional beam element (c).

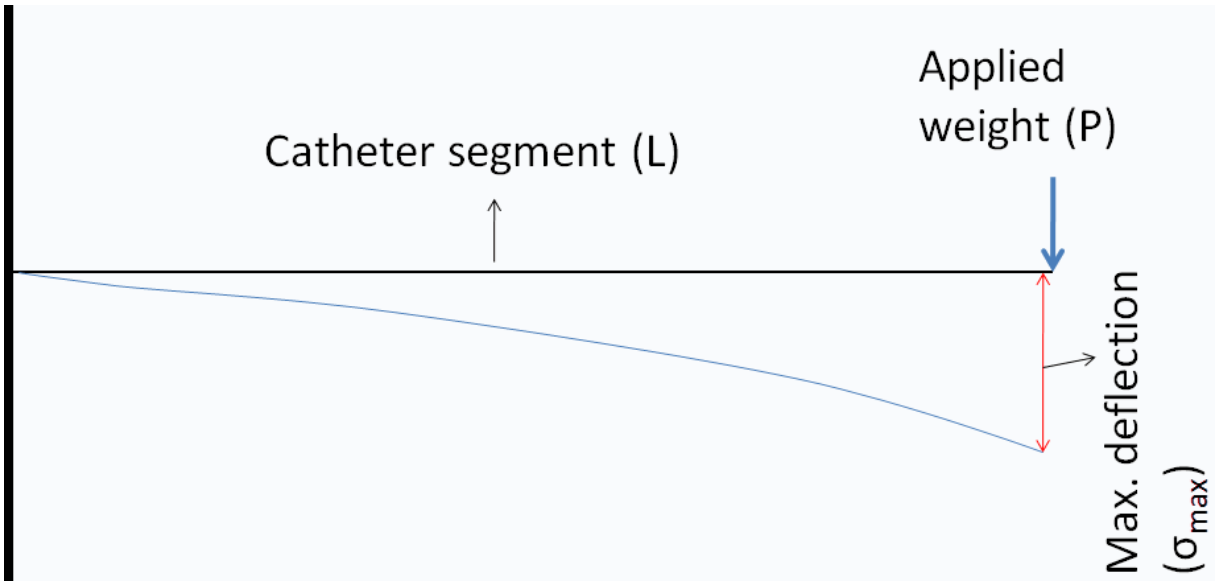

Figure 3.28.: Measuring catheter's elasticity.

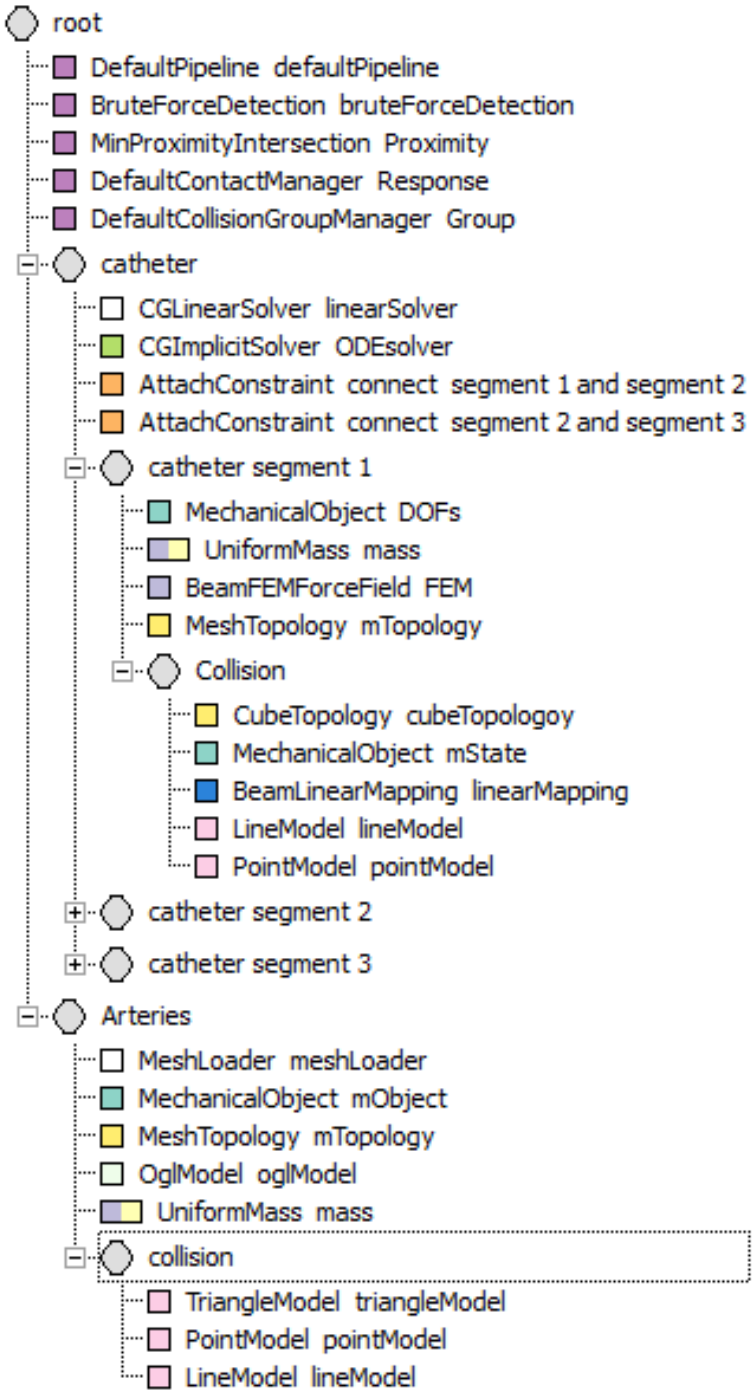

Figure 3.29.: SOFA scene graph of the catheter simulation

4. Experiments and Evaluation

4.1. Introduction

In the previous chapter, we presented an image processing based model for catheter selection. The purpose of this model is to replace the conventional *trial and error* based catheter selection during catheter angiography. For evaluating the model, different experiments were performed in collaboration with our clinical partner - the Uniklinikum Würzburg. The prerequisite of our model is the patient's image data (CT/MR) that is acquired prior to the angiography. For this purpose, our clinical partner selected different patients for these experiments and acquired image data of the patients. We created patient-specific arteries models from the segmented image data. The image processing based model used these arteries' model as well as the available catheters and suggested optimal catheters. In the clinic, angiography of different patients was performed and catheters were selected using clinical experience. These selected catheters, were then compared with the catheters suggested by the image processing based model. For suggesting catheters using our model, we tested different steps of the model. These step include segmentation of the patient arteries, skeletonization and parameters' estimation, parameters based models and simulation. The first step of the catheter selection pipeline is segmentation, which is presented in Section 4.2. In Section 4.3, the resulting skeletonization of the aorta and coronary arteries and geometric parameters' estimation is presented. In Section 4.4, we present results about catheter selection based on geometric parameter models. The results obtained from the algorithms are compared with the clinical data. In Section 4.5, we have shown how catheters' simulation affect the catheter choices. Summary of the chapter is given at the end.

4.2. Segmentation Results

The image data acquired prior to the angiography was a collection of CT and MR images. Initially, it was dictated by the clinical partner that the procedure has to be performed on special MRI data. For each patient, two sets of MR data were acquired i.e., one set of images contained the complete aorta but with low resolution ($0.83 \times 0.83 \times 1.5\,mm^3$) while the other set contained detailed high resolution images ($0.68 \times 0.68 \times 0.5\,mm^3$) of the coronary arteries. At a later stage of the project, CT data of twelve patients was also acquired. In CT data, the aorta and coronary arteries were imaged in the same set. We tested our automatic segmentation algorithm on MR data of eight patients. The algorithm was tested on low resolution aorta as well as high resolution coronary arteries. The segmentation quality was compared with the results of ITK-SNAP tool [YPCH*06, YPC*11] and were also judged visually by

an experienced cardiologist. In all cases, the aorta and coronary arteries were successfully segmented. The segmentation as well as the fusion of the two data sets were run successfully – judged again by an experienced cardiologist. For CT data, the same algorithm was executed twice, once for segmenting the aorta and second for segmenting the coronary arteries. Data with bad quality was segmented manually. The segmentation results were visually inspected.
ITK-SNAP [YPCH*06, YPC*11] is a free software application used for the segmentation of 3D medical images. It provides semi-automatic segmentation using active contour methods and image navigation. ITK-SNAP has been used for segmenting heart [Coi08, CRG*07], Aortic thrombus segmentation [DMMS06] and for the aorta segmentation [Sta11]. Here we give a comparison between the segmentation results of ITK-SNAP and our algorithm. The comparison was made on a computer with 6 GB of RAM and 4 x 2.8 Ghz. The time that was used for preprocessing, segmentation and selection of the starting point was measured. Using ITK-SNAP, one always has to manually select a start point and the segmentation does not stop by itself where our algorithm is completely automatic.

4.2.1. Aorta Segmentation Results

In Figure 4.1 and Figure 4.2 the aorta segmentation results produced by ITK-SNAP and our algorithm, are shown. The input image dimension is 432 X 432 X 27 pixels. In Figure 4.1(a) the aorta is segmented using ITK-SNAP where in Figure 4.1(b), our segmentation results are shown. Here ITK-SNAP does not produce accurate results. Figure 4.2 shows that both segmentation results are correct where the segmentation time of our algorithm was twelve times faster than ITK-SNAP. Our algorithm is also able to remove carotid arteries that are not needed for our target goal i.e., catheter simulation.

4.2.2. Coronary Arteries Segmentation Results

In Figure 4.3 the coronary arteries segmentation results are shown. These results show that ITK-SNAP is faster but the results are not correct. Our algorithm is slow but produces accurate results for the two coronary arteries. Visual inspection of the results shows that ITK-SNAP has not extracted the coronary arteries (see Figure 4.3(a)) while our segmentation algorithm has successfully extracted the coronary arteries (see Figure 4.3(b)).

4.2.3. Fusing the Aorta and Coronary Arteries

Once, both image data sets i.e., the aorta and coronary arteries are segmented, a fused image data set is computed (see Figure. 4.4)

4.2.4. Processing Time

The average time for the aorta segmentation and for the coronary arteries segmentation was 22 sec and 55 sec, respectively, running on a system with an *Intel* 2.67 GHz processor. There, the preprocessing of

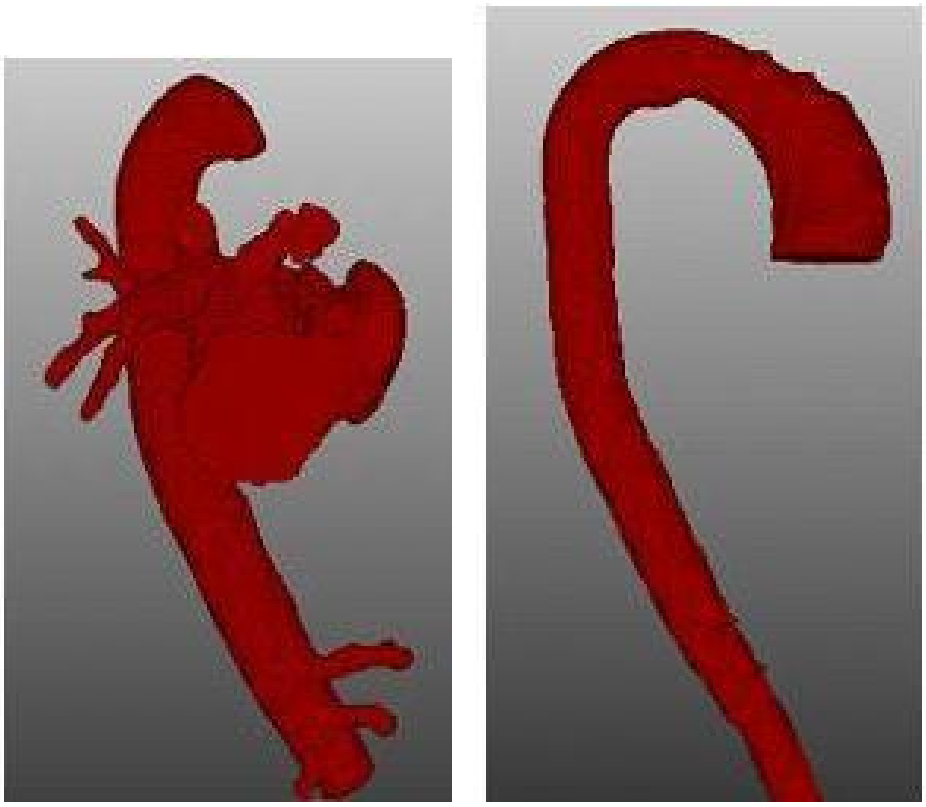

(a) Segmentation time: 1 minute 45 seconds (b) Segmentation time: 21 second

Figure 4.1.: (a) Segmentation using ITK-SNAP where the aorta is wrongly segmented, (b) Our automatic segmentation algorithm

the image data sets – smoothing, gradient as well as sigmoid filtering and the computation of the vesselness in case of the coronary arteries – consumed a significant amount of time. This initial processing step took about 15 *sec* for the low resolution aorta data sets and approximately 20 *sec* for the coronary artery data sets.

4.2.5. Discussion

Our automatic segmentation algorithm is ten times faster than ITK-SNAP for aorta segmentation. The coronary arteries segmentation takes a bit longer than the ITK-SNAP but produces precise results as compared to ITK-SNAP. The seed point selection is automatic where in ITK-SNAP, one has to select the seed point. Similarly, the algorithm automatically terminates when the aorta is completely segmented. The algorithm automatically segments the aorta and the coronary arteries from two 3-D MRI data

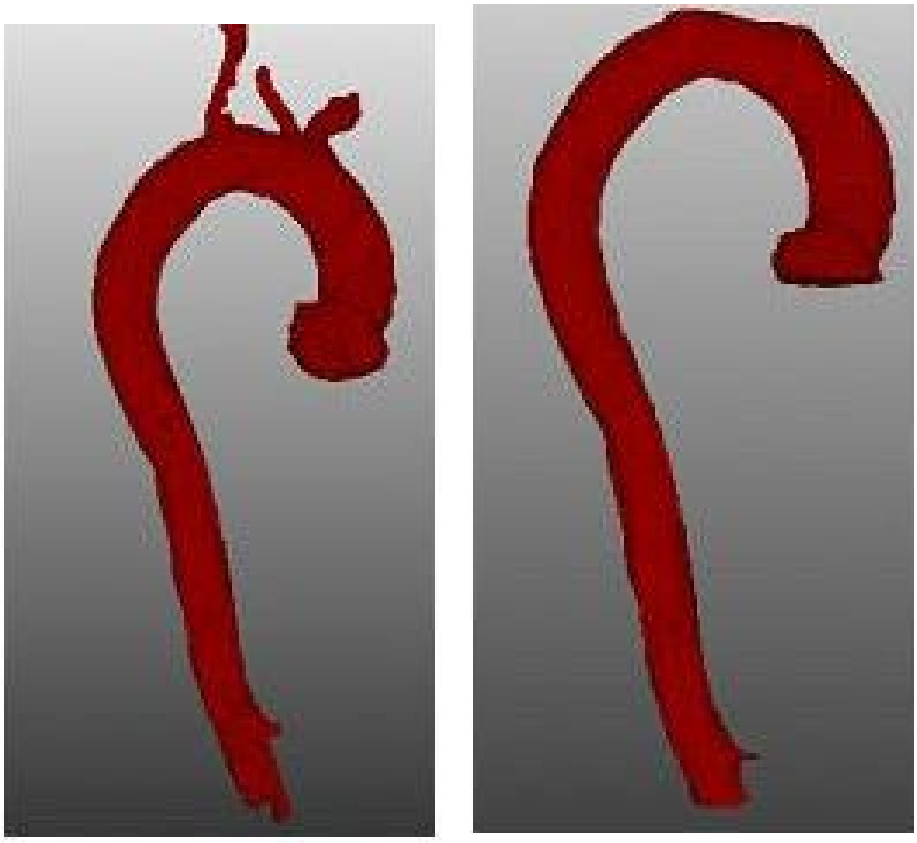

(a) Segmentation time: 4 minutes 10 seconds (b) Segmentation time: 22 second

Figure 4.2.: (a) Segmentation using ITK-SNAP, (b) Our automatic segmentation algorithm, Our algorithm is also able to remove carotid arteries which are not needed for our target goal.

sets and merge these two sets into a binary 3D data set. Our algorithm also avoids carotid arteries' segmentation which is good because these are not used in our target goal, i.e., simulation.

4.3. Parameters' Computation Results

Automatic geometric parameters' computation is one of the important parts of our contribution. Clinically important parameters like aortic valves' position, coronary arteries' ostia, coronary arteries' angle, radii of the aorta and coronary arteries and tip of the arteries are automatically computed from the segmented images. Measurements of these parameters are important for finding optimal catheters. In our evaluation methodology, we have obtained these measurements manually from the image data and have

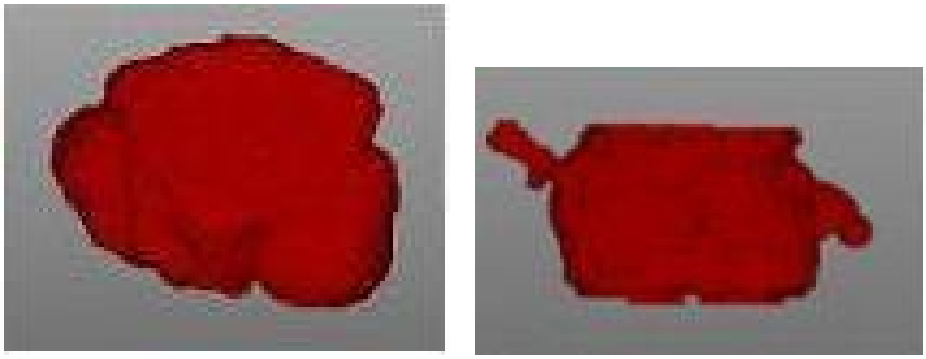

(a) Segmentation time: 30 seconds (b) Segmentation time: 55 second

Figure 4.3.: (a) Segmentation using ITK-SNAP where the coronary arteries are wrongly segmented, (b) Our automatic segmentation algorithm correctly segments the coronary arteries.

compared these with measurements obtained from our automatic computations and have computed the average error.

4.3.1. Centerline Extraction

The centerline of the aorta and coronary arteries is used for computing the diameter of the aorta, coronary artery ostium and coronary artery angle. A *binary thinning* algorithm for 3D image data [Hom07] has been used in this work to get the centerline of the image. The extracted centerline is visually examined. Figure 4.5 shows the segmented image and its centerline.

4.3.2. Aorta Diameter

For computing the diameter of the ascending as well as descending aorta, a plane is created, which is normal to each of the centerline's points of the aorta. Along that plane, the averaged distances of the points lying on the surface of the segmented region are determined, providing values for the aorta. In Table 4.1 the automatic computation and the manual computation are compared. The average error for the ascending aorta is $0.61mm$ and for the descending aorta is $0.41mm$.

4.3.3. Coronary Arteries' Ostia Position and Height

The position of the coronary artery's ostium and its distance from the aortic valves are very important parameters. These information are key to know about the takeoff of the arteries and catheter selection. These parameters are computed automatically using the method presented in Section 3.3. A comparison of the automatic and manual computation is shown in Table 4.2 and Table 4.3.

	Aorta Diameter (mm)		
Patient No.	Manual	Automatic	Error (mm)
1	41	42.4	1.4
2	39	40.1	1.1
3	29	29.1	0.1
4	35	36.1	1.1
5	35	36.5	1.5
6	37	37.3	0.3
7	42	43.3	1.3
8	44	44.5	0.5
9	29	27	2
10	31	31.1	0.1
11	23	24.3	1.3
12	25	24.7	0.3
13	23	24.8	1.8
14	25	26.1	1.1
15	28	28.3	0.3
16	26	27	1

Table 4.1.: Measurements for diameter of the aorta. The average error is 0.95*mm*

	Manually computed ostia position			Automatically computed ostia position			
patient. No.	X	Y	Z	X	Y	Z	Error (mm)
1	82.6	127.4	42	82.9	127.2	43.1	0.4
2	53.9	65.1	66	54.1	66.7	66.5	1.4
3	56	74.9	50.7	56.4	74.4	53.3	1.2
4	72.4	57.05	41.3	74.1	56.6	43.1	1.7
5	128.8	161.7	95.5	128.8	163.1	95.3	0.9
6	130.2	205.1	57.8	130.4	204.6	59.3	0.1
7	110.7	136.9	70.8	111.1	136.5	71.9	0.4
8	107.8	147	51.5	108.9	147	51.1	0.6
9	79.8	94.1	82	80.5	94.4	82.1	0.7
10	77.7	98.3	66.6	77.6	98.5	66.5	0
11	92.7	67.2	60.1	92.2	67.4	60.3	0.1
12	159.6	189.7	95.5	158.2	190.5	96.5	0.1
13	163.8	223.8	62.5	163.2	222.6	61.1	1.5
14	139.5	160	92.6	137.6	160.5	91.7	1

Table 4.2.: Automatic compution of the ostia is compared with the manual computation. The average error is $0.9mm$

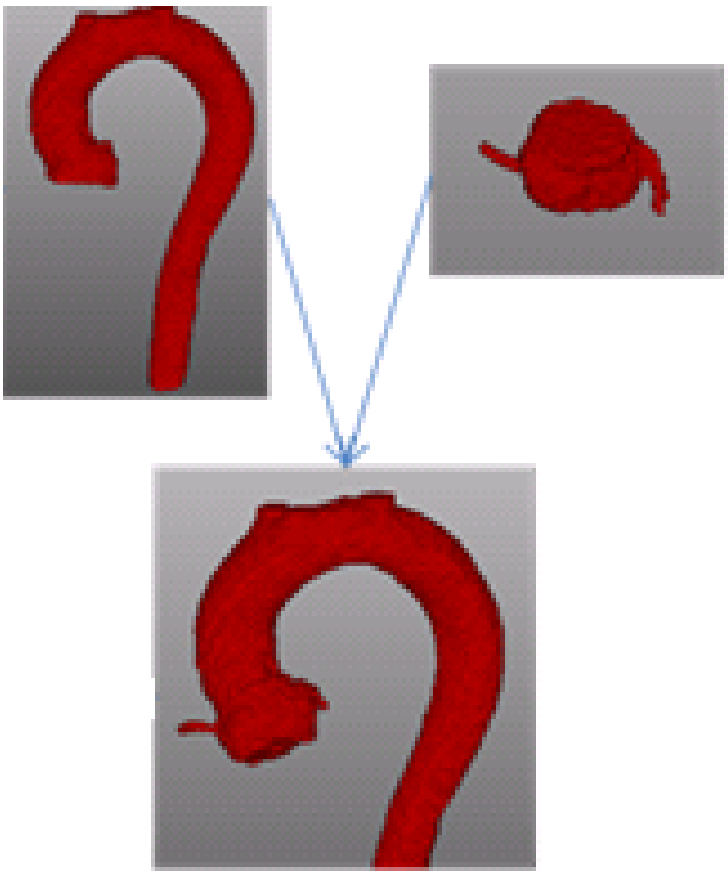

Figure 4.4.: Fusing the aorta and coronary arteries.

4.3.4. Coronary Arteries' Angles

For the computation of the angles of both coronaries arteries with respect to the aorta, the coronary arteries' skeleton parts as well as the skeleton part belonging to the ascending aorta are projected onto a 2D plane. Straight lines are interpolated for these projected segments and the corresponding angles between them are computed. For details please look [RWV11a, RWV11b].

4.3.5. Discussion

Using the image data, all these parameters are computed automatically. These parameters are of great help for the cardiologists to investigate different treatment and diagnoses. Finding the diameter of the aorta helps to know about the stenosis and aneurysm. The diameter of the coronary arteries helps to know whether the artery has become thin or not. The position of the coronary arteries ostium and its

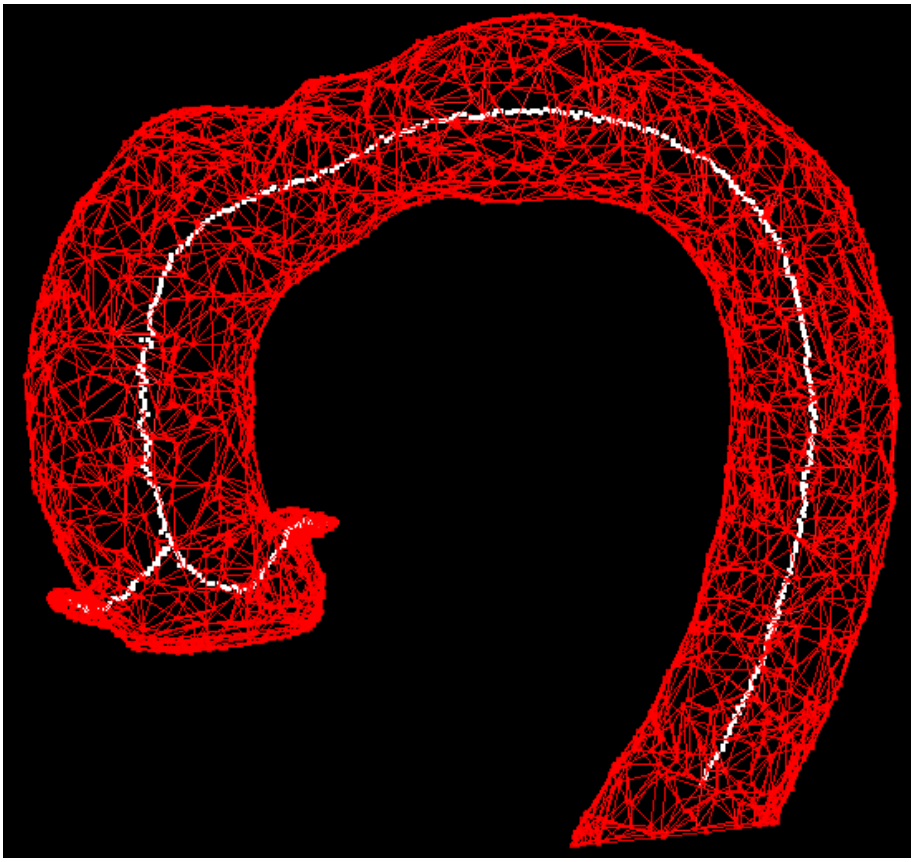

Figure 4.5.: Centerline extraction

distance from the aortic valves helps to know whether the coronary arteries have high takeoff or low takeoff. Similarly, the angle of the coronary arteries with the aorta helps to know whether the takeoff is horizontal, inferior or superior. These parameters are the basis for the image processing based catheter selection model.

4.4. Models Evaluation

4.4.1. Introduction

A two step approach for catheter selection was presented in Section 3.1. The first step which will be discussed in this section, is a geometric parameters based model for reducing the number of catheter choices. In Section 3.4, we have presented models for reducing the catheter choices for right and left coronary angiography as well as for angiography where the coronary arteries have an anomalous origin.

	Ostium Height(mm)		
Patient No.	Manual	Automatic	Error(mm)
1	8	9.20	1.20
2	6	6.1	0.10
3	5	6	1.00
4	6	7.3	1.30
5	14	12	2.00
6	20	21	1.00
7	9	10	1.00
8	20	21	1
9	18	18.3	0.3
10	14	15.1	1.1
11	32	32.5	0.5
12	14	15.2	1.2
13	23	22.7	0.3
14	24	24.3	0.3

Table 4.3.: Distance of the ostia from the aortic valves. Automatic compution of the ostia height is compared with the manual computation. The average error is 0.88*mm*.

In these models different weights are assigned to the parameters (see Equations 3.2, 3.4, and 3.6). The intuition for considering the difference in weights is to have more contribution from the clinically important parameters compared to less important parameters. Finding optimal weights will be discussed in this section. For creating ground truth, a team from our clinical partner led by an experienced cardiologist performed a series of experiments. They performed angiography of twenty four cases where twelve cases were for the right coronary angiography, and twelve cases were for the left coronary angiography. They selected catheters based on their experience and knowledge in the field. These final catheters selected by the clinical experts were considered as ground truth. In the next step, catheters were suggested using the image processing based models. Patient's image data was acquired before staring angiography. This data was preprocessed, segmented and the clinically important parameters were computed. Using the image processing based models, costs were assigned to each catheter for a given patient. For every patient catheters were ranked from the lowest cost to the highest cost. Lowest cost meant that the catheter parameters had closest values to the patient's parameters. For every patient, the top three catheters with the lowest costs were suggested. Then for every patient, the top three suggested catheters were compared with the catheter selected by the experienced cardiologist. If the catheter selected by the cardiologist was similar to any of the three suggested catheters, the decision was considered as correct, otherwise false. This means that if the cardiologist selection is second or third choice in the model based suggestions, the decision is still correct because it is not clear whether the cardiologist choice is really an optimal one. It is shown that sometimes the cardiologist's selection

does not satisfy some clinical recommendations where as the image based model fully incorporates these recommendations. The catheters selected by the cardiologist and catheters suggested by the model are visualized inside the arteries. These experiments show that the image based model will help the cardiologist to have suggestions for catheter selection before conducting angiography procedure.

4.4.2. Evaluating Model for the Right Coronary Angiography

Although there is a large number of catheters available in the market for right coronary angiography, we have restricted our experiments to different catheters that are used by our clinical partner. The model was evaluated on image data of twelve different patient cases that were provided by our clinical partner. For these patients, the catheterization was performed by an experienced cardiologist who selected catheters based on his knowledge and experience in the field. Then the image based model was used to select the three most optimal catheters for each patient and to compare our suggestions with the catheters actually selected by the cardiologist. For this, we computed parameters from the patient arteries, parameters from the catheters and then used the model for catheter selection.

4.4.2.1. Arteries Parameters Computation

For evaluating the model, we got CT data of twelve patients from our clinical partner. This data was acquired prior to the angiography. The dimension of these images was 512 X 512 X 260 pixels with a resolution 0.351563 X 0.351563 X 0.599976 mm^3. We segmented the aorta and coronary arteries from these images and obtained the different parameters. The right coronary curve was obtained from the arteries' centerline. Since 2D catheters were used, the patient's 3D data was projected onto a 2D plane. The coronary arteries' skeleton parts as well as the skeleton part belonging to the ascending aorta was projected onto a 2D plane. The right coronary arteries' curve, curve angle and distance of the ostium from the aortic valves were computed for all the patients. The different parameters that were computed for all patients are shown in Figure 4.6. In the next step, the related parameters for all the catheters were computed.

4.4.2.2. Catheters' Parameters Computation

For the right coronary angiography, ten different catheters were selected for our experiments. These catheters are mostly used by our clinical partner. For all these catheters, the curve angles and curve lengths were computed manually. The different catheters that were used in our experiments are shown in Figure 4.7.
After computing the curve lengths and curve angles for all the catheters, and curve angles and curve lengths for the right coronary artery of all the patients, the next step was using the catheter selection model to suggest optimal catheters.

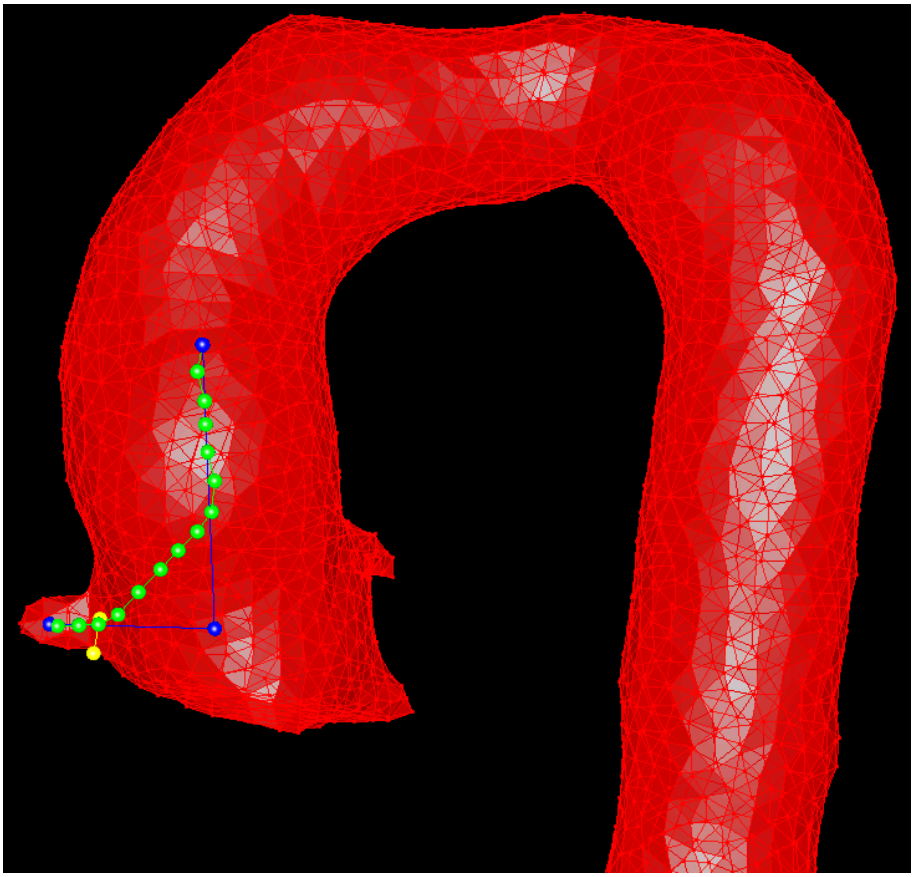

Figure 4.6.: Computing right coronary arteries curve (green), curve angle (blue) and ostium height from the aortic valves (yellow).

4.4.2.3. Ranking Catheters for Patients

For catheter recommendation, all catheters for a given patient were ranked. For this ranking we used the following model (see Section 3.4.2 for details).

$$OC = \arg\min_i \{CC_i\} \tag{4.1}$$

where i is the i^{th} catheter and

$$CC_i = a\sqrt{\left(\frac{5}{1}N_{CL}\left((CHCL)_i - RCAHCL\right)\right)^2} + b\sqrt{\left(\frac{1}{N_{CA}}\left((CA)_i - RCACA\right)\right)^2} \tag{4.2}$$

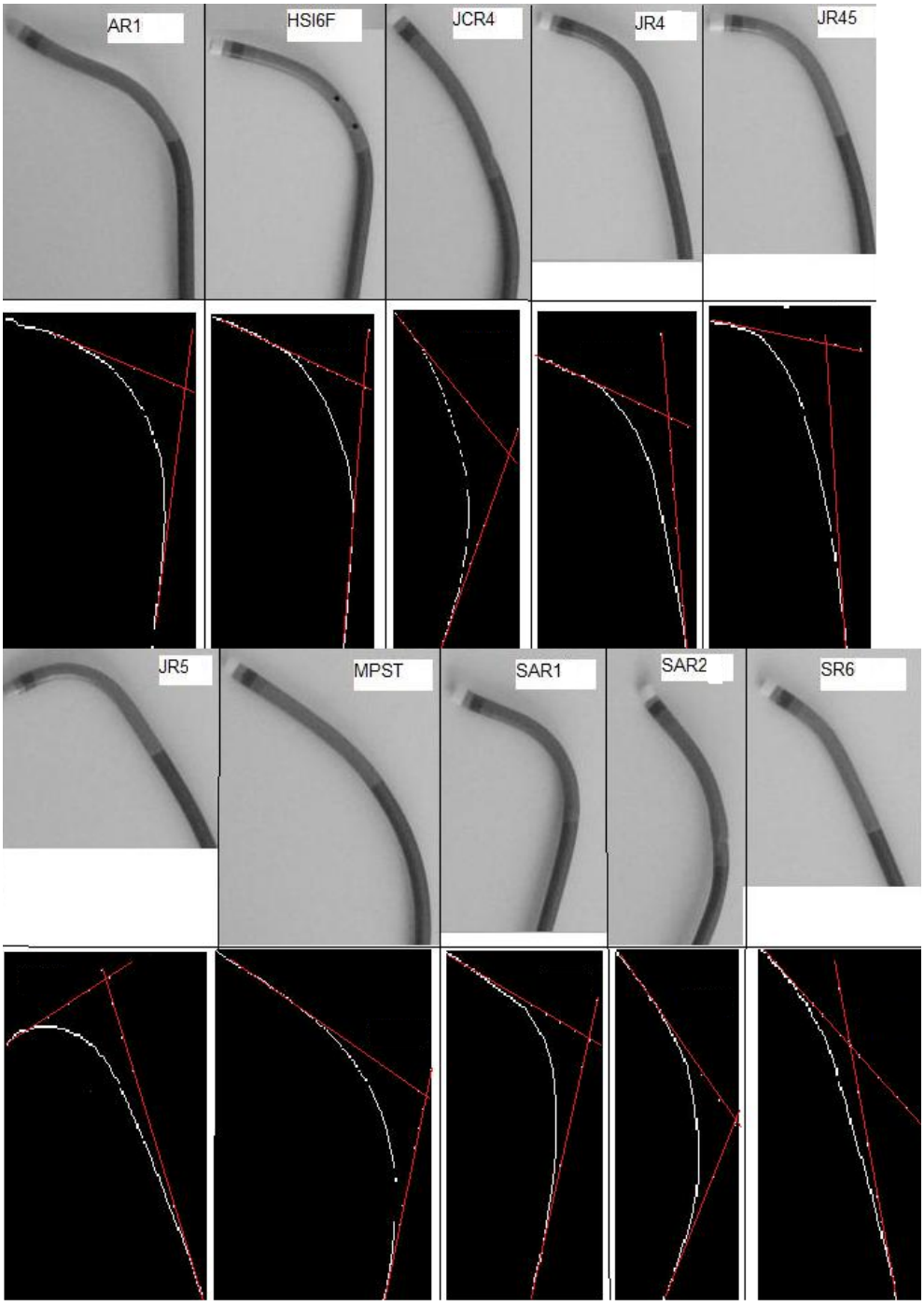

Figure 4.7.: Catheters that were used for right coronary angiography

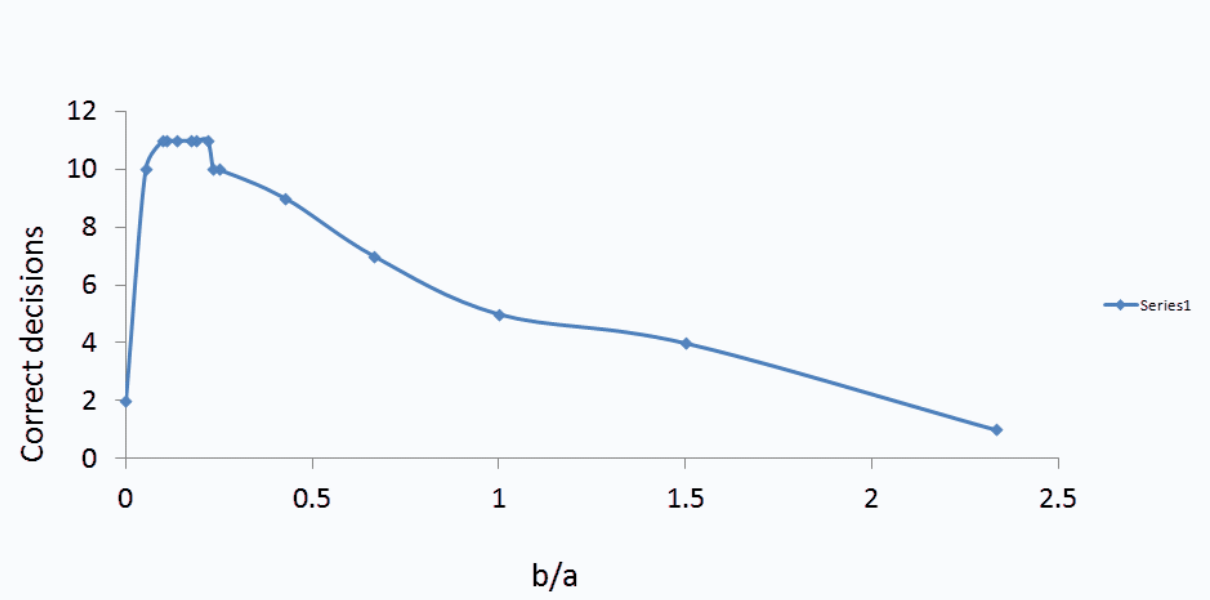

Figure 4.8.: The graph of weight factors $a = 1$ and $b = b/a$. The best results are obtained when b/a is in the range of .09 and .21

In this model, weight factors a and b are assigned to their respective parameters. Clinically, curve length is more important than the curve angle therefore, weight factor a should get more weight than the weight factor b. To find optimal values for these weight factors, we have heuristically tested different values (see Table 4.4). In Figure 4.8 it is shown that the best results are obtained when the ratio for weight factors a and b is 9 to 1.

4.4.2.4. Analysis of Catheters Ranking

We analyzed the top three ranking catheters for every patient and compared these with the catheters used by the cardiologist. Table 4.5 shows our top three suggested catheters as well as catheters selected by the cardiologist for the twelve patients. From this table, we get the information that in 41% cases, our top suggestion is the same as that of the cardiologists. For example, in Figure 4.10 catheter JR4 is selected by the cardiologist and the model also suggest it as the most optimal catheter. In 25% cases the cardiologist's selection is our second priority. Now we need to know whether our suggestion is really better than the actual catheter used. We simulated the two catheters and found that our suggestion has slightly better angle matching. For example, in Figure 4.11 a case is shown where the catheter actually used during the angiography is JR4 (green) and our recommendation is MP. In 25% cases the cardiologist selection is our third priority (see Figure 4.11) and in 9% cases the cardiologist's selection

Weight factor (a)	Weight factor (b)	Correct decisions)
0	1	8 %
0.1	0.9	8 %
0.2	0.8	16 %
0.3	0.7	24 %
0.4	0.6	32 %
0.5	0.5	40 %
0.6	0.4	56 %
0.7	0.3	72 %
0.8	0.2	80 %
0.81	0.19	80 %
0.82	0.18	80 %
0.84	0.16	80 %
0.85	0.15	88 %
0.88	0.12	88 %
0.9	0.1	88 %
0.91	0.09	80 %
0.95	0.05	80 %
0.98	0.1	40 %
1	0	16 %

Table 4.4.: Right coronary arteries model: The model was tested for different values of weight factor a and b. These values were heuristically selected. The table shows that we get better results when weight factor a gets greater value than weight factor b. The clinical requirements also demand higher values for weight factor a.

is not included in our top three priorities (see Figure 4.13). In Figure 4.9 a summary of the comparision of clinical decisions and model based suggestion is shown.

From these experiments, we have seen that the model for the right catheter selection can suggest a suitable catheter before starting the angiography. The visualization shows that in cases where the cardiologist's selection is our second or third option, our catheters seem to fit better visually. However for this, we need further scientific experiments.

4.4.3. Evaluating Model for the Left Coronary Angiography

The model for the left coronary angiography uses a different set of parameters as compared to the model for right coronary angiography. The number of parameters as well as the weighting factors are also different from the right coronary model. However, evaluation strategy for both the models is same.

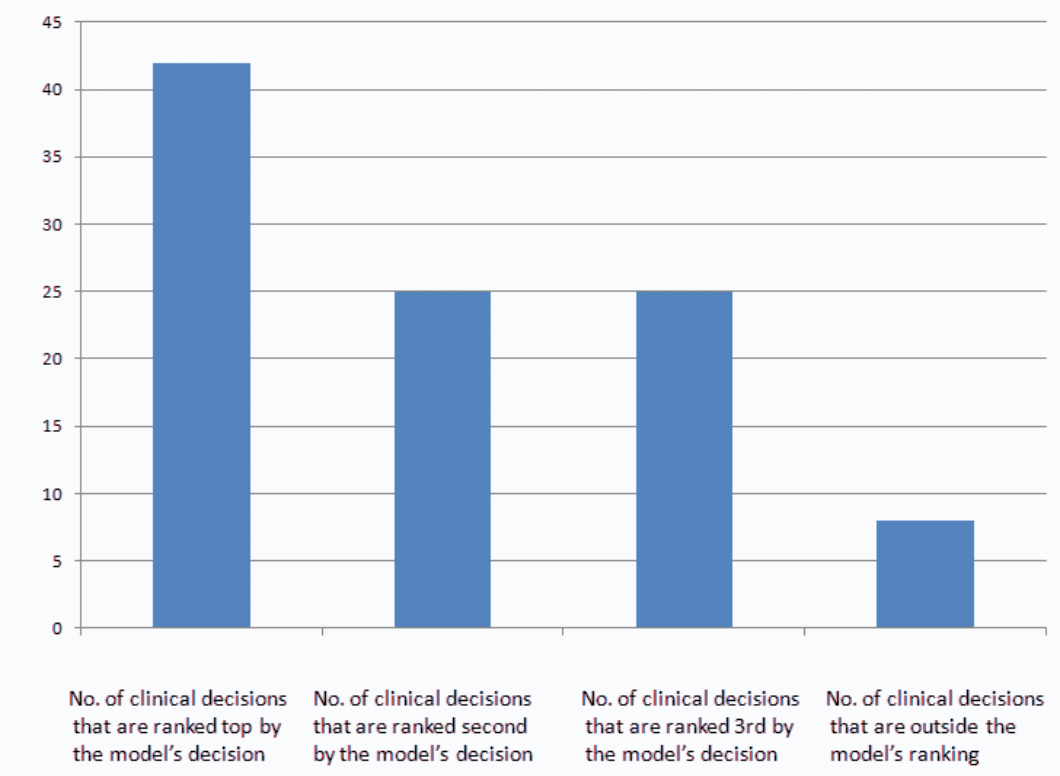

Figure 4.9.: Right coronary angiography: For every patient, the model suggests three top ranked catheters. These three top ranked catheters are compared with the catheter selected in the clinic. The clinical decision is either equal to any one of these three top ranked catheters or sometimes the clinical decision is outside the model's suggested range.

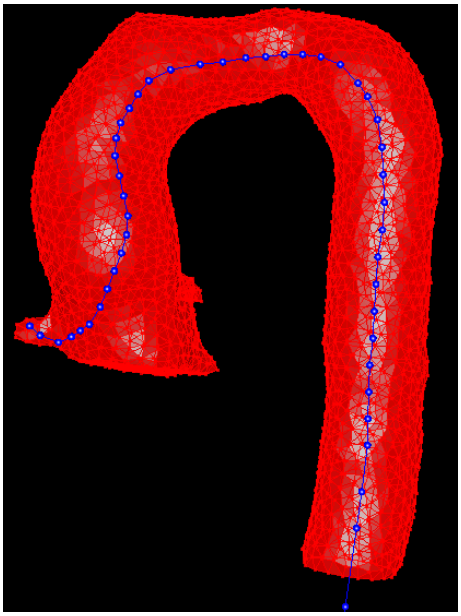

Figure 4.10.: Right coronary angiography: Catheter JR4 is used by the cardiologist and is also suggested by the model.

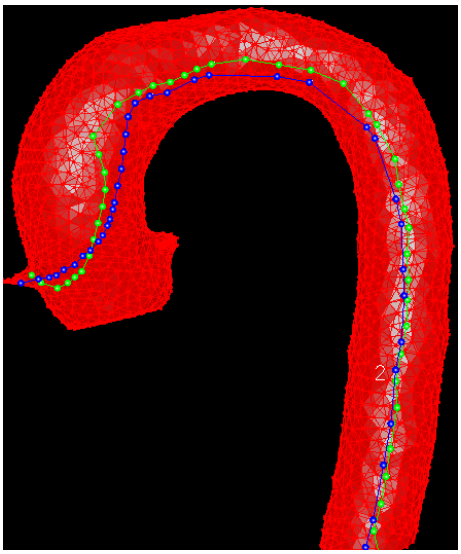

Figure 4.11.: Right coronary angiography: Cardiologist decision is catheter JR4 (Green). Model's suggestion is MP (Blue). The angle of catheter MP is more close to the arteries' angle compared to the catheter JR4. JR4 is the model's 3rd choice.

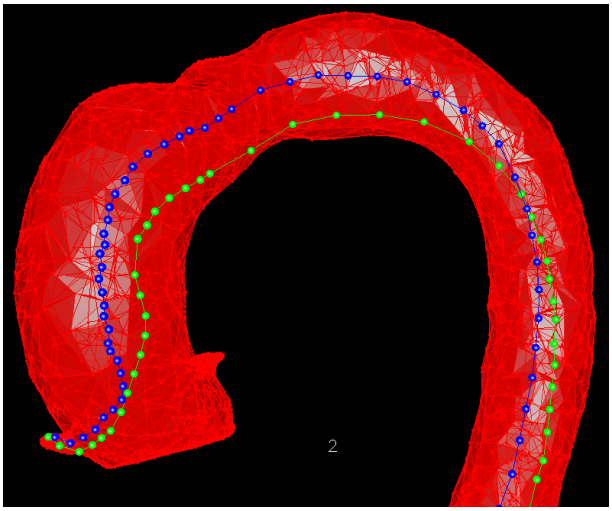

Figure 4.12.: Right coronary angiography: Cardiologist decision is the catheter JR4 (Green), Model's suggestion is the catheter JR5 (Blue). Catheter JR4 is the model's second choice.

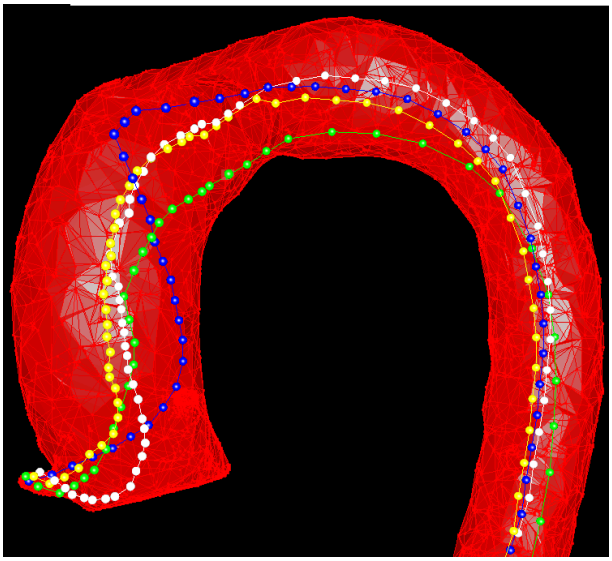

Figure 4.13.: Model's three suggested catheters HSISH (white), MB2 (blue), JR5 (yellow) and the cardiologist selection is the catheter JR4(green). Although the model's three suggestions do not contain the catheter used by the cardiologist the figure shows that the tip of each suggested catheter has reached the ostium and the angles are appropriate.

Patient No.	Model based suggestions			Selection by the cardiologist
0	1st	2nd	3rd	
1	JR5	JR4	HSISH	JR4
2	AR2	JR4	JR35	AR2
3	JR35	3DRC	JR4	JR4
4	JR4	MB2	JR35	JR4
5	JR4	3DRC	JR5	JR4
6	AR1	JL5	MB2	JL5
7	JR4	JR35	HSISH	JR4
8	MP	3DRC	JR4	JR4
9	JR35	JR4	HSISH	JR4
10	JR5	HSISH	MB2	JR4
11	JR4	JR35	AR2	JR4
12	JR3	AR1	JR4	JR4

Table 4.5.: Right coronary arteries model: Comparison of the 'model based catheter suggestions' and the cardiologist's selection

As for the right model, here too, catheterization was performed by an experienced cardiologist who selected catheters based on his knowledge and experience in the field. CT data of twelve patients was acquired before starting the angiography. From this image data, different parameters were computed. The related parameters from the catheters were also computed. Using these parameters, three catheters were suggested by the image based model for each patient. Then, for every patient, the suggested three catheters were compared with the catheter selected by the cardiologist. If any of the three suggested catheters was similar to the cardiologist's selection, then the model decision was considered as correct otherwise incorrect. The reason of considering three catheters is that we are not sure if the cardiologist selection is an optimal one.

4.4.3.1. Arteries Parameters Computation

First, we needed to extract the clinically important parameters from the patient's CT image data. We got CT data of twelve patients from our clinical partner. The aorta and the left coronary arteries were segmented from these images and the different parameters like the left coronary curve angle, aorta cavity length and the amount of backup support were computed. Since 2D catheters are used, the patient's 3D data was projected onto a 2D plane. The coronary arteries' skeleton parts as well as the skeleton part belonging to the ascending aorta was projected onto a 2D plane. The left coronary artery curve angle, aorta cavity length, backup support and distance of the ostium from the aortic valves were

computed for all the patients. The different parameters that were computed for all patients are shown in Figure 4.14. In the next step, the related parameters for all the catheters were computed.

4.4.3.2. Catheter's Parameters Computation

For left coronary angiography, we considered different catheters that are used by our clinical partner. The different catheters that were used in our experiments are shown in Figure 4.15. For all these catheters, the different parameters like the curve angles and length as well as the distances between the two curves were manually computed for all the catheters. After computing the parameters for the catheters and parameters for the patients, the next step was using the catheter selection model to assign a cost to each catheter and rank these catheters according to their costs.

4.4.3.3. Ranking Catheters for Patients

Using the model presented in Section 3.4.3, every catheter is assigned some cost CC_i for a given patient. All catheters are ranked based on these costs.

$$OC = \arg\min_i \{CC_i\} \tag{4.3}$$

where i is the i^{th} catheter and

$$CC_i = a\sqrt{\left(\frac{1}{N_1}\left((CSSL)_i - ACL\right)\right)^2} + b\sqrt{\left(\frac{1}{N_2}\left((CC2A)_i - LCACA\right)\right)^2} + c\sqrt{\left(\frac{1}{N_3}\left((CC1A)_i - CWCA\right)\right)^2} \tag{4.4}$$

Different weight factors (a, b and c) are assigned to each parameter. Proper selection of values for a, b and c is important for the optimal catheter selection. For the left coronary angiography, the most important parameter from the clinical point of view is the catheter's segment length (see Figure 4.16). During left catheter selection, it is important to ensure that the catheter's distance between the two curves has enough length to reach the ostium. It means this parameter (CSSL) should be assigned more weight as compared to the other two parameters. The next important parameter is the coronary artery curve angle. Catheter having a suitable angle for the left artery angle, ensures coaxial placement and avoids artery injury. Therefore, this parameter should be given more weight than the backup support. Keeping in mind these clinical requirements, different weights were tried for these coefficients.

In our experiments, different values for a, b and c were used (see Table 4.6). We started by assigning equal weights to all coefficients, observed the results and then changed the parameters according to the clinical importance of different parameters. The best results are obtained when the ratio between weight factors a, b and c is 1, 0.2, and 0.1, respectively (see Figure 4.17)

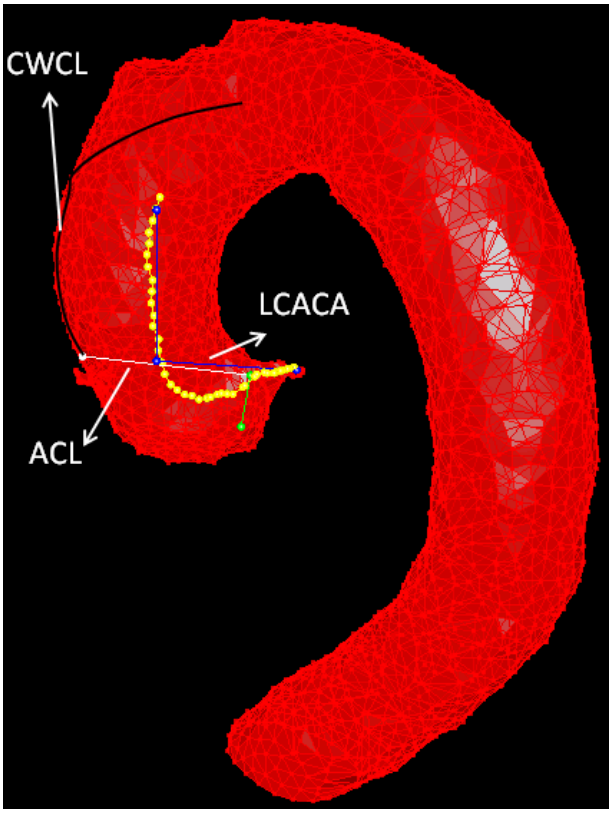

Figure 4.14.: Left coronary angiography: Computing left coronary artery curve angle (LCACA), Aorta Cavity Lenght (ACL), Contralateral Wall Curve Length (CWCL) and ostium height from the aortic valves.

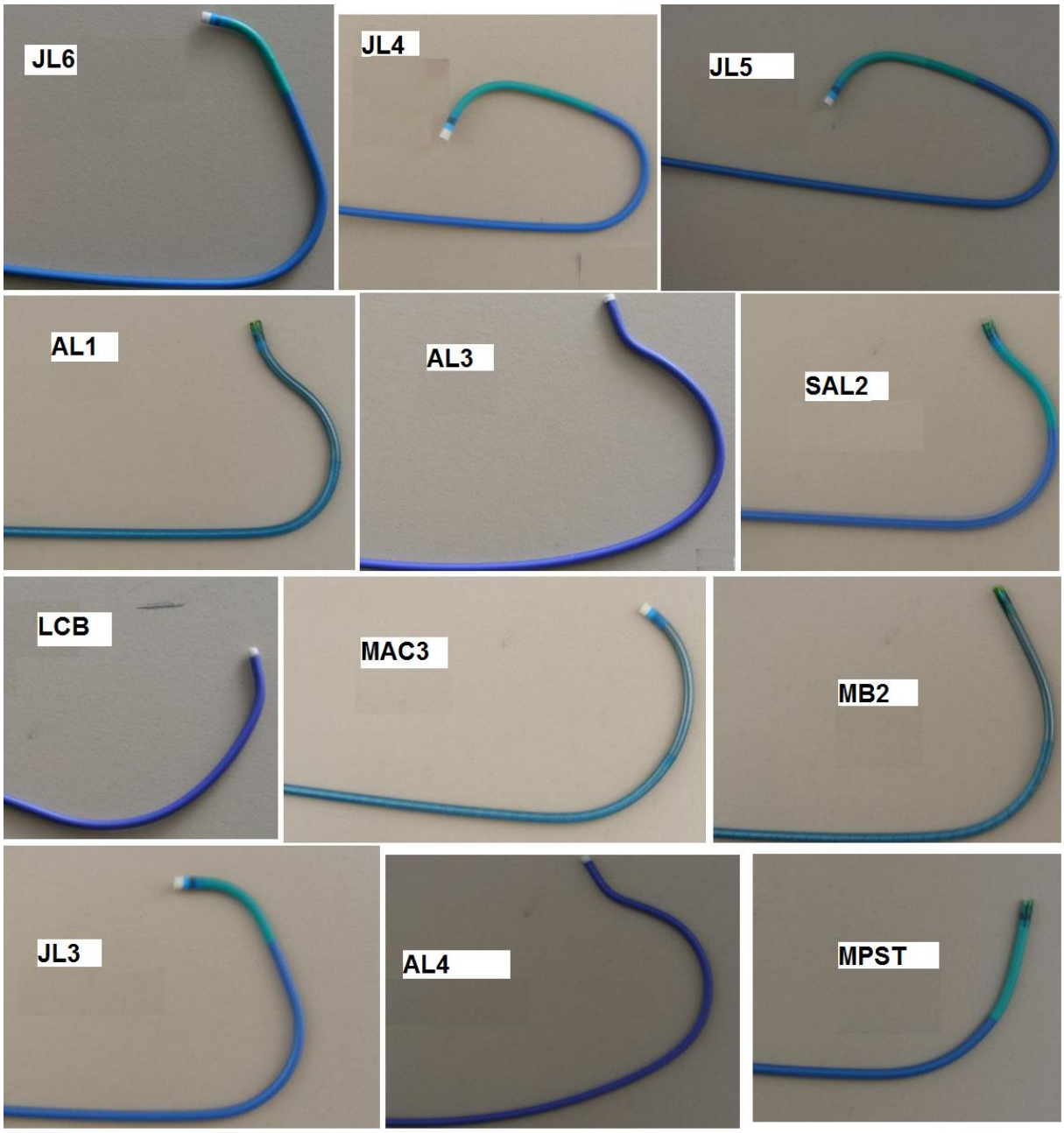

Figure 4.15.: Catheters that were used for left coronary angiography.

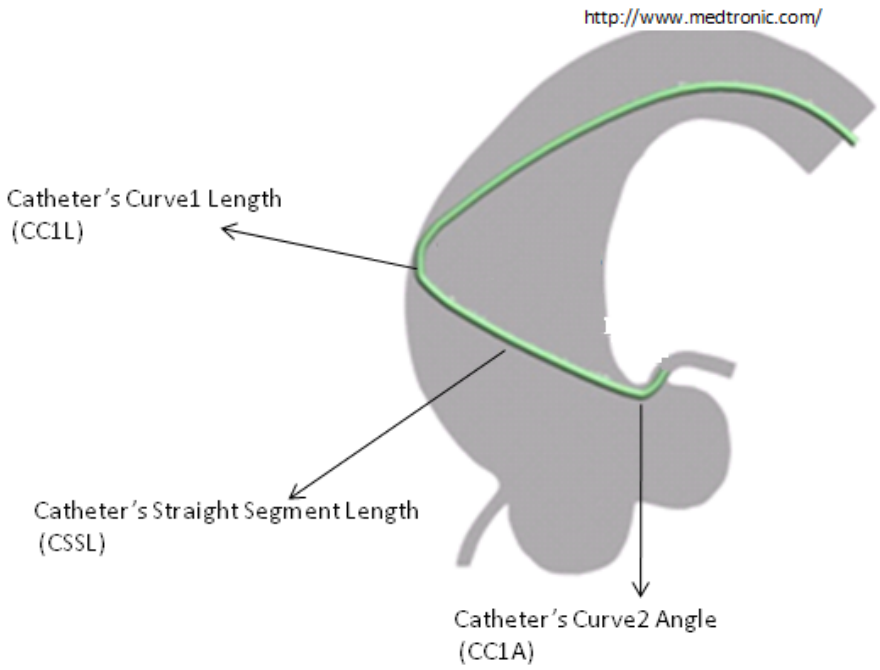

Figure 4.16.: Left coronary angiography: It is important to see that the catheter's distance between the two cures should have enough lenght to reach the ostium. It means this parameter should assign more weight as compared to the other two parameters.

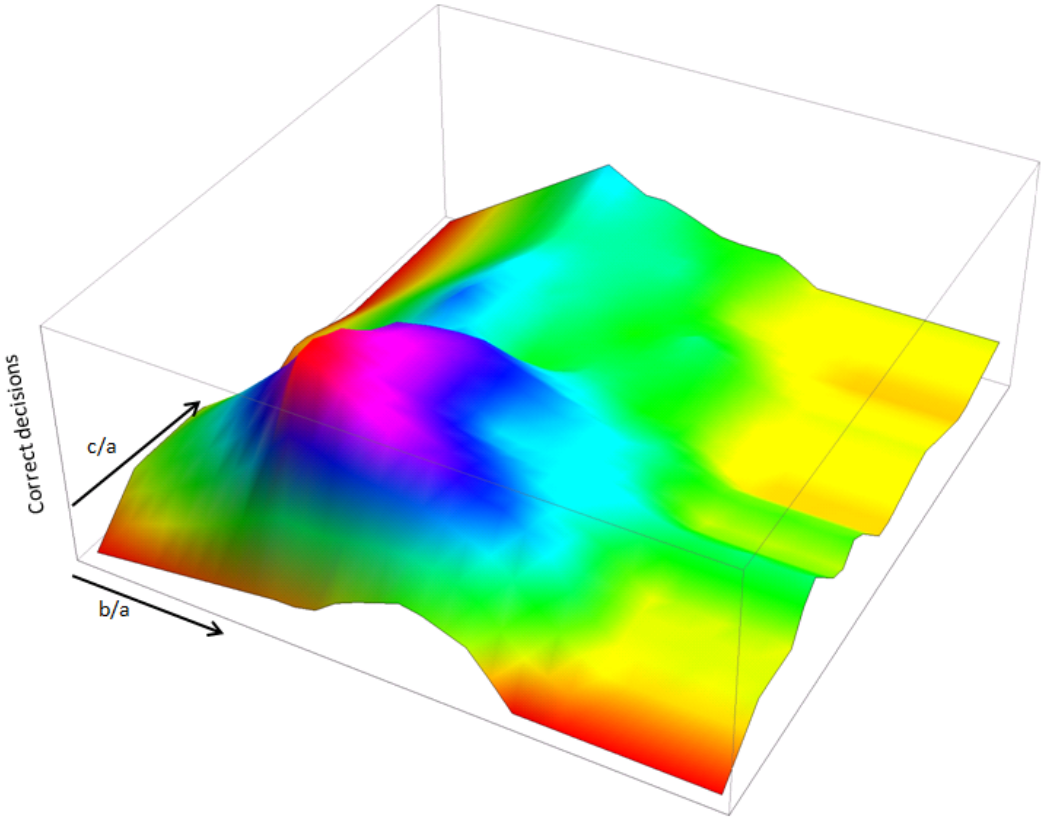

Figure 4.17.: The graph of weight factors $a = 1$, $b = b/a$, and $c = c/a$. The best results are obtained when the ratio between weight factors a, b and c is 1, 0.2, and 0.1, respectively.

Weight factor (a)	Weight factor (b)	Weight factor (c)	Correct decisions
0.34	0.33	0.33	16 %
0.38	0.32	0.3	24 %
0.42	0.31	0.27	24 %
0.46	0.3	0.24	24 %
0.5	0.29	0.21	32 %
0.54	0.28	0.18	48 %
0.6	0.25	0.15	56 %
0.65	0.23	0.12	64 %
0.7	0.21	0.09	80 %

Table 4.6.: Left coronary angiography: The model was tested for different values of weight factors *a*,*b* and *c*. These values were heuristically selected. The table shows that better results are obtained when weight factor *a* gets greater value than weight factor *b* and weight factor *b* gets greater value than weight factor *c*. These differences are according to the clinical importance of the parameters.

4.4.3.4. Analysis of Catheter Ranking

The top three ranking catheters for every patient were analyzed and compared with the catheters used by the cardiologist (see Figure 4.18). It was observed that in 41% cases, our top suggestions are the same as that of the cardiologist's decision. In 25% cases the cardiologist's selection is our second priority. In 17% cases the cardiologist's selection is our third priority and in 17% cases the cardiologist's selection is not included in our top three priorities. We wanted to know whether our suggestion is better than the actual catheter used. Therefore, our suggested catheters as well as the cardiologist's selected catheters were visualized. These visualizations gave promising results about our suggested catheters. For example, in Figure 4.19 the two catheters are shown. JL4 (green) is the cardiologist's selection which is ranked third in the model based suggestions. According to the model based suggestions, the first choice is AL4 (blue). Here, the coronary takeoff is high so according to medical literature AL should be used, which is correctly suggested by the model based procedure. However, a further scientific validation would be needed for those catheters where the cardiologist's choice is not our first choice. These experiments would show the difference of performance between the model based suggestions and the catheter selected by the cardiologist.

From these experiments, we have seen that the model for left catheter selection is able to suggest a suitable catheter before starting the angiography. The visualization shows that in cases where the cardiologist's selection is our second or third option, our catheters seem to fit better visually. However, for this we need further scientific experiments.

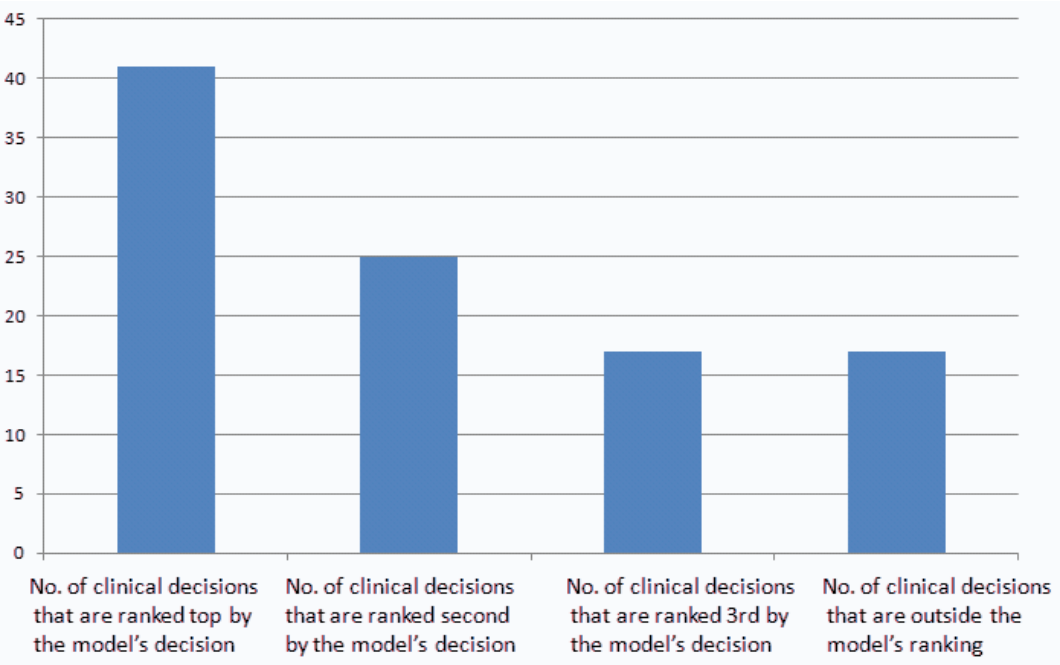

Figure 4.18.: Left coronary angiography: For every patient, the model suggest three top ranked catheters. These three top ranked catheters are compared with the catheter selected in the clinic. The clinical decision is either equal to any one of these three top ranked catheters or sometimes the clinical decision is outside the model's suggested range.

4.4.4. Evaluating Model for the Coronary Arteries with High Takeoff

If the distance between the aortic valves and coronary arteries ostia is greater than 1.5 *cm* then such anatomy is referred as high takeoff coronary arteries. High takeoff coronary artery is a haemodynamically minor, but surgically important coronary anomaly [TWT10]. Special catheters called *Amplatz* are used for this purpose. Amplatz catheters seat deeply at the aortic valves for the stable position (see Figure 3.24) and the backup support is provided from the aortic valves as well as from contralateral wall of the aorta. The image data, we got from the clinic had only two cases where the coronary arteries had high takeoff. For these data sets, we measured the coronary arteries angle, height of the ostium and the aortic diameter near the ostium. Then important parameters from the Amplatz catheters were computed. The important parameters are Catheter Secondary Curve Width (CSCW), Catheter Secondary Curve Depth (CSCD), Catheter Primary Curve Angle (CPCA). Using the model presented in Section 3.4.4, cost was assigned to each catheter for a given patient.

$$CC_i = a\sqrt{\left(\frac{1}{N_1}\left((CSCD)_i - OH\right)\right)^2} + b\sqrt{\left(\frac{1}{N_2}\left((CSCB)_i - AD\right)\right)^2} + c\sqrt{\left(\frac{1}{N_3}\left((CPCA)_i - CACA\right)\right)^2} \tag{4.5}$$

where i is the i^{th} catheter and

$$OC = \arg\min_i \{CC_i\} \tag{4.6}$$

Different weight factors (a, b and c) are assigned to each parameter. In case of using Amplatz catheter, the most important parameter from the clinical point of view is the Catheter's Secondary Curve Width (CSCW) (see Figure 3.25). For optimal catheter selection, it should be ensured that the width is enough, and the catheter is tightly positioned at the contralateral wall. So highest weight should be assigned to this parameter. Next, it is important to ensure that the Catheter's Curve Depth is enough so that it touches the aortic valves and the second curve reaches the ostium. Therefore, next highest weight should be assigned to this parameter.
We used parameters' weight similar to the weights for the normal left coronary angiography and ranked the Amplatz catheters. Limited data of only two cases was available where the coronary arteries had a high takeoff. So we were unable to compare our model to enough data. The cardiologist has used an amplatz catheter in only one case. The case where the cardiologist has not used amplatz is shown in Figure 4.19. The coronary takeoff is high so according to medical literature Amplatz Left should be used which is correctly suggested by the model.

.

4.4.5. Execution Time

The catheter selection procedure is completely automatic. The segmentation (including preprocessing) takes 1.5 minutes, centerline extraction takes 40 seconds, and the parameters estimation and catheter

selection computation needs 10 seconds. The cardiologist gets a decision about an optimal catheter within 2.5 minutes (see Table 4.7).

Module	Processing time (seconds)
Segmentation including preprocssing	90
Skeletonization	50
Geometric parameters computation	5
Catheter selection	5

Table 4.7.: Execution time

4.4.6. Discussion

Knowing which one is the best catheter prior to coronary angiography significantly reduces the exposure time of the patient to radiation. An optimal catheter selection dramatically reduces the risk of artery punctures and internal bleeding. In this section, we evaluated image processing based models that replace the conventional catheter selection procedure. For this validation process, the ground truth was provided by the Uniklinkum Würzburg. They performed angiography of twenty four cases where twelve cases, were for the right coronary angiography and twelve cases were for the left coronary angiography. An experienced cardiologist selected catheters based on his experience and knowledge in the field. In the next step, the image data acquired prior to the angiography was used to find optimal catheters. For every patient, three catheters were suggested.

For the right model, in 41% cases the model's top suggested catheters were the same as that selected by the cardiologist. In 25% cases, the cardiologist's selection was second choice according to the model based selection. In 25% cases the cardiologist's selection was third choice of the model based selection. In 9% cases the cardiologist' selection was not included in the model's suggestions. For the left coronary model, in 41% cases the model's first suggestion is the same as that of the cardiologist's selection. In 25% cases the cardiologist's selection is model's second priority. In 17% cases the cardiologist's selection is model's third priority. In 17% cases the cardiologist' selection was not included in the model's suggestions. For anomalous arteries, only two cases were available in which in one case, model suggestion was same as that of cardiologist's selection and in the second case the model suggested a different catheter. Total of 25 catheters were used in these experiments. This is the first time that an image processing based method is introduced for catheter selection. The method is clinically applicable and only requires patients' image data before angiography. The whole method is completely automatic and needs two minutes for segmentation and catheter suggestion. Since 2D catheters are used, the patient's 3D data is projected onto a 2D plane. Sometimes this may lead to an angle computation which is not very exact. But in this case the system can suggest more than one choice. In any case the system will help the cardiologists to reduce the number of catheters to be tested on a given patient.

Catheter Type	Catheter Segment	w_{max} real catheter	w_{max} virtual catheter	error in %
JR35	1	0.001	0.00107584	3.792
	2	0.003	0.0032275	11.375
JR1	1	0.002	0.0022175	13.588
	2	0.004	0.00454356	13.589
SAR2	1	0.002	0.00215167	7.584
MB1	1	0.002	0.00182501	8.75
	2	0.001	0.00091252	8.748
	3	0.003	0.00273752	8.749

Table 4.8.: Deflection measurements of the virtual catheters compared to the deflection of the real catheters.

4.5. Evaluating Simulation Model

The first step of an image processing based catheter selection model is reducing the catheter choices from many to few using a geometric parameters based model. The second step is to simulate these reduced number of catheters and find a final suggestion. In this section, experiments related to simulation will be presented. First, we evaluate whether the catheter model is correct and then present different results about best catheter suggestion using catheter simulation.

4.5.1. Validating Catheter Simulation Model

For validating the catheter model, four different catheters (see Figure 4.20) were selected. These catheters differed in shape, size and elasticity. An ideal test for the simulation model would be the comparison of the final placement of a real catheter in a real artery and the final placement of the virtual catheter in patient-specific arteries' model, but such an experimental set up was not possible.

The evaluation was restricted to test the elastic behavior of the catheter models. The real catheters were compared to the virtual catheters with regard to their elastic behavior. Table 4.8 shows the elasticity values for the four catheters that were used in these experiments. First, the elasticity of real catheters was measured and computed using the procedure described in Section 3.5. The elasticity of each catheter was checked at different segments. Catheters JR35 and JR1 had two different elasticity levels at different segments. The elasticity for SAR2 was constant for the whole catheter everywhere. MB1 had three different elasticity levels. To compute the elasticity of the virtual catheters we followed the same procedure described in section 3.5 in our virtual environment. Figure 4.21 shows a segment of virtual catheter and the maximum deflection under the applied force of 1N. In the SOFA environment, we fixed one end of the segment and applied force at the other end. Then the deflection w_{max} was measured and compared to the deflection of the real catheters. Table 4.8 shows the deflection difference for real and virtual catheters. The average error is 9.52%.

4.5.2. Catheter Simulation Tests

After validating the catheter simulation model, a series of experiments was performed for optimal catheter selection. The reduced number of suggested catheters and the catheter selected by the cardiologist were simulated. All these catheters were visualized inside the patient's arteries. For all patients-specific arteries' models, surface meshes were created from the segmented images using series of VTK filters [SML06, Kit11]. The number of surface mesh triangles for different patients' models ranged from 90,000 to 120,000. In order to speed up the simulation, the meshes for all the patients were down sampled to 10,000 triangles using the mesh resampling algorithm presented by Simon et. al. [FAKG10]. The catheters were modeled as flexible beams. For catheter modeling, the catheter centerline was created and 3D triangulated surface mesh was created using the diameter of the catheter. The number of triangles for catheter models ranged from 800 to 1000. The guidewire was modeled as one dimensional bendable beam with a number of points ranged from 100 to 120. Same guidewire model was used for different catheters. For catheters and guidewires, denser sampling were taken at the curved area and sparse sampling at the straight area. The SOFA framework was used for simulation. Different steps of the catheter and guidewire simulation are shown in Figure 4.22. For simulation, first the guidewire was pushed inside the catheter until the guidewire reached the tip of the catheter. Then the combined catheter and guidewire were inserted into the aorta. Force was continuously applied at the proximal end of the guidewire as well as the catheter until the catheter reached the ostium. The catheter was rotated so that it can enter the coronary artery. After this, the tip of catheter was held fixed inside the coronary arteries by using a *FixedConstraint* component of the SOFA, and the guidewire was pulled back. Using Equations 3.10 and 3.11, the catheter placed closest to the centerline was selected as the optimal catheter.

We were specially interested in cases where the cardiologist's choice was not the first choice of the model. In Figure 4.13, the model's three suggested catheters HSISH (white), MB2 (blue), JR5 (yellow) and the cardiologist selection JR4 (green) are shown. Although the model's suggestions do not contain the catheter used by the cardiologist the figure shows that the tip of each suggested catheter has reached the ostium and the angles of the suggested catheters are appropriate. In Figure 4.12, the cardiologist decision JR4 (green) and the model's suggestion JR5 (blue) are shown. JR4 is the model's second choice. The angle of the suggested catheter is more suitable as compared to the selected catheter. In Figure 4.11, the cardiologist's decision JR4 (green) and the model's suggestion MP(Blue) are shown. The angle of MP is more suitable as compared to the JR4. JR4 is the model's 3rd choice. In Figure 4.19, the cardiologist's decision JL4 (green) and the model's suggestion AL4 (blue) are shown. The coronary takeoff is high so according to medical literature, AL should be used which is correctly suggested by our algorithms.
The current simulation implementation on CPU is slow and simulating one catheter takes thirty minutes. However, the simulation time can be reduced using parallel processing on GPU.

4.5.3. Discussion

In this section, a simulation based technique for patient-specific optimal catheter selection was presented. This simulation is used to further refine the catheter decisions from the geometric parameters based model. The geometric model does not consider the deformable nature of catheters and also consider the arteries as rigid bodies. In this simulation model, the catheter shape is obtained after simulation. The simulation takes more time as compared to simple parameters' computation but it guarantees more accurate decisions.

4.6. Summary

In this chapter, an evaluation of the different steps of an image processing based catheter selection procedure was presented. The clinical evaluation was conducted, and it was shown that the model is able to correctly identify an optimal catheter before starting the actual angiographic procedure. A series of validation tests were conducted for segmentation, geometric parameters' estimation, parameters based catheter selection model and simulation model. The segmentation results were compared with the results of ITK-SNAP tool as well as visual inspection was done. It was shown that completely *automatic initialization* and *termination* of the segmentation process takes less than a minute. After successful segmentation, the next validation was performed for the computation of different geometric parameters' computation. The automatically computed parameters were compared with the manually computed parameters. The average error between the manual and automatic computation was less than 1 *mm*. The most important step of the validation process was the catheter suggestion, using the geometric parameters based model. For this validation, the ground truth was obtained from the clinical partner. In the clinic, angiography of twenty four cases was performed. An experienced cardiologist selected catheters based on his experience and knowledge in the field. In the next step CT/MR image data that was acquired prior to the angiography was used for the image based catheter selection models to find optimal catheters. Catheters were suggested for every patient. Catheters suggested by the model were compared with the catheters selected by the cardiologist. It was found that for the right model, in 41% cases, model based top suggestions were the same as that of the cardiologist's selection. In 25% cases, the cardiologist's selection was the model's second priority. In 25% cases, the cardiologist selections were the model's third priority. In 9% cases the cardiologist's selection was not in the list of suggested catheters. For the left coronary model, in 41% cases, the model's top suggestions were same as that of the cardiologist's selection. In 25% cases the cardiologist's selection was the model's second priority. In 17% cases the cardiologist selections were athe model's third priority. In 17% cases the cardiologist's selection was not in the list of suggested catheters. For anomalous cases, only two cases were available. In one case, the model had the same result as that of cardiologist and in the second case, the model suggestion was different. Total of 25 catheters were used in these experiments. It was shown that the method is clinically applicable, and that the only requirement is to have patient's image data before angiography. The whole method is completely automatic and needs two minutes for segmentation and catheter suggestion. It was discussed that the angle computation may be not

very exact due to the projection of 3D data onto a 2D projection plane. But since the system suggests more than one catheter, in any case the system will help the cardiologists to reduce the number of catheters to be tested on a given patient. For further refining these geometric parameters based model, simulation was done. This simulation was done because the geometric model does not consider the deformable nature of catheters and also considers the arteries as rigid bodies. The simulation takes more time as compared to simple parameters computation but it guarantees more accurate decisions. It was shown that since the geometric parameters based approach does not consider the flexible nature of the catheters, sometimes it excludes a catheter that can be used after angle adjustment.
All these tests showed that the method of an image processing based catheter selection is clinically applicable, and the only requirement is to have patient's image data before starting angiography. It was shown that this tool will be of great help for the experienced as well as the non experienced cardiologists to have a catheter suggestion before starting the angiography.

[p] 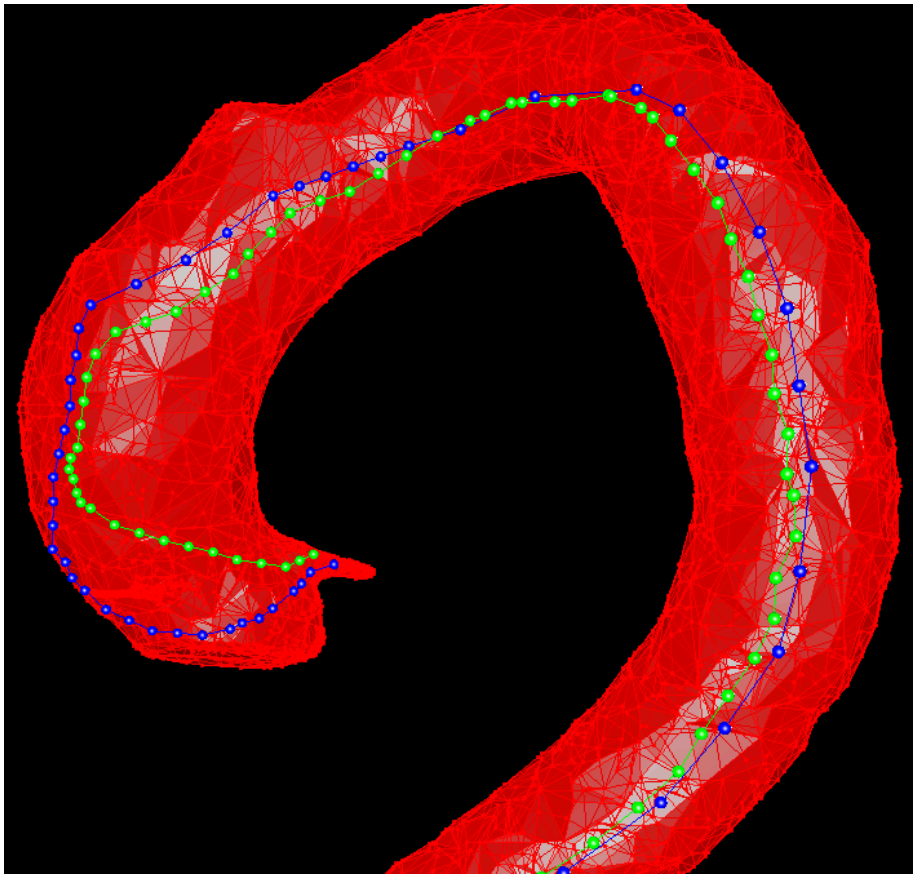

Figure 4.19.: Left coronary angiography (arteries with high takeoff): Cardiologist decision is the catheter JL4 (Green), Model's suggestion is the catheter AL4(Blue). The coronary take-off is high so according to the optimality criterion, AL should be used which is correctly suggested by the model

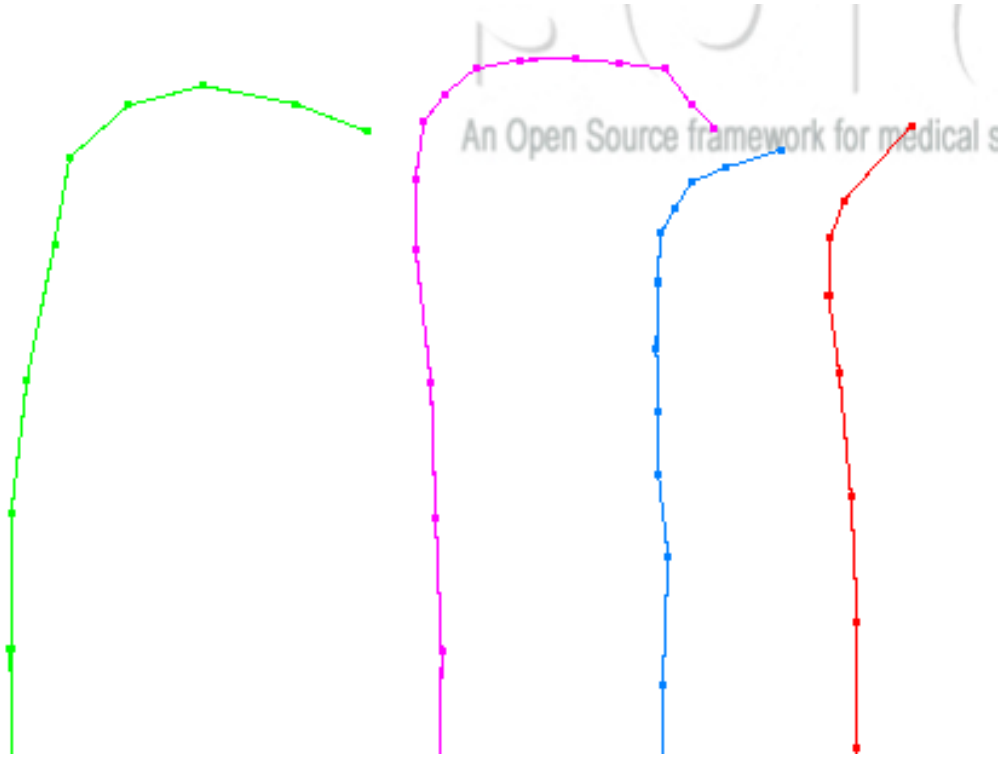

Figure 4.20.: Four different catheters that were used for elasticity tests, from left: MB1 (green), JR35 (pink), JR10 (blue), SAR20 (red)

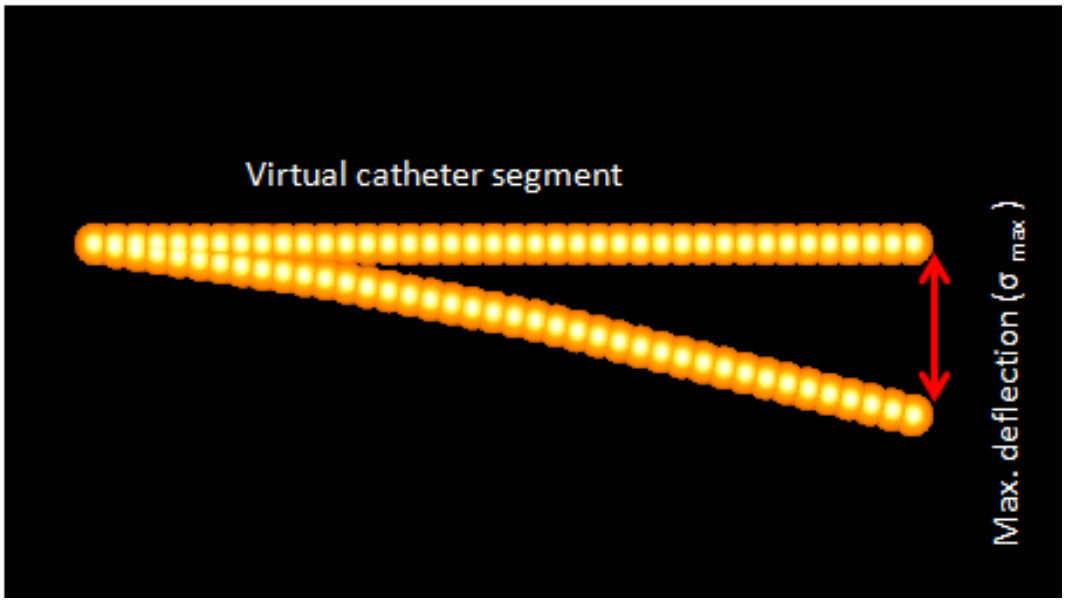

Figure 4.21.: Measuring virtual catheter's elasticity using SOFA framework

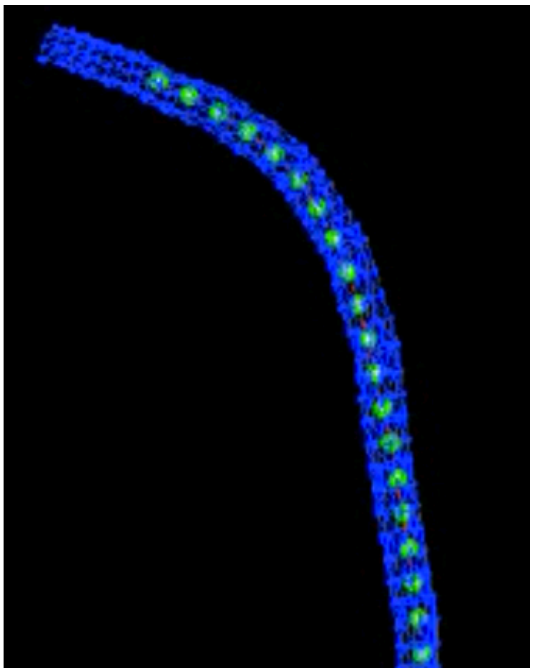

(a) Guidewire (green) is pushed inside catheter (blue)

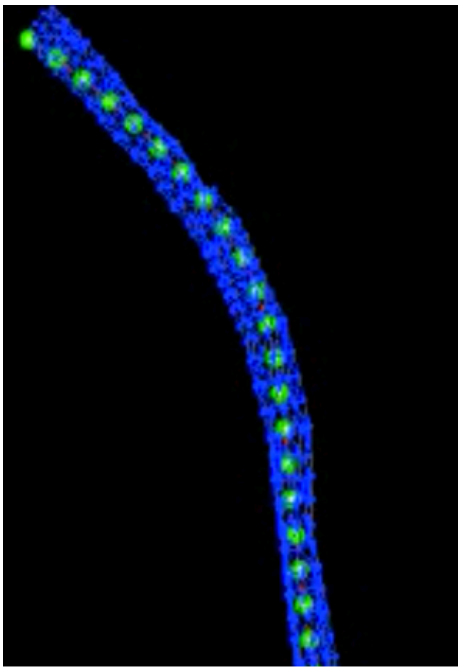

(b) Catheter curve becomes straight due to the guidewire stiffness

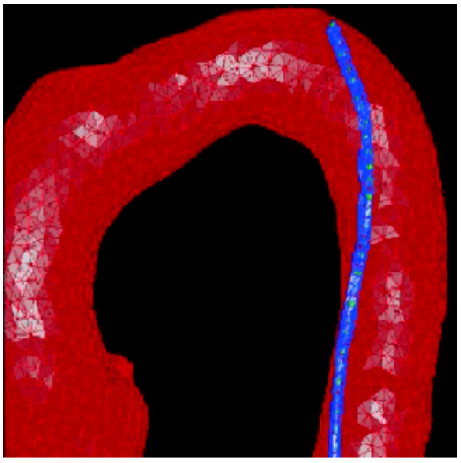

(c) Catheter and guidewire is pushed inside the arteries

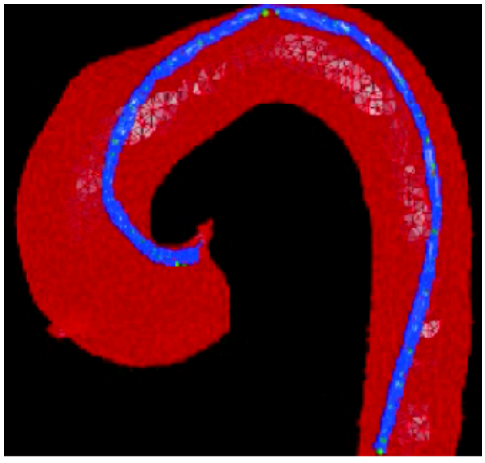

(d) Catheter is rotated towards the left coronary artery

Figure 4.22.: Catheter and guidewire simulation inside the arteries.

5. Conclusion and Future Work

The advancement in CT and MR imaging technology has made it possible to acquire a large amount of 3D and 4D image data in a short time. Due to the easy availability of patient's image data, the trend of patient-specific treatment and diagnosis is increasing. But at the same time, it is also challenging to get the required information from the bulk of this image data. Sometimes, the physicians need information that is scattered in different sets of images, which need manual work for getting the required information. Therefore, it is important to collect information from these different images and present it in a simple manner. In this thesis, we have presented models that collect information from different MR and CT images and provide patient-specific information for different treatment planning and diagnosis. The major contributions and distinctive features of this research work are: giving models for collecting useful information from different images, models for planning angiography, and simulation based guidance before the actual procedure.

Our first contribution is collecting information from different 3D images. In clinical imaging practice, different sets of high resolution and low resolution 3D images are acquired. For example, different sets of high resolution images of small objects like the coronary arteries, and low resolution images of the bigger objects like the aorta, are acquired. Clinically, it is highly desirable to have information from all these images in one 3D image. In this thesis, we presented a solution, which based on segmentation and registration, for fusing information from different images. A complete automatic segmentation model for specially acquired MR images of low resolution aorta and high resolution coronary arteries is presented. The 3D model is able to collect information from the different images with different resolution, into a single image. The segmentation results were compared with the results of ITK-SNAP tool as well as a visual inspection was done. It has been shown that completely automatic initialization and termination of the segmentation process takes less than a minute, and this procedure saves image acquisition time by decreasing the target resolution for the larger objects.

Second contribution is in the field of quantitative measurements of different clinically important parameters. A 3D model is computed from 3D MR or CT images, and then clinically important parameters are automatically computed. These parameters are of great help for the cardiologists to investigate different treatments and diagnoses. Finding the diameter of the aorta helps to know about the stenosis and aneurysm. The diameter of the coronary arteries helps to know whether the artery has become thin. The position of the coronary arteries ostium and its distance from the aortic valves helps to know whether the coronary arteries have a high takeoff or a low takeoff. Similarly, the angle of the coronary arteries with the aorta helps to judge whether the takeoff is horizontal, inferior or superior. For evalua-

tion, the automatically computed parameters were compared with the manually computed parameters. The average error between the manual and automatic computation was less than 1 *mm*.

The innovative aspect of the thesis is in the field of catheter angiography and catheter selection. Different models are defined for a very challenging task of catheter selection. Different image processing based patient-specific models for best catheter selection have been defined. These models are compatible to replace the conventional *trial and error* based catheter selection procedure. The models are for right coronary angiography, left coronary angiography and for angiography of the coronary arteries with a high takeoff. These models are able to reduce the catheter choices from many to a few and will facilitate a cardiologist, especially the inexperienced, in conducting the angiography procedure with greater accuracy. The models under discussion will also be a benefit for the patients such as time wise less exposure to radiation and less incidence of injuries to the arteries. A series of validation tests were performed and it was found that for half of the cases, model based top suggestions were the same as that of the cardiologist's selection. In one fourth of the cases, the cardiologist's selection was the model's second priority. It was shown that the method is clinically feasible, easily applicable with the only requirement to have patients' image data before angiography. The whole method is completely automatic and needs two minutes for segmentation and catheter selection.

The last contribution is in the field of catheter simulation. Although there exist catheter simulation systems but all these are used only for training purposes and these systems are non patient-specific. Under the current research study, the current simulation strategies for catheter selection purposes have been extended and value added. The proposed simulation system uses patient-specific models and simulates different catheters. The final placement of different catheters are computed and a catheter, suitable according to some medical criteria are considered as an optimal catheter.

5.1. Comparison with the Current Approaches

The different contributions in this thesis improve state of the art in the areas of segmentation, parameters' estimation, catheter selection and simulation. In this section, we compare our methods with the available approaches.

Our segmentation approach is based on the existing "Fast Marching Method". In the available literature, this approach has been used for segmenting specific objects [DC02] as well as for generalized segmentation algorithms [YPCH*06, YPC*11] for the 3D objects. However, these approaches involve user interaction. We have automated the seed point selection procedure using Hough peaks [Bal81] and have used registration of the aorta and the coronary arteries for the seed point selection in the coronary arteries.

Our work on parameters' estimation also extends the current state of the art. In the literature, there are some semiautomatic approaches for computing parameters from the image data and there are also approaches for the patient-specific quantification of some parameters like aortic valves and mitral valves landmark. In our work, we have extended these approaches to the complete automatic computation of the aorta and the coronary arteries' diameters, curves, angles, ostium, and aortic valves position.

We have seen that in the medical literature, there are some general approaches and recommendations for the best catheter selection but cardiologists are not able to decide in advance for an optimal catheter. We have used these recommendations and guidelines for a complete novel automatic patient-specific catheter selection. To the best of our knowledge, no such approach is available in the current medical literature.

Our catheter simulation approach extends the state of the art by considering both the guidewire and the catheter in the simulation system. In the current systems, people have either considered only guidewire simulation [LBGB09, LZL*10] or catheter-guidewire composite model [J. 06]. In the composite model, the same FEM model dynamically adapts its material properties to locally described combination of both devices. In this model, catheter and guidewires or not considered two different objects as these are in the physical world. There are also other systems for catheter simulation [Meg96, AR98, NC01, CDM*00] but all these systems are still far from the real environment. Moreover, these systems do not handle the problem of patient-specific optimal catheter selection. In our work, we have considered the two instruments the same way as these are used in the physical world. However, the disadvantage of our system is the required amount of simulation time. The complete simulation of catheter and guidewire need 30 minutes per catheter.

5.2. Improvement of the Models

The algorithms developed during this thesis work can be improved to be more general, dynamic and more robust with a wider scope of improvement. There are many dimensions in which the current approaches can be improved.

In the current validation tests, we have seen that the catheter selection model is able to identify the catheters, that are selected by the clinicians after a series of attempts. We have seen that if clinician select an optimal catheter then the model agrees with that suggestion but if the clinician select a non optimal catheter then the model does not agree with that selection and suggest a different catheter. However, we do not yet know that the alternate suggestion of the model is an optimal choice. For these, we need further scientific experiments. It would be very interesting to perform a series of experiments by first performing catheter selection in conventional way and afterwards usage of the catheters , which is proposed by the automatic catheter selection procedure.

In MR and CT images, the orientation of the acquired images remains the same with slight devia-

tion in the rotation or translation. The current segmentation algorithm has assumed these standard orientations. These algorithms can be modified to be orientation independent. Similarly, during geometric parameters computations, the algorithms assume the standard orientation but these parameters can be computed in a way to be independent of the image orientation.

Besides, the used skeletonization algorithm is highly dependent on the exact segmentation results. A minor segmentation error may lead to a very bad skeletonization result. Therefore, it would be necessary to have skeletonization that can tolerate minor segmentation errors.

Computing the position of the aortic valves can also be improved by incorporating the anatomical information. The current computations consider only the intensity information for the aortic valves identification.

Another area of improvement is about generality of the segmentation algorithm. The current segmentation approach was developed for a special clinical requirement of having separate images of the coronary arteries and the aorta. However, the algorithm can be extended for segmenting the images where the aorta and coronary arteries are acquired in the same image.

For simulation, the FEM has been used, which is very slow due to which real time computation is not possible. In order to get real time computation, the FEM based technique is needed to be replaced by some other technique like spring model, which is faster.

The most important and interesting improvement is possible in the geometric parameters based models. These models use different parameters and each parameter needs tuning of the parameter's weight for obtaining correct results. It is possible to avoid weight tuning by comparing patient's parameters with the catheters' parameters and use some threshold value for excluding catheters from the optimality list.

The current model does not include many cases having anomalous origin of the coronary arteries. For examples, the cases with anomalous right coronary artery where the right coronary artery originates from the left coronary sinus or anomalous left coronary artery where the left main coronary artery originates from the right coronary sinus and following prepulmonic course. The catheter selection algorithm can be modified to include these cases.

Similarly, in the current work we have not considered the cases of coronary bypass surgery angiography and interventions. New parameters will be needed to select catheter for post bypass angiography.

5.3. Future Work

The models presented in the current research study, can be extended in many directions for patient-specific treatment and diagnostic procedures. The different directions for extension are brain angiogra-

phy, heart catheterization, inventing new catheters and fusing 3D and 4D images.

The current models for suggesting optimal catheters can be extended for catheter selection during cerebral angiography. The treatment and diagnosis of strokes and arteriovenous malformation (abnormal connection between veins and arteries) need brain catheterization and due to the complex arteries structure, the selection of suitable catheter is challenging. The models developed as outcome of this research, can be modified to fit to the problem of catheter selection for cerebral angiography.

Another research direction is the heart catheterization. Crossing the aortic valves during left heart catheterization is also a time consuming task. The cardiologists find a suitable catheter for crossing the aortic valves using the 'trail and error' procedure. The existing models for the catheter selection can be used by changing the parameters.

The work can also be extended for inventing new catheters. A study of the anatomies of different patients and different catheters shows that sometimes the parameters of the available catheters do not fit well for a given patient's anatomy. The idea of inventing new catheters that fulfill the need of many patients can be an interesting research area.

Another extension of the current work is fusion of 3D images of the different parts of the human body. For example the aortic valves can be imaged using high resolution (because of its smaller size) and the aorta can be imaged using low resolution. Clinically, it would be desirable to combine the high resolution aortic valves and the low resolution aorta in a single 3D image which will reduce patient's exposure time to radiation.

The current simulation strategies can be extended to integrate a Haptic device. This will help to have more realistic simulation environment for training as well as catheter selection.

The current geometric based catheter selection model has the potential for commercial use. The only requirements is to add a user interface for easy use and adding a component for visualization of the catheters inside the arteries and having user feedback for handling noisy data for seed point selection during segmentation and marking the aortic valves position.

A. Publications and Talks

The thesis is partially based on the following publications:

Publications

1. Flehmann, Eugen; Rahman, Sami ur; Wesarg, Stefan; Völker, Wolfram. : Towards Patient Specific Catheter Selection: Computation of Aortic Geometry Based on Fused MRI Data. In Functional Imaging and Modeling of the Heart, Metaxas D., Axel L., (Eds.), vol. 6666 of Lecture Notes in Computer Science. Springer Berlin / Heidelberg, 2011, pp. 145–152
2. Rahman, Sami ur; Wesarg, Stefan; Völker, Wolfram.: Patient specific optimal catheter selection for right coronary artery. In Society of Photo-Optical Instrumentation Engineers (SPIE) Conference Series (Mar. 2011), vol. 7964 of Society of Photo-Optical Instrumentation Engineers (SPIE) Conference Series.
3. Rahman, Sami ur; Thoene, Clara; Wesarg, Stefan; Völker, Wolfram.: Simulation based patient specific optimal catheter selection for right coronary angiography. In Society of Photo-Optical Instrumentation Engineers (SPIE) Conference Series (Feb. 2012), vol. 8316 of Society of Photo-Optical Instrumentation Engineers (SPIE) Conference Series.
4. Rahman, Sami ur; Wesarg, Stefan; Völker, Wolfram.: Patient specific optimal catheter selection for the left coronary artery. In Informatik 2011, Emerging Technologies for Medical Diagnosis and Therapy (2011).
5. Rahman, Sami ur; Wesarg, Stefan.: Combining short-axis and long-axis cardiac MR images by applying a super-resolution reconstruction algorithm. In Society of Photo-Optical Instrumentation Engineers (SPIE) Conference Series (Mar. 2010), vol. 7623 of Society of Photo-Optical Instrumentation Engineers (SPIE) Conference Series.
6. Rahman, Sami ur; Wesarg, Stefan.: Upsampling of cardiac MR images: Comparison of averaging and super-resolution for the combination of multiple views. In ITAB 2010 (2010), University of Ioannina and et al., IEEE, Inc., New York, p. 4.
7. Rahman, Sami ur; Tsvetoslava, Vateva; Wesarg, Stefan.: Enhancing super-resolution reconstructed image quality in 3D MR images using simulated annealing. In Society of Photo-Optical Instrumentation Engineers (SPIE) Conference Series (Feb. 2012), vol. 8314 of Society of Photo-Optical Instrumentation Engineers (SPIE) Conference Series

B. Supervising Activities

The following list summarizes the student bachelor, diploma and master thesis supervised by the author. The results of these works were partially used as an input into the thesis.

B.1. Diploma and Master Thesis

1. Catheter simulation using spring model. Metlewski, Eduard; Rahman, Sami ur (supervisor). Master thesis, TU-Darmstadt, Darmstadt, 2012.
2. Optimal Catheter Selection for Anomalous Right Coronary Arteries. Rauf, Usman; Rahman, Sami ur (supervisor). Master thesis, Blekinge Institute of Technology Sweden, 2011.
3. Segmentierung der Aorta, Koronararterien und Bestimmung der geometrischen Parameter. Flehmann, Eugen; Rahman, Sami ur (supervisor). Master thesis, TU-Darmstadt, Darmstadt, 2010.

B.2. Bachelor Thesis

1. Catheter simulation for optional selection prior to coronary angiography, Thoene, Clara; Rahman, Sami ur (supervisor). Bachelor thesis, TU-Darmstadt, Darmstadt, 2011.
2. Evaluating a super-resolution reconstruction algorithm and enhancing image quality using simulated annealing technique, Vateva, Tsvetoslava ; Rahman, Sami ur (supervisor). Bachelor thesis, TU-Darmstadt, Darmstadt, 2011.

C. Curriculum Vitae

Personal Data

Name	Sami ur Rahman
Birth date & place	01.01.1976 in Swat Pakistan
Family status	Married
Nationality	Pakistani

Education

2007 – 2009	M.Sc (Applied Computer Science), Alfred-Ludwig Universität Freiburg, Germany
1999 – 2001	M.Sc (Computer Science), University of Peshawar, Pakistan
1995 – 1999	B.A (Hons), University of Peshawar, Pakistan

Work Experience

2009 –	Researcher, Interactive Graphics Systems Group, Technische Universität Darmstadt, Germany, Focus: Medical Imaging
2003–2006	Lecturer, Department of Computer Science, University of Malakand, Pakistan
2003–2003	Lecturer, Department of Computer Science, NWFP University of Engineering and Technology Peshawar, Pakistan
2002–2003	Lecturer, Department of Computer Science, Qurtuba University of Science and Information Technology Peshawar, Pakistan
2001–2002	Lecturer, Department of Computer Science, CECOS University of IT and Emerging Sciences Peshawar, Pakistan

Bibliography

[AAE*10] ARLICOT A., AMOURIQ Y., EVENOU P., NORMAND N., GUEDON J.-P.: A single scan skeletonization algorithm: application to medical imaging of trabecular bone. In *Medical Imaging: Image Processing* (2010), Dawant B. M., Haynor D. R., (Eds.), vol. 7623, SPIE, p. 762317. 20

[ACF*07] ALLARD J., COTIN S., FAURE F., BENSOUSSAN P., POYER F., DURIEZ C., DELINGETTE H., GRISONI L.: SOFA an Open Source Framework for Medical Simulation. In *Medicine Meets Virtual Reality (MMVR'15)* (Long Beach, USA, February 2007). xiv, 68

[AKN04] ALDERLIESTEN T., KONINGS M. K., NIESSEN W.: Simulation of minimally invasive vascular interventions for training purposes. *Computer Aided Surgery 9*, 1-2 (2004), 3–15. ix, 32, 33

[AR98] ANDERSON J., RAGHAVAN R.: A vascular catheterization simulator for training and treatment planning. *Journal of Digital Imaging 11* (1998), 120–123. 10.1007/BF03168278. ix, 29, 32, 113

[ATC*08] AU O. K.-C., TAI C.-L., CHU H.-K., COHEN-OR D., LEE T.-Y.: Skeleton extraction by mesh contraction. In *ACM SIGGRAPH 2008 papers* (New York, NY, USA, 2008), SIGGRAPH '08, ACM, pp. 44:1–44:10. 19

[Bal81] BALLARD D.: Generalizing the Hough transform to detect arbitrary shapes. *Pattern Recognition 13*, 2 (1981), 111 – 122. ix, 40, 112

[BBN*94] BRINKMAN A., BAKER P., NEWMAN W., VIGORITO R., FRIEDMAN M.: Variability of human coronary artery geometry: An angiographic study of the left anterior descending arteries of 30 autopsy hearts. *Annals of Biomedical Engineering 22* (1994), 34–44. 10.1007/BF02368220. viii, 21, 26

[Bn97] BRO-NIELSEN M.: Simulation Techniques for Minimally Invasive Surgery. *Journal of Minimally Invasive Therapy and Allied Technologies 6* (1997), 106–110. 29

[Bor84] BORGEFORS G.: Distance transformations in arbitrary dimensions. *Computer Vision, Graphics, and Image Processing 27*, 3 (1984), 321 – 345. 20

[BRB*08] BOURAOUI B., RONSE C., BARUTHIO J., PASSAT N., GERMAIN P.: Fully automatic 3D segmentation of coronary arteries based on mathematical morphology. In *Biomedical Imaging: From Nano to Macro, 2008. ISBI 2008. 5th IEEE International Symposium on* (May 2008), pp. 1059–1062. 19

[BS00] BOUIX S., SIDDIQI K.: Divergence-based medial surfaces. In *Sixth European Conference on Computer Vision* (2000), pp. 603–618. 20

[CDL*05] COTIN S., DURIEZ C., LENOIR J., NEUMANN P., DAWSON S.: New approaches to catheter navigation for interventional radiology simulation. In *Proceedings of medical image computing and computer assisted intervention (MICCAI), Palm* (2005), pp. 300–308. ix, 31, 32

[CDM*00] COTIN S., DAWSON S., MEGLAN D., SHAFFER D., FERRELL M., BARDSLEY R., MORGAN F., NAGANO T., NIKOM J., SHERMAN P., WALTERMAN M., WENDLANDT J.: ICTS, an interventional cardiology training system. In *Westwood JD, Hoffman HM, Mogel GT, Robb A, Stredney D, editors. Medicine Meets Virtual Reality: Studies in Health Technology and Informatics (Proceedings of MMVR 2000). Amsterdam: IOS Press* (2000), pp. 59,65. 30, 31, 113

[CNW*12] CHUI C., NGUYEN H., WANG Y., MULLICK R., RAGHAVAN R.: User interface for davinci. `http://www.nlm.nih.gov/research/visible/vhp_conf/chui/index.htm`, June 2012. [Accessed Jun. 22, 2012]. 30

[Coi08] COIS C. A.: *Variable Scale Statistics For Cardiac Segmentation and Shape Analysis*. PhD thesis, January 2008. 76

[CRG*07] COIS A., ROCKOT K. J., GALEOTTI J. M., TAMBURO R. J., GOTTLIEB D., MAYER J. E., POWELL A., SACKS M., STETTEN G. D.: Automated segmentation of the right heart using an optimized shells and spheres algorithm. In *ISBI* (2007), pp. 876–879. 76

[DC02] DESCHAMPS T., COHEN L. D.: Fast extraction of tubular and tree 3d surfaces with front propagation methods. In *Proceedings of the 16 th International Conference on Pattern Recognition (ICPR'02) Volume 1 - Volume 1* (Washington, DC, USA, 2002), ICPR '02, IEEE Computer Society, pp. 10731–. 18, 19, 34, 112

[DMMS06] DAS B., MALLADI R., MALLYA Y., SRIKANTH S.: Aortic thrombus segmentation using narrow band active contour model. *Conf Proc IEEE Eng Med Biol Soc 1*, 1 (2006), 408–411. 76

[EGM*94] EBERLY D., GARDNER R., MORSE B., PIZER S., SCHARLACH C.: Ridges for image analysis. *J. Math. Imaging Vis. 4*, 4 (Dec. 1994), 353–373. 20

[EMGF07] EGGER J., MOSTARKIC Z., GROSSKOPF S., FREISLEBEN B.: A fast vessel centerline extraction algorithm for catheter simulation. In *Proceedings of the Twentieth IEEE International Symposium on Computer-Based Medical Systems* (Washington, DC, USA, 2007), IEEE Computer Society, pp. 177–182. 20

[FAKG10] FUHRMANN S., ACKERMANN J., KALBE T., GOESELE M.: Direct resampling for isotropic surface remeshing. In *VMV* (2010), pp. 9–16. 104

[FC06] FALLAVOLLITA P., CHERIET F.: Towards an Automatic Coronary Artery Segmentation Algorithm. In *Engineering in Medicine and Biology Society, 2006. EMBS '06. 28th Annual International Conference of the IEEE* (30 2006). 19

[FNH*99] FRANGI A., NIESSEN W., HOOGEVEEN R., VAN WALSUM T., VIERGEVER M.: Quantitation of Vessel Morphology from 3D MRA. In *MICCAI, 2nd International Conference* (1999), Taylor C., Colchester A., (Eds.), vol. 1679 of *LNCS*, Springer, pp. 358–367. x, 42

[FRWV11] FLEHMANN E., RAHMAN S., WESARG S., VÖLKER W.: Towards Patient Specific Catheter Selection: Computation of Aortic Geometry Based on Fused MRI Data. In *Functional Imaging and Modeling of the Heart*, Metaxas D., Axel L., (Eds.), vol. 6666 of *Lecture Notes in Computer Science*. Springer Berlin / Heidelberg, 2011, pp. 145–152. 57, 58, 67

[FW06] FERCHICHI S., WANG S.: A Clustering-based Algorithm for Extracting the Centerlines of 2D and 3D Objects. *Pattern Recognition, International Conference on Pattern Recognition 2* (2006), 296–299. 20

[HBF*05] HENNEMUTH A., BOSKAMP T., FRITZ D., KÜHNEL C., BOCK S., RINCK D., SCHEUERING M., PEITGEN H.-O.: One-click coronary tree segmentation in CT angiographic images. *International Congress Series 1281* (2005), 317–321. CARS 2005: Computer Assisted Radiology and Surgery. viii, 19

[Hib10] HIBBELER R. C.: *Mechanics of Materials; 8th ed.* Pearson, Upper Saddle River, NJ, 2010. 68

[Hom07] HOMANN H.: Implementation of a 3D thinning algorithm. *Oxford University, Wolfson Medical Vision Lab* (2007). xi, 52, 79

[HSKR96] HIGGINS W. E., SPYRA W. J. T., KARWOSKI R. A., RITMAN E. L.: System for analyzing high-resolution three-dimensional coronary angiograms. *Medical Imaging, IEEE Transactions on 15*, 3 (June 1996), 377–385. 20

[IVG*10] IONASEC R. I., VOIGT I., GEORGESCU B., 0001 Y. W., HOULE H., HIGUERA F. V., NAVAB N., COMANICIU D.: Patient-Specific Modeling and Quantification of the Aortic and Mitral Valves From 4-D Cardiac CT and TEE. *IEEE Trans. Med. Imaging 29*, 9 (2010), 1636–1651. viii, 26, 27

[J. 06] J. LENOIR AND S. COTIN AND C. DURIEZ AND P. NEUMANN: Interactive physically-based simulation of catheter and guidewire. *Computers and Graphics 30*, 3 (2006), 416 – 422. ix, 32, 113

[JLZ*10] JOHN M., LIAO R., ZHENG Y., NOETTLING A., BOESE J. M., KIRSCHSTEIN U., KEMPFERT J., WALTHER T.: System to Guide Transcatheter Aortic Valve Implantations Based on Interventional C-Arm CT Imaging. In *MICCAI (1)* (2010), Jiang T., Navab N., Pluim J. P. W., Viergever M. A., (Eds.), vol. 6361 of *Lecture Notes in Computer Science*, Springer, pp. 375–382. viii, 17, 26

[KCA*06a] KOVÁCS T., CATTIN P., ALKADHI H., WILDERMUTH S., SZÉKELY G.: Automatic Segmentation of the Aortic Dissection Membrane from 3D CTA Images. In *Medical Imaging and Augmented Reality (MIAR)* (2006). vii, 17, 19, 34

[KCA*06b] KOVÁCS T., CATTIN P., ALKADHI H., WILDERMUTH S., SZÉKELY G.: Automatic Segmentation of the Vessel Lumen from 3D CTA Images of Aortic Dissection. In *Bildverarbeitung für die Medizin 2006*, Brauer W., Handels H., Ehrhardt J., Horsch A., Meinzer H.-P., Tolxdorff T., (Eds.), Informatik aktuell. Springer Berlin Heidelberg, 2006, pp. 161–165. vii, 17, 18, 19, 34, 40

[KFHN76] KIRKS D. R., FITZ C. R., HARWOOD-NASH D. C.: Pediatric abdominal angiography: Practical guide to catheter selection, flow rates, and contrast dosage. *Pediatric Radiology 5* (1976), 19–23. 10.1007/BF00988657. viii, 21

[KISB78] KIMBIRIS D., ISKANDRIAN A., SEGAL B., BEMIS C.: Anomalous Aortic Origin of Coronary Arteries. *Circulation 58*, 4 (1978), 606–615. viii, 6, 11, 21

[Kit11] KITWARE I.: VTK Visualization Toolkit, May 2011. [Accessed Aug. 16, 2012]. 67, 104

[Kit12] KITWARE I.: Insight Segmentation and Registration Toolkit (ITK). `http://www.itk.org/ITK/help/documentation.html`, June 2012. [Accessed Jun. 24, 2012]. 40

[KM90] KATZ W., MERICKEL M.: Aorta detection in magnetic resonance images using multiple artificial neural networks. In *Engineering in Medicine and Biology Society, 1990., Proceedings of the Twelfth Annual International Conference of the IEEE* (nov 1990), pp. 1302 –1303. 17

[KMA*00] KRISSIAN K., MALANDAIN G., AYACHE N., VAILLANT R., TROUSSET Y.: Model-Based Detection of Tubular Structures in 3D Images. *Computer Vision and Image Understanding 80*, 2 (2000), 130–171. 20

[KS96] KRIETE A., SCHWEBEL T.: 3-D TOP-A software package for the topological analysis of image sequences. *J. Structural Biol. 116*, 1 (1996), 150–154. 20

[KSK*04] KIVINIEMI T. O., SARASTE M., KOSKENVUO J. W., AIRAKSINEN K. E. J., TOIKKA J. O., SARASTE A., PÄRKKÄ J. P., HARTIALA J. J.: Coronary artery diameter can be assessed reliably with transthoracic echocardiography. *American Journal of Physiology - Heart and Circulatory Physiology 286*, 4 (Apr. 2004), H1515–H1520. 26

[KWT88] KASS M., WITKIN A., TERZOPOULOS D.: Snakes: Active contour models. *INTERNATIONAL JOURNAL OF COMPUTER VISION 1*, 4 (1988), 321–331. 18

[LBGB09] LUBOZ V., BLAZEWSKI R., GOULD D., BELLO F.: Real-time guidewire simulation in complex vascular models. *The Visual Computer 25* (2009), 827–834. 10.1007/s00371-009-0312-x. ix, 32, 33, 113

[LGW*12] LI S., GUO J., WANG Q., MENG Q., CHUI Y.-P., QIN J., HENG P.-A.: A catheterization-training simulator based on a fast multigrid solver. *Computer Graphics and Applications, IEEE 32*, 6 (nov.-dec. 2012), 56 –70. 33

[Lin96] LINDEBERG T.: Edge detection and ridge detection with automatic scale selection. *International Journal of Computer Vision 30* (1996), 465–470. 20

[LKC94] LEE T., KASHYAP R., CHU C.: Building Skeleton Models via 3-D Medial Surface Axis Thinning Algorithms. *CVGIP: Graphical Models and Image Processing 56*, 6 (1994), 462 – 478. 20, 21, 34, 47

[LRSB03] LORENZ C., RENISCH S., SCHLATHOELTER T., BUELOW T.: Simultaneous segmentation and tree reconstruction of the coronary arteries in MSCT images. Clough A., Amini A., (Eds.), vol. 5031, SPIE, pp. 167–177. vii, 19

[LUM11] LUMEN: Radiological Anatomy of Heart and Vessels in Thorax. http://www.meddean.luc.edu/lumen/MedEd/Radio/curriculum/Vascular/Structure_Vessels_thorax_f.htm, Apr. 2011. [Accessed Jun. 10, 2012]. 4

[LZL*10] LUBOZ V., ZHAI J., LITTLER P., ODETOYINBO T., GOULD D., HOW T., BELLO F.: Endovascular guidewire flexibility simulation. In *Biomedical Simulation*, Bello F., Cotin S., (Eds.), vol. 5958 of *Lecture Notes in Computer Science*. Springer Berlin / Heidelberg, 2010, pp. 171–180. 10.1007/978-3-642-11615-5-18. ix, 32, 33, 113

[MBA93] MALANDAIN G., BERTRAND G., AYACHE N.: Topological segmentation of discrete surfaces. *International Journal of Computer Vision 10* (1993), 183–197. 10.1007/BF01420736. 20

[MBCS90] MYLER R., BOUCHER R., CUMBERLAND D., STERTZER S.: Guiding catheter selection for right coronary artery angioplasty. *Catheterization and Cardiovascular Diagnosis 19* (1990). 23, 24

[Meg96] MEGLAN D.: Making surgical simulation real. *SIGGRAPH Comput. Graph. 30* (November 1996), 37–39. ix, 28, 32, 113

[MPN*11] MENDIS S., PUSKA P., NORRVING B., ORGANIZATION. W. H., FEDERATION W. H., ORGANIZATION. W. S.: *Global atlas on cardiovascular disease prevention and control / editors, Shanthi Mendis, Pekka Puska and Bo Norrving*. World Health Organization in collaboration with the World Heart Federation and the World Stroke Organization, Geneva :, 2011. vii, 1

[MS96] MA C. M., SONKA M.: A fully parallel 3D thinning algorithm and its applications. *Comput. Vis. Image Underst. 64*, 3 (Nov. 1996), 420–433. 20, 47

[MT96] MCINERNEY T., TERZOPOULOS D.: Deformable models in medical image analysis: a survey. *Medical Image Analysis 1*, 2 (June 1996), 91–108. 18

[NC01] NOWINSKI W. L., CHUI C.-K.: Simulation of interventional neuroradiology procedures. In *Proceedings of the International Workshop on Medical Imaging and Augmented Reality (MIAR '01)* (Washington, DC, USA, 2001), MIAR '01, IEEE Computer Society, pp. 87–. ix, 30, 32, 113

[NHS12] NHSCHOICES I.: Cardiac catheterisation and coronary angiography. http://www.nhs.uk/Conditions/CoronaryAngiography/Pages/Introduction.aspx, Apr. 2012. [Accessed Jun. 10, 2012]. 3

[Phi12] PHILIPS I.: Heartnavigator. http://www.healthcare.philips.com/de_de/products/interventional_xray/product/interventional_cardiac_surgery/interventional_tools/heartnavigator/, May 2012. [Accessed Aug. 30, 2012]. 26, 28

[Pil02] PILKEY W.: *Analysis and Design of Elastic Beams: Computational Methods*. Wiley, 2002. 68

[PK09] PINAR KOSAR ELIF ERGUN C. Z. U. K.: Anatomic variations and anomalies of the coronary arteries: 64-slice CT angiographic appearance. *Diagn Interv Radiol 15*, 4 (2009), 275–83. 6, 8, 9, 10

[PM90a] PERONA P., MALIK J.: Scale-space and edge detection using anisotropic diffusion. *IEEE Transactions on Pattern Analysis and Machine Intelligence 12* (1990), 629–639. 19

[PM90b] PERONA P., MALIK J.: Scale-space and edge detection using anisotropic diffusion. *IEEE Transactions on Pattern Analysis and Machine Intelligence 12* (1990), 629–639. 40

[Poh01] POHLE R.: Segmentation of medical images using adaptive region growing. *Proceedings of SPIE 4322*, 3 (2001), 1337–1346. 16

[RBF*97] RUECKERT D., BURGER P., FORBAT S., MOHIADDIN R., YANG G.: Automatic tracking of the aorta in cardiovascular MR images using deformable models. *Medical Imaging, IEEE Transactions on 16*, 5 (1997), 581–590. vii, 17

[RPJN98] RUBIN G. D., PAIK D. S., JOHNSTON P. C., NAPEL S.: Measurement of the aorta and its branches with helical CT. *Radiology 206*, 3 (1998), 823–829. viii, 26

[RTWV12] RAHMAN S. U., THOENE C., WESARG S., VOELKER W.: Simulation based patient-specific optimal catheter selection for right coronary angiography. In *Society of Photo-Optical Instrumentation Engineers (SPIE) Conference Series* (Feb. 2012), vol. 8316. 69

[RWV11a] RAHMAN S. U., WESARG S., VÖLKER W.: Patient specific optimal catheter selection for right coronary artery. In *Society of Photo-Optical Instrumentation Engineers (SPIE) Conference Series* (Mar. 2011), vol. 7964 of *Society of Photo-Optical Instrumentation Engineers (SPIE) Conference Series*. 58, 82

[RWV11b] RAHMAN S. U., WESARG W., VÖLKER W.: Patient specific optimal catheter selection for the left coronary artery. In *Informatik 2011 – Emerging Technologies for Medical Diagnosis and Therapy* (2011). 82

[Sch03] SCHNEIDER P.: *Endovascular Skills: Guidewire and Catheter Skills for Endovascular Surgery*, "second edition" ed. Marcel Dekkar Inc., 2003. viii, 21, 22, 25

[Set99] SETHIAN J.: Fast Marching Methods. *SIAM Rev. 41* (June 1999), 199–235. ix, 40

[SJYW10] SHOUJUN Z., JIAN Y., YONGTIAN W., WUFAN C.: Automatic segmentation of coronary angiograms based on fuzzy inferring and probabilistic tracking. *BioMedical Engineering OnLine 9*, 1 (2010), 40. viii, 19

[SKB*08] SAUR S. C., KÜHNEL C., BOSKAMP T., SZEKELY G., CATTIN P. C.: Automatic Ascending Aorta Detection in CTA Datasets. Tolxdorff T., Braun J., Deserno T. M.,

Handels H., Horsch A., Meinzer H.-P., (Eds.), Informatik Aktuell, Springer, pp. 323–327. vii, 17

[SML06] SCHROEDER W., MARTIN K., LORENSEN B.: *Visualization Toolkit: An Object-Oriented Approach to 3D Graphics, 4th Edition*, 4th ed. Kitware, Dec. 2006. xiv, 67, 104

[SSK09] SARKAR K., SHARMA S., KINI A.: Catheter Selection for Coronary Angiography and Intervention in Anomalous Right Coronary Arteries. *Journal of Interventional Cardiology 22* (2009), 234–239. viii, 23

[Sta11] STALDER A.: Aorta Segmentation using ITK-SNAP. http://picsl.upenn.edu/data/pauly/itksnap-v3-cinepak-32fps_crop_resized3_cinepack90_15fps_15s.avi, May 2011. [Accessed Jun. 27, 2012]. 76

[TAA05] TEK H., AKOVA F., AYVACY A.: Region competition via local watershed operators. In *Proceedings of the 2005 IEEE Computer Society Conference on Computer Vision and Pattern Recognition (CVPR'05) - Volume 2 - Volume 02* (Washington, DC, USA, 2005), CVPR '05, IEEE Computer Society, pp. 361–368. 16

[TAL80] TRIVELLATO M., ANGELINI P., LEACHMAN R. D.: Variations in coronary artery anatomy: Normal versus abnormal. *Cardiovasc Dis*, 4 (1980), 357–370. 6

[TOY*09] TAKASHIMA K., OHTA M., YOSHINAKA K., MUKAI T., OOTA S.: Catheter and guidewire simulator for intravascular surgery (comparison between simulation results and medical images). In *IFMBE proceedings*, vol. 25. 2009, pp. 128–131. ix, 32, 33

[TWT10] TSAI W.-L., WEI H.-J., TSAI I.-C.: High-take-off coronary artery: a haemodynamically minor, but surgically important coronary anomaly. *Pediatric Radiology 40* (2010), 232–233. 10.1007/s00247-009-1413-4. 101

[Uni11] UNIVERSITY M.: Visible human project. http://vhp.med.umich.edu/, May 2011. [Accessed Apr. 20, 2012]. 31

[VBM*96] VERDONCK B., BLOCH L., MAITRE H., VANDERMEULEN D., SUETENS P., MARCHAL G.: Accurate segmentation of blood vessels from 3d medical images. In *Image Processing, 1996. Proceedings., International Conference on* (sep 1996), vol. 3, pp. 311 –314 vol.3. 17

[Vod92] VODA J.: Long-tip guiding catheter: Successful and safe for left coronary artery angioplasty. *Catheterization and Cardiovascular Diagnosis 27*, 3 (1992), 234 – 242. viii, 23, 26, 57

[WCL*98] WANG Y., CHUI C., LIM H., CAI Y., MAK K.: Real-time interactive simulator for percutaneous coronary revascularization procedures. *Computer Aided Surgery 3*, 5 (1998), 211–227. ix, 29, 32

[WF04] WESARG S., FIRLE E. A.: Segmentation of vessels: the corkscrew algorithm. Fitzpatrick M. J., Sonka M., (Eds.), vol. 5370, SPIE, pp. 1609–1620. 19

[WL09] WANG Y., LIATSIS P.: A Fully Automated Framework for Segmentation and Stenosis Quantification of Coronary Arteries in 3D CTA Imaging. In *Developments in eSystems*

Engineering (DESE), 2009 Second International Conference on (2009), pp. 136–140. viii, 19

[WNV00] WINK O., NIESSEN W. J., VIERGEVER M. A.: Fast delineation and visualization of vessels in 3-D angiographic images. *IEEE Transactions on Medical Imaging 19*, 4 (2000), 337–346. 16

[WR07] WÖRZ S., ROHR K.: Segmentation and Quantification of Human Vessels Using a 3-D Cylindrical Intensity Model. *Image Processing, IEEE Transactions on 16*, 8 (2007), 1994–2004. vii, 17

[WvH*10] WÖRZ S., VON TENGG-KOBLIGK H., HENNINGER V., RENGIER F., SCHUMACHER H., BÖCKLER D., KAUCZOR H.-U., ROHR K.: 3-D Quantification of the Aortic Arch Morphology in 3-D CTA Data for Endovascular Aortic Repair. *Biomedical Engineering, IEEE Transactions on 57*, 10 (2010), 2359–2368. vii, 17

[Yan06] YANG Y.: A robust region based level set framework for medical image segmentation. In *Proceedings of the 11th Iberoamerican conference on Progress in Pattern Recognition, Image Analysis and Applications* (Berlin, Heidelberg, 2006), CIARP'06, Springer-Verlag, pp. 336–344. 19

[YPC*11] YUSHKEVICH P. A., PIVEN J., CODY H., HO S., GEE J. C., GERIG G.: ITK-SNAP. http://www.itksnap.org/pmwiki/pmwiki.php?n=Main.HomePage, Feb. 2011. [Accessed Jun. 27, 2012]. 75, 76, 112

[YPCH*06] YUSHKEVICH P. A., PIVEN J., CODY HAZLETT H., GIMPEL SMITH R., HO S., GEE J. C., GERIG G.: User-guided 3D active contour segmentation of anatomical structures: Significantly improved efficiency and reliability. *Neuroimage 31*, 3 (2006), 1116–1128. 75, 76, 112

[ZJL*10] ZHENG Y., JOHN M., LIAO R., BOESE J., KIRSCHSTEIN U., GEORGESCU B., ZHOU S. K., KEMPFERT J., WALTHER T., BROCKMANN G., COMANICIU D.: Automatic aorta segmentation and valve landmark detection in C-Arm CT: application to aortic valve implantation. In *Proceedings of the 13th international conference on Medical image computing and computer-assisted intervention: Part I* (Berlin, Heidelberg, 2010), MICCAI'10, Springer-Verlag, pp. 476–483. 17, 26

[Zse05] ZSEMLYE G.: *Shape prediction from partial information*. PhD thesis, ETH Zurich, 2005. 17

[ZZW*06] ZHAO F., ZHANG H., WAHLE A., SCHOLZ T. D., SONKA M.: Automated 4D segmentation of aortic magnetic resonance images. In *The 17th BMVC* (Edinburgh, Sept. 2006), vol. 1, British Machine Vision Association, pp. 247–257. 18